Information Fusion 26 (2015) 1–35

Contents lists available at ScienceDirect

Information Fusion

journal homepage: www.elsevier.com/locate/inffus

# Ocular biometrics: A survey of modalities and fusion approaches

Ishan Nigam, Mayank Vatsa *, Richa Singh

*IIIT Delhi, India*

ARTICLE INFO

*Article history:*
Received 12 December 2014
Received in revised form 17 March 2015
Accepted 28 March 2015
Available online 15 April 2015

*Keywords:*
Ocular biometrics
Iris
Periocular
Retina
Information fusion

ABSTRACT

Biometrics, an integral component of *Identity Science*, is widely used in several large-scale-county-wide projects to provide a meaningful way of recognizing individuals. Among existing modalities, ocular biometric traits such as iris, periocular, retina, and eye movement have received significant attention in the recent past. Iris recognition is used in Unique Identification Authority of India's Aadhaar Program and the United Arab Emirate's border security programs, whereas the periocular recognition is used to augment the performance of face or iris when only ocular region is present in the image. This paper reviews the research progression in these modalities. The paper discusses existing algorithms and the limitations of each of the biometric traits and information fusion approaches which combine ocular modalities with other modalities. We also propose a path forward to advance the research on ocular recognition by (i) improving the sensing technology, (ii) heterogeneous recognition for addressing interoperability, (iii) utilizing advanced machine learning algorithms for better representation and classification, (iv) developing algorithms for ocular recognition at a distance, (v) using multimodal ocular biometrics for recognition, and (vi) encouraging benchmarking standards and open-source software development.



## 1. Introduction

With the increasing requirement of establishing the identity of individuals, a number of identity programs are being instituted across the globe. Therefore, the design of accurate and robust methods for identity recognition has become a very important research challenge. Traditional approaches rely on the use of identification cards, passwords, or PINs to determine or verify one's identity. However, due to several challenges associated with traditional methods such as the ease to forge or forget, use of biometrics is gaining significant importance. Biometrics refers to the use of physiological and behavioral characteristics of humans for establishing their identity. Among physiological characteristics, several body parts have been studied that demonstrate biometric properties such as universality, uniqueness, permanence, and collectability. It has been observed that the ocular region, including iris, is one of the most stable ones and can be effectively used for recognition [1].

The field of ocular biometrics has undergone significant progress in the last decade. Researchers have developed a number of techniques to leverage the information present in the ocular region. Ocular region is an important and interrelated system (organ) that consists of several subsystems such as cornea, lens, optic nerve, retina, pupil, iris, and the periocular region. Out of these, iris, periocular, retina, and sclera have been well studied for being potential biometric modalities (Fig. 1). Related research started with iris recognition in 1987 [2], followed by sclera [3], retina [4], and then periocular recognition [5] in 2009. A number of noteworthy contributions have been made to improve the state-of-the-art in ocular related biometrics. Currently, there are several identification and verification systems in deployment that use one or more of these ocular biometric modalities. For instance, the United Arab Emirate's immigration program, deployed in 2001, uses iris recognition for frequent travelers [6]. Retina recognition is being used in high security military and nuclear instalments [7].

After decades of research in individual biometric modalities by the research community, it is observed that none of the individual modalities can satisfy every biometric characteristic at every point in time. For instance, fingerprint of laborers and farmers and iris patterns of individuals suffering from certain eye diseases can change over time. To address such instances, researchers and practitioners have proposed multi-modal fusion or selection of biometric modalities to improve the recognition performance [8]. The Aadhaar program in India is using iris and fingerprint for de-duplication and verification [10]. Office of Biometric Identity Management (OBIM), formerly US-VISIT, is using fingerprints and face for recognition [11]. Therefore, the current best practice is to combine or fuse multiple modalities for improved coverage and performance. Under the same principle, ocular modalities are also

* Corresponding author. Tel.: +91 11 26907434.
*E-mail address:* mayank@iiitd.ac.in (M. Vatsa).

http://dx.doi.org/10.1016/j.inffus.2015.03.005
1566-2535/

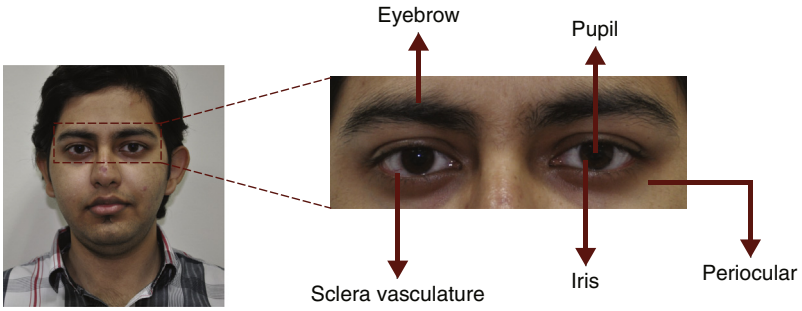


**Fig. 1.** Ocular biometric modalities.

combined with other ocular and non-ocular modalities for improved performance.

In this survey article, we review the advancements made in individual ocular biometric modalities and the research that has been conducted in combining multiple ocular modalities or ocular and other non-ocular modalities. The advancements and developments are measured in terms of the contributions provided to higher recognition performance, to higher computational efficiency, and to the collection of databases that help researchers in addressing interesting and important challenges which continue to emerge. Therefore, the paper summarizes the contributions in terms of both technologies and databases prepared. Section 2 provides a review of technical contributions made in individual ocular biometric modalities and Section 3 summarizes the contributions in terms of combining multiple ocular biometric modalities. Section 4 summarizes publicly available databases related to ocular biometric modalities. Section 5 discusses the authors' view of the path forward in ocular biometrics – where the technology should be heading to improve recognition performance.

## 2. Ocular biometrics

As discussed earlier, multiple biometric modalities have been established in the ocular region. This section presents a detailed summary of the research conducted in the field of ocular biometrics between 2010 and 2014.[1] Section 2.1 presents a comprehensive survey of iris biometrics, Section 2.2 explores the advances in periocular biometrics, Section 2.3 covers the work done in the field of retina biometrics, and Section 2.4 summarizes several emerging ocular modalities.

### 2.1. Iris

Ocular biometrics has become an established biometric trait, primarily due to the extensive efforts made by the biometrics community in the field of iris recognition. The possibility that the iris may be used as an optical fingerprint was first explored by Flom and Safir [2]. Since then, it has evolved into a reliable biometric trait and has been explored extensively by the biometric research community. The popularity of iris biometrics has resulted in the large-scale deployment of commercial and public iris recognition systems around the world. One of the foremost examples of such a system includes the Aadhaar Unique Identification Authority of India (UIDAI) Program [10], which performs approximately 100 trillion iris matches everyday.

Daugman's IrisCode algorithm [14] has served as the basis for a number of efforts made by researchers in the biometrics community. The feature descriptor consists of a compact sequence of multi-scale quadrature 2D Gabor wavelet coefficients. In [15], Daugman analyzes the statistical variability which forms the basis of iris recognition. The principle driving the algorithm is the failure of a test of statistical independence on the iris sample image encoded by multi-scale quadrature wavelets as discussed in [14]. The combinatorial complexity of this method of information description across individuals spans approximately 249 degrees-of-freedom. It generates a discrimination entropy of about 3.2 bits/mm$^2$ over the iris such that it enables real-time identification to support exhaustive searches through very large databases. In [16], Daugman presents (1) several advances towards the IrisCode algorithm for iris recognition: more accurate detection and modeling of iris boundaries with active contours, (2) statistical inference methods for detecting and excluding eyelashes, and (3) the possibility of employing score normalizations, depending on the amount of valid iris data available.

Kong et al. [17] also analyze the IrisCode algorithm. The study proves the equivalent relationship between bit-wise hamming distance and bit-wise phase distance and studies the role of the Gabor function as a phase-steerable filter. These studies lead up to the most significant contribution of the paper, which is the precise phase-representation algorithm for iris recognition. Experiments conducted on the WVU Iris database show precise phase representation is more accurate than IrisCode, though its computation time is considerably longer. The authors propose that the precise phase representation may be considered as a flexible representation for balancing the trade-off between matching speed and identification accuracy.

As shown in Fig. 2, the flow of information in an iris recognition system can be organized as acquisition, preprocessing, segmentation, feature extraction, and matching. Section 2.1.1 reviews iris acquisition in visible light and near infrared light. Section 2.1.2 presents the various preprocessing techniques developed for treating iris images and improving recognition performance. Section 2.1.3 examines the segmentation methodologies that have evolved to handle ideal as well as non-ideal iris images. A brief overview of feature selection techniques is provided in Section 2.1.4. Publications focusing on matching and indexing of iris templates are surveyed in Section 2.1.5. The emerging field of non-ideal iris recognition and associated methodologies are presented in Section 2.1.6.

#### 2.1.1. Acquisition

Researchers have explored multiple kinds of acquisition techniques in iris recognition. These techniques vary in spectrums, devices, and also the distances at which the images are captured. Early research in iris recognition relied exclusively on the acquisition of high-resolution iris images. Daugman [14] proposed the use of the Near Infrared (NIR) spectrum in the wavelength range 750–950 nm for iris acquisition. The evolution of sensor technology has permitted greater flexibility in the development of acquisition modalities. Some recent advances in iris acquisition systems have

[1] For a literature review prior to 2010, readers are referred to [12,13].


**Fig. 2.** Flow of information in an iris biometric system.

involved the use of lower resolution systems, visible spectrum cameras, and set-ups which permit the user to walk through them, allowing image acquisition at multiple distances. Moreover, acquisition by mobile devices has also been explored.

Proença and Alexandre [18] designed a setup to capture iris images in the visible spectrum. A Nikon E5700 camera with a halogen lamp set up behind the acquisition apparatus and the subject, captures grayscale images of size $400 \times 300$. They created the first large visible spectrum iris database known as the UBIRIS v1 [18] database that contains 1877 images collected from 241 persons. The UBIRIS v2 [19] database is the second version of the database collected using a Canon EOS 5D at distances of 3–10 m. The database contains 11,102 color images from 261 subjects and is the largest database collected for irises in the visible spectrum.

Venugopalan and Savvides [20] investigate unconstrained iris acquisition and recognition using a single pan-tilt-zoom camera. The apparatus acquires images at a distance of 1.5 m from the subject, yielding an iris diameter in the range of 150–200 pixels. Face detection is used to localize the position of the user and track the user's movements. Active Shape Models are applied for localization of facial landmarks. The camera captures the face when the user is detected. The authors claim that the proposed system eliminates the need for calibration adjustments prior to acquisition. The hardware entirely consists of Commercial Off-The-Shelf equipment. Experiments are conducted on 12 test subjects using the proposed apparatus to demonstrate the efficacy of the system.

McCloskey et al. [21] explore the problem of capturing sharp iris images from subjects in motion. Images are captured using the computational photography flutter-shutter technique. Instead of capturing an image with traditional motion blur, the shutter is opened and closed several times during capture in order to effect invertible motion blur. Following automated blur estimation and de-blurring, de-convolution is used to estimate the sharp image from the captured image. Multiple synthetic experiments are performed on the Iris Challenge Evaluation dataset. Motion-blurred capture and deblurring is simulated and compared to the original images. The results with synthetic images illustrate the potential upper bound of the performance of the system.

Venugopalan et al. [22] present the design of an acquisition system for non-cooperative subjects. The equipment consists of Commercial-Off-The-Shelf hardware and an infrared sensor. The authors incorporate velocity estimation and focus tracking modules for acquisition so that images may be acquired from subjects on the move as well. For mobile subjects, a sensor is included with a wide angle lens to track the subject's movement during the acquisition process. While the subject is moving, their speed is estimated and used to continuously tune the focus of the system.

Connaughton et al. [23] compare three commercially available iris sensors – the LG TD100, the LG IrisAccess 4000, and the IrisGuard AD100. The performance of each sensor is analyzed and single-sensor as well as cross-sensor experiments are performed to investigate how factors such as changes in environmental conditions and pupil dilation affect sensor performance, in what manner cross-sensor performance corresponds to single-sensor performances, whether relative sensor performance is consistent across matching algorithms, and whether a ranking of sensors can be established. The sensors are evaluated using three iris recognition algorithms – one of the three matchers is an in-house implementation by the authors, while two are commercially available systems.

Tankasala et al. [24] design and implement a hyper-focal imaging system for acquiring iris images in the visible spectrum. The proposed acquisition system uses a DSLR Canon T2i camera to capture videos of the ocular region at multiple focal lengths. The video frames are fused in order to yield a single image with higher precision. The authors use a combination of focus bracketing with lateral white LED lighting to overcome problems associated with RGB iris exposure and adjustment of the depth-of-field. It is observed by the authors that the proposed hyper-focal imaging system produces better results compared to fixed focus systems.

Boehnen et al. [25] present a standoff biometric system having an operation range of up to 7 m. The proposed system captures high quality 12 megapixel Near Infrared videos allowing for multi-sample and multi-modal comparisons. The proposed system is used to capture data from 50 subjects in order to demonstrate the efficacy of the system. Experiments show a 100% rank-1 recognition performance for the system on standoff recognition of non-cooperative subjects. Recognition experiments for multiple samples achieve an improvement of 24% in Rank-1 accuracy. However, a non-significant improvement is observed for multi-modal recognition.

Ortiz et al. [26] present a dilation-aware iris enrollment scheme based on assuming a linear relationship between match scores and dilation difference. The paper analyzes several eye images per subject to determine the optimal choice based on pupil dilation. Several observations are made by the authors: the optimal image for enrollment has a pupil dilation near the mean or median depending on the measure used for dilation difference, minimization of the difference in dilation between pairs of images is more critical even though a constricted pupil has a greater pixel resolution of the iris, accounting for dilation in the enrollment phase overcomes a few differences introduced due to difference in dilation. Experiments performed on image samples collected by the authors over the period 2008–2013 show the effectiveness of the enrollment scheme.

Table 1 summarizes the acquisition methods in the literature. The current acquisition systems are generally constrained towards capturing images at a distance of approximately one feet (Fig. 3). To increase the usability of iris as a biometric, researchers are attempting to design hardware that can capture good quality images without requiring significant cooperation from the user. Sarnoff is designing one such system that can function as a "walk through" recognition system. The possibility of combining information in the ocular region is also prompting researchers to explore the possibility of moving towards iris recognition in the visible spectrum. The acquisition of ocular images in the visible spectrum serves the purpose of permitting the extraction of multiple ocular modalities from the same image.

### 2.1.2. Pre-processing

In the last five years, iris recognition has moved towards exploring real-word large-scale applications. Due to the unconstrained nature of image acquisition in current research, quality assessment and preprocessing of biometric samples has become an important challenge for researchers. Different types of imperfect images may be acquired which require quality assessment based pre-processing techniques to be applied to them prior to recognition (Fig. 4). Bharadwaj et al. [27] discuss different image features utilized in the literature for quality assessment, and the application of relevant pre-processing methods. This sub-section expands upon

**Table 1**
Summary of iris acquisition research.

| Authors | Database | Summary |
|---|---|---|
| Daugman [14] | In-house collection | Proposed NIR imaging (750–950 nm) for iris recognition |
| Venugopalan and Savvides [20] | In-house collection | Proposed apparatus that acquires images at 1.5 m from subject. Face detection is used to localize user's face. Tracks face and segments iris region |
| McCloskey et al. [21] | ICE [28] | Images captured using computational photography flutter-shutter technique. Deconvolution is used to estimate sharp image from captured image |
| Venugopalan et al. [22] | In-house collection | Hardware constitutes Commercial Off The Shelf (COTS) components. Incorporate velocity estimation and focus tracking modules. Subject's speed is estimated and used to tune focus of system |
| Connaughton et al. [23] | In-house collection | Compare three commercially available iris sensors. Performance of each sensor is analyzed. Experiments are performed to investigate how external factors affect acquisition |
| Tankasala et al. [24] | In-house collection | Capture video sequence of ocular region at multiple focal lengths. Fuse frames to yield single image. Combination of focus bracketing and lateral white LED lighting is used |
| Boehnen et al. [25] | In-house collection | System captures high quality Near Infrared videos. Significant improvements in recognition on increasing images are reported |
| Ortiz et al. [26] | In-house collection | [Acquisition] Dilation-aware iris enrollment scheme; shows that optimal dilation is near the median or mean if relationship between match scores and dilation is linear |

several important techniques that have been used to process the image before the iris texture is segmented from the image. Table 2 summarizes these pre-processing techniques.

Liu et al. [29] propose a novel image deblurring method to enhance the quality of defocused and motion blurred iris images. Each image is classified as either defocused or motion blurred. The initial point spread function is refined based on selected gradient maps in conjunction with a noise model. Image deconvolution is performed by adopting a more accurate noise model. Extensive experiments are performed on a dataset collected for the purpose of the study. The experiments demonstrate that the proposed technique improves accuracy and robustness, and enhances the effective capture range of iris recognition systems.

Ortiz and Bowyer [30] posit that the incorporation of pupil dilation information obtained during iris image acquisition results in a noticeable improvement in recognition rates. The study examines a strategy to improve system performance by incorporating a dilation-aware enrolment phase that selects eye images based on their respective dilation ratio distribution. Experimental results from the study show that there is significant improvement when pupil dilation is accounted for during the enrolment phase as compared to the random scenario.

Robustly estimating iris masks is one of the key factors to achieve high iris recognition rates. Li and Savvides [31] propose to use Figueiredo and Jain's Gaussian Mixture Models (FJ-GMMs) to model distributions of regions on iris images for robust occlusion estimation. The authors find that Gabor Filter Bank (GFB) descriptors provide the most discriminative information. Simulated Annealing technique is applied to optimize the parameters of GFB to achieve a high recognition accuracy. Experimental results show that the masks generated by the proposed algorithm increase recognition accuracy on both the ICE dataset as well as the UBIRIS v1 dataset, verifying the effectiveness of the method. The major contributions of the work are: formulating a feature set which is an optimal combination of visual features, sequential optimization of the parameters for GFB, the requirement of a single training image from each class to obtain satisfactory results for

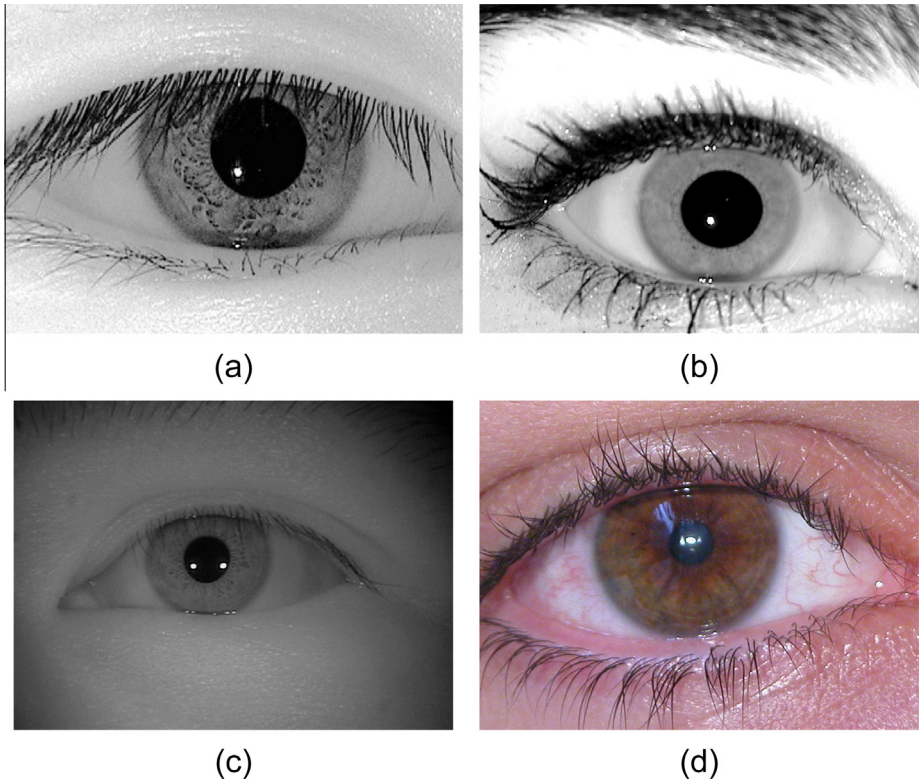


**Fig. 3.** Iris images captured with different acquisition devices.

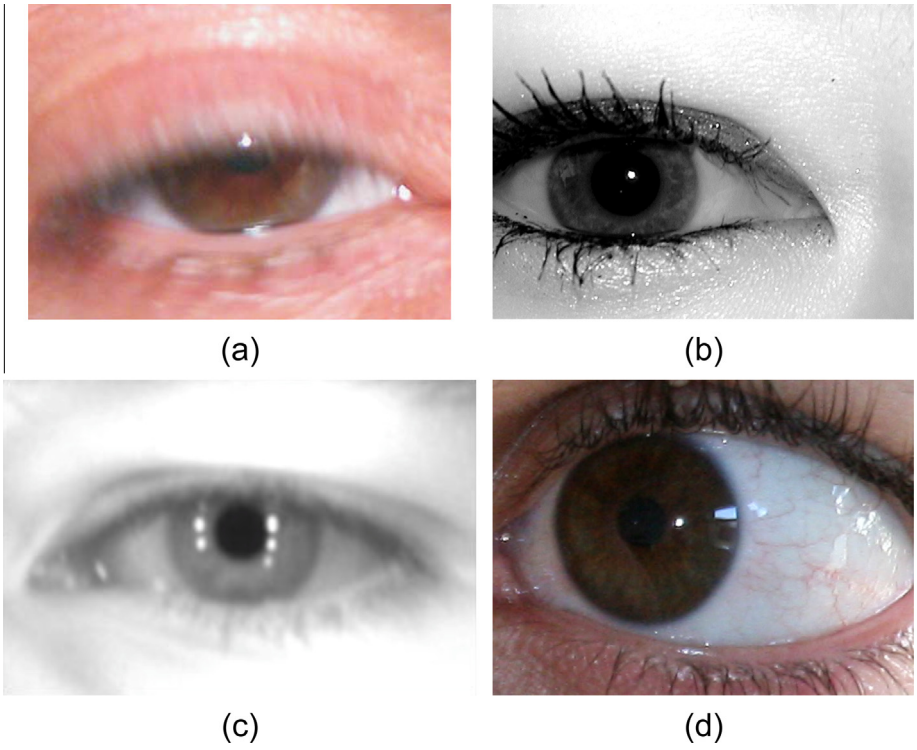


**Fig. 4.** Iris images which require pre-processing.

**Table 2**
Summary of iris preprocessing techniques.

| Authors | Database | Summary |
|---|---|---|
| Liu et al. [29] | In-house collection | Image is classified as either defocused or motion blurred. PSF is refined based on gradient maps and noise model. Image deconvolution is performed |
| Ortiz and Bowyer [30] | Notre Dame Iris [28] | Implement dilation-aware enrolment phase to choose image based on empirical dilation ratio distribution |
| Li and Savvides [31] | ICE, UBIRIS v1 [18] | GMMs used to model probabilistic distributions of valid and invalid regions on iris images. Simulated Annealing technique is applied to optimize parameters |
| Sgroi et al. [32] | In-house collection | Propose diffuse illumination system. Matching algorithms are used to study diffused image templates |
| Tan and Kumar [33] | CASIA v4 [34], UBIRIS v2 [19] | Noise treated as inconsistent fragile bits. Model relationship between iris codes and noise. Features are extracted using 1D log Gabor filters |

estimating iris masks, and the computational efficiency associated with the evaluation of the Gaussian function.

Sgroi et al. [32] propose a diffuse illumination system to reduce specular reflections in iris template acquisition. For the purpose of this study, the authors collected a database of more than 8000 images using an LG IrisAccess 4000 sensor and an in-house apparatus assembly to cause diffusion of the infrared illumination. Matching algorithms are used to study the resulting diffused image templates. The authors observe that an (in-house) recognition system performs significantly better for diffused illumination compared to normal illumination. This observation supports the authors' hypothesis regarding diffused illumination as a hardware level pre-processing technique.

Tan and Kumar [33] propose to model the relationship between the bit consistency of iris codes and the accompanying noise using a non-linear relationship. The noise perturbed bits are modeled using small weights while consistent bits are given high weights. The noise estimation can be regarded as a process of determining the inconsistent bits in iris codes. The relationship between the iris code stability and the accompanying noise in feature space is modeled as a power-law. The effectiveness of the proposed iris matching strategy is demonstrated using 1D log Gabor filters on the CASIA v4-distance and UBIRIS v2 datasets. The proposed method results in an improvement of the rank-1 accuracy for the CASIA v4-distance database by 13.9%, and an improvement of the rank-1 accuracy for the UBIRIS v2 database by 47.2%.

### 2.1.3. Segmentation approaches

Iris sensors acquire not only the iris but also some surrounding regions. Depending on the acquisition device, the amount of neighboring regions varies. Therefore, it is important to have a robust iris segmentation algorithm. Fig. 5 shows some sample iris images with significantly different amount of acquired ocular areas that require adaptive and robust segmentation algorithms.

Daugman [14] initially proposed circular edge detection using an integro-differential operator to segment the iris boundaries. However, this model assumed circular iris and only accounted for occlusion due to upper eyelid and specular reflections. It did not consider non-circular boundaries and occlusion due to eyelashes. Since then iris recognition has steadily moved towards unconstrained acquisition and matching. This has led to the need for a robust class of segmentation schemes which can tolerate occluded, noisy, and off-angle iris images. In 2007, Daugman [16] proposed a new segmentation scheme, using active contour

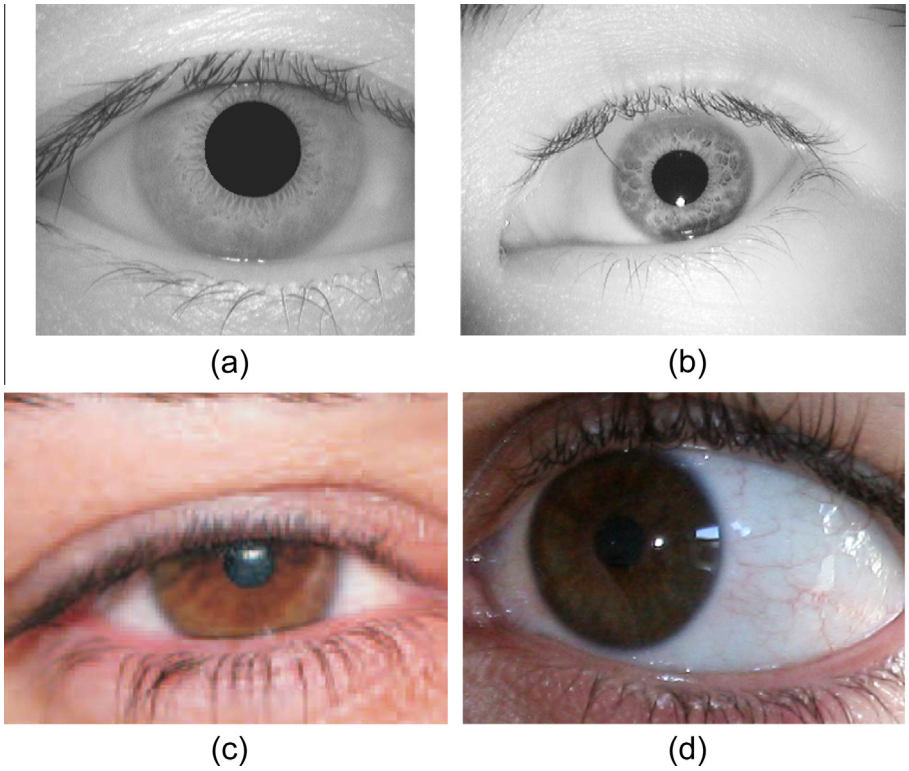


**Fig. 5.** Sample images showing variations in the difficulty of segmentation of iris images.

models, which is capable of modeling non-circular non-concentric irises and pupils. The improved segmentation scheme also accounted for variations in the boundaries due to eyelashes occluding the iris pattern.

Tan et al. [35] present an efficient algorithm for noisy non-cooperative iris segmentation. An eight-neighbor connection based clustering scheme is proposed to cluster iris image pixels in different regions. The genuine iris region is extracted, and the non-iris regions are explicitly identified and excluded to reduce the possibility of mis-localizations on non-iris regions. An integro-differential constellation is applied to enhance global convergence for pupillary and limbic boundary localization. A horizontal rank filter and an eyelid curvature model are applied to account for eyelashes and shape irregularity, respectively. The eyelash and shadow occlusions are detected through a learned prediction model based on intensity statistics between iris regions. Exhaustive experiments are performed on the UBIRIS v1 database [18] and the algorithm performs optimally among all submissions to the NICE v1 Contest [36].

Zhang et al. [37] propose the removal of local gradient extremes for robust iris segmentation. Orthogonal ordinal filters are applied to obtain a robust gradient map. Hough transform is used to localize the iris region on the gradient map. A Semantic Iris Contour Map is generated by combining spatial information of the coarse iris location and the gradient map. A new convergence criterion and an adaptive parameter are proposed by the authors to improve the performance of the level set method. Experiments performed on the ICE dataset and CASIA v3 dataset show the effectiveness of the proposed method.

Roy et al. [38] apply a parallel game-theoretic decision making procedure to segment iris images. The proposed algorithm integrates region based segmentation and gradient based boundary localization methods and fuses the complementary strengths of each of these individual methods. Experiments are performed on the ICE 2005 dataset [39], the CASIA v3 dataset, and the UBIRIS v1 dataset [18]. The reported genuine accept rate at a false accept rate of 0.001% is 98.23% for ICE, 97.18% for CASIA v3, and 97.61% for UBIRIS v1 databases. The genuine accept rate on the combined dataset is 97.47%.

Pundlik et al. [40] describe a non-ideal iris segmentation approach based on graph cuts. The image texture gradient is used to discriminate between eyelash and non-eyelash regions. The intensity differences between the iris, the pupil, and the background are utilized for the segmentation process. The image is modeled as a Markov Random Field and energy minimization is achieved via graph cuts to assign each image pixel to iris, pupil, background, or eyelash classes. The authors further model the iris region as an ellipse to refine the segmented region. Experiments performed on the WVU Non-Ideal Iris Database and the WVU Off-Angle Iris Database demonstrate significantly improved results as compared to prior state-of-the-art approaches.

Zuo and Schmid [41] propose a methodology for robust iris segmentation, which is directed towards treating non-ideal irises. The pupil is pre-processed and segmented by fitting an ellipse to the pupil boundary. In order to be able to reliably detect the iris boundary under the condition of uneven illumination, a contrast-balancing pre-processing step is introduced, which is followed by segmentation of the iris. An ellipse based model is used to contour the estimated boundaries for pupil and iris regions, which demonstrates the robustness of the algorithm towards evaluating non-frontal iris images. Exhaustive experiments performed on the CASIA v3, ICE, WVU, and WVU-OA datasets confirm the effectiveness of the algorithm compared to prior methods.

De Marisco et al. [42] present an iris segmentation method, $IS_{IS}$ (Iris Segmentation for Identification Systems). Pre-processing is performed by applying a posterization filter to the image. Canny filtering and Taubin method for circle fitting are applied to the image to locate the pupil boundary. The image is then transformed to polar coordinates to be able to identify the boundary between the iris and the sclera. The authors compare the results of the

proposed system with prior state-of-the-art for segmentation as well as recognition. Experiments are performed on the UBIRIS v1 and CASIA v3 databases. It is observed that $IS_{IS}$ improves the performance of Daugman's approach to recognition. The run-time of the algorithm also suggests that $IS_{IS}$ supports high resolution iris images, with a higher precision compared to a stand-alone implementation of Daugman's approach.

Proença [43] makes significant contributions to segmenting degraded iris images in the visible wavelength. The author suggests that the sclera is the most easily distinguishable part of the eye in degraded images, and proposes a novel feature that measures the proportion of sclera in each direction. Specific color components are used to calculate local features for segmentation of the sclera. The iris is segmented by exploiting the mandatory adjacency between the iris and the sclera and using the proportion-of-the-sclera as a feature to localize the iris. A constrained polynomial fitting procedure is used after classification to compensate for classification inaccuracies. Experiments on the UBIRIS v2 dataset show that the entire procedure runs in deterministically linear time with respect to the size of the image, making the procedure suitable for real-time applications.

Koh et al. [44] propose a robust localization method that uses an active contour model and a circular Hough transform to segment the pupillary boundary and the limbic boundary. Histograms are generated from the binarized image. The center of the pupil is estimated based on the histograms. Iris segmentation based on active contour models is performed to correct for possible false estimates of the pupil center. The pupillary boundary is computed by applying the Hough transform. The Hough transform is used again for localizing the limbic boundary. Experiments performed on 100 images from the CASIA v3 database show that the proposed method is accurate and approximately 2.5 times faster than Daugman's approach in segmenting the iris.

Du et al. [45] propose a video based non-cooperative iris image segmentation scheme. The method incorporates a quality filter to eliminate images that do not consist of a valid iris and employs a coarse-to-fine segmentation scheme, which uses a direct least-squares ellipse fitting function to model the deformed pupil and limbic boundaries. A window gradient based method is employed to remove noise in the iris region. Experiments are performed on images acquired from a customized iris acquisition system set up to collect non-cooperative iris video images. Experimental results suggest that the proposed method can segment irises accurately from non-cooperative iris video images.

Tan and Kumar [46] tackle the problem of segmenting iris images acquired at-a-distance using visible spectrum imaging. Iris features are extracted by exploiting localized Zernike moments. Sclera features are extracted using discriminant color features. The authors also propose a robust approach for post-processing of classified iris image pixels. Such post-classification is shown to be effective in reducing iris segmentation errors by overcoming limitations in the classification stage. Rigorous experiments performed on the UBIRIS v2 database corroborate the usefulness of the proposed approach. An improvement of 42.4% in the average segmentation error is achieved. The best of the segmentation results are obtained using feed-forward network (FFN) classifier. However, they require rigorous training. The authors suggest that the SVM classifier is used as an alternative to the FFN. However, the performance achieved using FFN is reported to be marginally superior to SVM.

Tan and Kumar [47] present an iris segmentation framework which uses multiple higher order dependencies among local pixels to robustly classify the eye region pixels into iris or non-iris regions using visible wavelength as well as Near Infrared imaging. Face and eye detection modules are incorporated in the framework to provide localized eye region from facial image for segmentation. The authors develop robust post-processing operations to effectively tackle the noisy pixels caused by misclassification. One of the novel features of the proposed approach is its ability to segment iris images acquired under varying illumination conditions. Experimental results presented suggest significant improvement in segmentation errors over other previously proposed approaches on the UBIRIS v2, the FRGC, and the CASIA v4 databases. The experimental results suggest improvement in the iris segmentation error by 32–47% for these databases.

Sutra et al. [48] present an iris segmentation technique that finds the contour of the iris by optimizing a cost function which maximizes the summation of gradients. An optimal path is searched for, joining points of significant gradients, using the Viterbi algorithm. The iris is pre-processed by anisotropic smoothing before computing the gradient by a Sobel filter. The Viterbi algorithm is first applied at a high resolution to find precise contours. It is applied again to retrieve coarse contours to improve the accuracy of the normalization. The authors conduct experiments on the ICE 2005, the ND-IRIS-0405, and the CASIA v3 datasets. The results indicate state of the art performance for the proposed algorithm.

Iris edge detection techniques suffer from generation of a large number of noisy edge points in non-ideal scenarios. Li et al. [49] propose a robust iris segmentation method based on specific edge detectors to overcome this problem. Intensity, gradient, and texture features are used to characterize edge points on the iris boundary. The AdaBoost algorithm is employed to learn six class-specific boundary detectors for localization of pupillary boundaries, limbic boundaries, and eyelids. The inner and outer boundaries of the iris are localized using weighted Hough transforms. Finally, the edge points on the eyelids are detected and fitted as parabolas using robust least squares fitting. Experiments performed on the CASIA Iris-Thousand database demonstrate the efficacy of the proposed method.

Fernandez et al. [50] present a method for iris segmentation which focuses on NIR iris recognition in low-constrained environments. The algorithm is based on energy minimization of one-directional graphs. Pupil localization is achieved by a sliding average pattern, model fitting by direct search, and defocusing of irrelevant regions. The Herta Iris Database [51] is collected for iris segmentation. The authors claim accurate segmentation is possible in presence of clutter, lenses, glasses, motion blur, and variable illumination using the proposed methodology.

Tan and Kumar [52] present an efficient iris segmentation approach based on the cellular automata using the grow-cut algorithm. The authors propose that the computational simplicity of the approach is its advantage compared to prior methods, without any compromise in recognition performance. Experiments performed on the UBIRIS v2, the FRGC, and the CASIA v4 databases achieve an average improvement of 34.8%, 31.5%, and 31.4%, respectively, in the average segmentation error. The results indicate the superiority of the proposed segmentation approach in terms of computational complexity as well as recognition performance for segmentation of distantly acquired iris images.

Uhl and Wild [53] propose a novel two-stage algorithm for localization and mapping of the iris texture. The work aims to achieve robust segmentation independent of the acquisition sensor. An adaptive Hough transform is applied at multiple resolutions to estimate the approximate position of the iris center. A subsequent polar transform detects the first elliptic pupillary boundary, and a subsequent ellipsopolar transform finds the second boundary based on the results of the detection of the first boundary. Experiments conducted on the CASIA VI database, the CASIA-L database, and the Notre Dame ND-IRIS-04055 database confirm the robustness of the proposed method.

Li et al. [54] present an efficient segment search algorithm that takes advantage of shape information and learned iris boundary detectors. An efficient segment search algorithm, which utilizes both shape information and Learned Boundary Detectors (LBD), designed for assembling pupillary contour segments. The assembled pupillary contour segments exclude (most) noises and can be accurately fitted as an ellipse. The limbic boundary points are detected by the LBD. Unseen boundary points are inferred in the eyelid occluded regions. Extensive experiments on a challenging subset of the CASIA v4 database demonstrate that the proposed method achieves state-of-the-art iris localization accuracy.

Alonso-Fernandez and Bigun [55] present an iris segmentation algorithm based on the Generalized Structure Tensor (GST). Circular complex filters encode local orientations. The response is penalized in case of disagreement of local orientations of the image with those of the filter. The algorithm accommodates a certain degree of non-circularity through the control of the filter width. Experimental results reported on the CASIA v3 Interval database show the efficacy of the proposed algorithm, either performing at par with or outperforming prior segmentation methods. The GST segmentation methodology is used by Alonso-Fernandez and Bigun [56] to evaluate iris segmentation performance by employing quality measures such as defocus blur, motion blur, edge contrast, edge circularity, grayscale spread, and occlusion. Experimental results on the BioSec baseline corpus [57] show that local measures are generally better predictors of the segmentation performance. The authors also evaluate the impact of quality components in the performance of two iris matchers based on Log-Gabor wavelets and SIFT key-points. Recognition experiments with the two matchers indicate that segmentation and matching performance may not necessarily be affected by the same factors.

Tan and Kumar [58] develop a segmentation approach which exploits a random walker algorithm to estimate coarsely segmented iris images. The input image is preprocessed to enhance the quality of the image. The image is segmented using the random walker algorithm followed by post-processing techniques to refine the coarsely segmented result. The iris is modeled as a graph such that each pixel corresponds to a node and the linkage between any two pixels corresponds to the edge of a graph. Experiments are performed to measure segmentation accuracy using the proposed algorithm. The algorithm demonstrates improvements of 9.5%, 4.3%, and 25.7%, respectively, for the UBIRIS v2, the FRGC, and the CASIA v4 databases. The authors also exploit periocular features to study their effect on improvements in the recognition performance. The joint segmentation and combination strategy achieves average improvements of 132.3%, 7.45%, and 17.5% on the UBIRIS v2, FRGC, and CASIA v4 databases.

Jillela and Ross [59] explore the suitability of using iris texture for biometric recognition in mobile devices. The study focuses on iris segmentation in the visible spectrum, while succinctly describing the complete iris recognition process. The authors utilize the color component analysis approach, the Zernike moments approach, the multi-stage refinement approach, the boundary regularization approach, and the clustering and semantic rules approach. The paper summarizes the challenges and future directions associated with iris segmentation in the visible spectrum.

Hu et al. [60] propose an algorithm for color iris segmentation that demonstrates the utility of sparsity induced by $l_1$-norm in overcoming noise and degradations in color iris images. The limbic and pupillary boundary and eyelids are fitted using $l_1$-norm regression on a set of estimated boundary points. A coarse iris region is determined by super-pixel based correlation histogram method; the technique is capable of locating iris region in images captured at a distance in the presence of noise such as specular reflection and glasses. Experiments performed on the UBIRIS v2 and FRGC databases show the effectiveness of the proposed segmentation method.

Table 3 presents a summary of iris segmentation; it also shows that the growing interest in unconstrained recognition ensures active interest in optimizing segmentation schemes. Researchers are also actively pursuing the development of novel *non-linear* algorithms to meet the demands of the increasing complexity of iris biometric systems.

#### 2.1.4. Feature extraction methods

The extraction of useful features from the iris has been one of the most well-explored areas in iris biometrics. Daugman [14] proposed the use of 2D Gabor filters to capture the textural information present in iris codes. The DC response to the Gabor filter output is suppressed, which allows for robustness towards illumination. The Gabor filter, due to its intrinsic properties, has reciprocal effects on Fourier transforms without any change in functional form. This motivates researchers to actively pursue Gabor filters and other robust texture modeling techniques. The diversification of acquisition modalities has allowed a number of feature descriptors to be explored for accurate recognition. The remainder of this section outlines the feature extraction techniques which have been developed for iris recognition in the last five years.

Sunder and Ross [65] investigate the use of macro-features for iris matching and retrieval, and their feasibility as a soft biometric trait. The macro-features correspond to structures such as moles, freckles, nevi, melanoma. Given a macro-feature image, the goal is to determine if it can successfully retrieve the associated iris from the database. The Scale-Invariant Feature Transform descriptor is used to represent the macro-features. Experiments are performed on high resolution images taken from the Miles Research Database [66]. Data captured in visible spectrum suggests that these structures may be used in addition to traditional features for the purpose of iris retrieval.

Zhou and Kumar [67] propose an approach for the extraction and modeling of iris features using Localized Radon Transforms. The dominant orientation from these Radon transform features is used to generate a compact feature representation. The similarity between two feature vectors is computed using matching distances. The feasibility of the proposed method is evaluated on the IITD Iris Image Database v1 and the CASIA v3 Database. The algorithm achieves equal error rates of 0.53% and 2.82% on IITD v1 and CASIA v3 databases respectively. It is worth noting that the proposed approach requires significantly smaller computational operations for feature extraction.

Scotti and Piuri [68] present an adaptive design methodology for reflection detection and localization systems in irises. The authors propose that a set of features is extracted from the iris pattern and an inductive classifier is used to perform the reflection segmentation. A significant contribution of this work is the introduction of the use of the Radial Symmetry Transform (RST) as a feature. The images in the dataset used for the study are created using a number of different sensors. Experimental results on the dataset establish that the RST is a robust feature to detect and localize reflections in a computationally fast manner. The low computational complexity of the proposed system indicates that it is suitable for real-time applications.

Hosseini et al. [69] explore a noise-resistant pigment melanin based feature descriptor for iris recognition in visible light. The algorithm encodes the pattern of pigment melanin in visible light, independent of the iris texture in near infrared spectrum. Three features are proposed: Radius Vector Function, Support Function, and Tangent Angle Function to extract shape information from the pigment melanin. Each iris is captured in near infrared as well

**Table 3**
Summary of iris segmentation approaches.

| Authors | Database | Summary |
|---|---|---|
| Tan et al. [35] | UBIRIS v1 [18] | Clustering based coarse iris localization. Localization of pupillary and limbic boundaries and localization of eyelids is performed |
| Zhang et al. [37] | ICE 2005, CASIA v3 [61] | Robust gradient map is used for iris localization. SIMC generated using spatial information and coarse iris location. Segmentation achieved by level set method |
| Roy et al. [38] | ICE 2005, CASIA v3, UBIRIS v1 | Game-theoretic decision making procedure to segment irises. Integrates region based segmentation and gradient based boundary localization |
| Pundlik et al. [40] | WVU Non-Ideal [62], WVU Off-Angle [63] | Image is modeled as MRF. Energy minimization is achieved via graph cuts. Model iris as ellipse to refine segmentation |
| Zuo and Schmid [41] | CASIA v3, ICE, WVU, WVU-OA | A combined scheme for pre-processing, pupil segmentation, iris segmentation, and occlusion detection is reported |
| De Marisco et al. [42] | CASIA v3, UBIRIS v1 | Pre-process using posterization filter. Canny filtering is applied to locate pupil boundary. Image is transformed to polar coordinates to identify boundary between iris and sclera |
| Proença [43] | UBIRIS v2 | Sclera and iris are segmented and classified. Polynomial fitting is applied |
| Koh et al. [44] | CASIA v3 | Center of pupil is estimated based on histograms. Pupillary boundary is computed using Hough transform. Apply Hough transform again to localize limbic boundary |
| Du et al. [45] | In-house collection | Method incorporates quality filter to eliminate non-valid images. Employs coarse-to-fine segmentation scheme and window gradient based method to remove noise |
| Tan and Kumar [46] | UBIRIS v2 | Iris features extracted using localized Zernike moments and sclera features are extracted using color features. A robust approach is proposed for post-processing classified iris pixels |
| Tan and Kumar [47] | UBIRIS v2, FRGC v1 [64], CASIA v4 | Multiple higher order local pixel dependencies are used to robustly classify eye region pixels into iris or non-iris regions. Post-processing operations effectively tackle noisy pixels |
| Sutra et al. [48] | ICE 2005, CASIA v3, ND-IRIS-0405 | Pre-processing is performed using anisotropic diffusion. Gradients are computed using Sobel filter and Viterbi algorithm is applied to find contours |
| Li et al. [49] | CASIA v4 | Locate edge points on iris boundary. Boundary detectors for pupillary, limbic, eyelid boundaries are learned and iris boundaries are localized. Eyelid edge points are modeled as parabolas |
| Fernandez et al. [50] | Herta Iris [51] | Based on energy minimization of one-directional graphs. Pupil localization is achieved by sliding average pattern, model fitting, and defocusing of irrelevant regions |
| Tan and Kumar [52] | UBIRIS v2, FRGC, CASIA v4 | Iris segmentation approach based on cellular automata using grow-cut algorithm is proposed. Reduces computational complexity while increasing recognition performance |
| Uhl and Wild [53] | CASIA Iris, ND-IRIS-0405 | Adaptive Hough transform estimates iris center. Polar transform detects first elliptic pupillary boundary. Ellipsopolar transform is used to find second boundary |
| Li et al. [54] | CASIA v4 | Assembled pupillary contour segments are fitted as an ellipse. Limbic boundary points detected by LBD. Unseen boundary points are extrapolated in eyelid occluded regions |
| Alonso-Fernandez and Bigun [55] | CASIA v3 | Pupil boundary is searched for and sclera is detected. Eyelid occlusion is computed and the iris is localized |
| Alonso-Fernandez and Bigun[56] | BioSec Baseline Corpus[57] | Study local and global quality measures for iris segmentation performance. Explore correlation between factors affecting segmentation and matching |
| Tan and Kumar [58] | UBIRIS v2, FRGC, CASIA v4 | Image is segmented using random walker algorithm. Coarsely segmented iris is refined and modeled as a graph |
| Hu et al. [60] | UBIRIS v2, FRGC | $l_1$-norm induces sparsity allowing coarse iris localization, limbic and pupillary boundary segmentation. Eyelid fitting and post-processing are performed |
| Jillela and Ross [59] | – | Explore suitability of using iris texture for recognition in mobile devices. Study focuses on iris segmentation in visible spectrum |

as visible light. The fusion of features extracted from the two spectra leads to higher classification accuracy. The authors assert that visible light imaging can be considered for iris, where the patterns of pigment melanin are highly meaningful and can produce valuable encoded data for classification and complementary features to NIR images.

Roy et al. [70] propose a framework to extract features from non-ideal irises for recognition. A region based active contour model is deployed to segment the irises. The Modified Contribution-Selection Algorithm, an efficient feature ranking scheme, is used to select a subset of informative features without affecting the recognition rate. Experiments are performed on the UBIRIS v1, the ICE 2005, and the WVU Non-ideal datasets to validate the proposed scheme.

A bit in an iris code is termed fragile if its value changes across codes representing different images of the same iris. Hollingsworth et al. [71] explore the possibility of improving iris recognition performance by masking these fragile bits. Rather than ignoring fragile bits completely, discriminative information from the fragile bits is considered towards classification of irises. It is observed by the authors that the locations of fragile bits tend to be consistent across multiple iris codes belonging to the same eye. A metric termed as the Fragile Bit Distance (FBD) is established, which quantitatively measures the coincidence of the fragile bit patterns in two iris codes. Low FBDs are associated with genuine comparisons between two iris codes. High FBDs are associated with impostor comparisons. It is observed that score fusion of FBD and Hamming distance works optimally for recognition compared to Hamming distance alone. The multiplication of FBD and Hamming distance reduces the equal error rate of the proposed recognition system by 8%, a statistically significant improvement from prior research. Proença [72] extends the concept of fragile bits by modeling the relationship between inter-class iris images. The concept of *bit discriminability* is proposed, which takes into account both the intra-class and the inter-class variabilities. The utility of the different regions of the iris is compared on the basis of bit discriminability. Experiments are performed on the UBath, FRGC, UBIRIS v2, and CASIA v4 databases to test the efficacy of the proposed descriptor.

Zhang et al. [73] describe the Deformable DAISY Matcher (DDM) for robust iris feature matching. Dense DAISY descriptors are extracted to represent regional iris features, which are robust against intra-class variations in iris images. The descriptor for each pixel consists of the weighted orientation gradient of the pixel itself as well as information from its neighbors. The DDM technique is robust to noise and illumination changes. A set of iris key points are localized on the feature map. The algorithm replaces fixed point matching with dynamic point matching. Thus, it is tolerant to misalignment caused due to deformation. All the extracted key points are matched for deformed iris matching. Experimental results on the CASIA Iris database demonstrate that DDM outperforms prior state-of-the-art iris recognition methods.

Bastys et al. [74] propose three new iris descriptors that are based on multi-scale Taylor expansion of the iris texture. The first descriptor is a phase based iris representation which uses binarized multi-scale Taylor expansion phase information. The second feature is based on local extrema of the multi-scale Taylor expansion. Approximations of the first and second order Taylor coefficients are averaged over multiple scales. The most significant local extrema of the Taylor expansion is used to define the most significant iris texture variations. The third method is a combination of the first and the second approach, combining the advantages of local maxima features with the phase based features. The efficacy of the proposed descriptors is validated using the CASIA v2, the ICE 2005 and the MBGC-3l datasets. Experiments show that the third descriptor is found to outperform prior state-of-the-art recognition systems.

Proença and Santos [75] propose a scheme based on partitioning the iris into disjoint regions to extract color and shape information. A color constancy technique is used for regularization. Data is normalized into a polar coordinate system of constant dimensions, from which global MPEG 7 color descriptors are extracted. Experiments are performed on the NICE II competition dataset. The data encoding and matching techniques of the proposed algorithm are radically different from prior state-of-the-art approaches. The authors obtain significant improvements in performance when the proposed algorithm is fused with other approaches using weighted sum rule.

Kumar et al. [76] investigate automated recognition of distantly acquired iris images using sparse representation of orientation features based on Local Radon Transform (LRT). Iris representation is modeled as a sparse coding solution based on a LRT dictionary, which is computed using a convex optimization approach. The iris recognition and verification performances for the distantly acquired iris images are evaluated using baseline 1-D log-Gabor filter and monogenic log-Gabor filter based approach, respectively. Experimental results are reported on the publicly available UBIRIS v2 dataset, the FRGC dataset, and the CASIA-Iris v4 database. The experimental results, for both verification and recognition, achieve significantly improved performance over baseline approaches.

Li and Wu [77] propose a method to represent iris texture by combining several image-cues in non-ideal imagery. The inner and outer iris boundaries, eyelids, and specular highlights are localized to generate the normalized iris image and binary mask image. Log-Euclidean Covariance Matrices (LECM) are utilized to model the local correlation of multiple cues: spatial coordinates, intensities, 1st-order and 2nd-order image derivatives. Ordinal measures are used to extract the order relationship of LECM features at different positions. The matching algorithm is based on Hamming distance. Equal error rates of 0.1809 and 0.0008 are reported for experiments performed on UBIRIS v2 dataset and CASIA v3 Iris Image dataset, respectively.

Rahulkar and Holambe [78] present a shift, scale, and rotation-invariant technique for iris feature-representation and decision-level fusion. Iris features are extracted on the basis of a class of Triplet Half-Band Filter Bank (THFB). A novel flexible k-out-of-n post-classifier is explored to achieve robustness against intraclass iris variations. The proposed approach is observed to be capable of handling artifacts, including segmentation error, eyelid/eyelashes occlusion, eyelid shadow, head-tilt, and specular reflections. Experimental results using the UBIRIS, MMU1, CASIA-Iris v3, and IITD v1 Iris databases show the effectiveness of the proposed approach in comparison to prior recognition algorithms. The proposed method provides low computational complexity which makes it feasible for online applications, and experimental results present an improvement in recognition accuracy for the proposed scheme under non-ideal environmental conditions.

Zhang et al. [79] propose a Perturbation-enhanced Feature Correlation Filter (PFCF) for robust iris matching. PFCF is performed on Gabor filtered iris images to encode both local and global features. Instead of using Hamming Distance, Gabor images are matched using correlation filters. Extensive experiments performed on the CASIA v4 and ICE 2005 databases demonstrate that the proposed method outperforms state-of-the-art methods in terms of robustness against deformation, rotation, occlusion, blurring, and illumination changes in iris images. This novel method produces higher intra-class and inter-class discrimination compared to traditional distance measures.

da Costa and Gonzaga [80] present a method to measure the dynamic movement of the human pupil and iris. The authors propose to capture images of one eye using NIR illumination while illuminating the other eye using visible-light. This methodology intends to capture information about the manner in which the human eye reacts to light. The results demonstrate that these features have significant discriminatory information. An average identification accuracy of 99.1% is obtained using the Euclidean distance measure on a dataset collected for the purpose of the study. An accuracy comparison between Daugman's algorithm and the proposed method suggests that the dynamic features presented in the paper provide comparable performance. The tests demonstrate that in addition to recognizing a person, the proposed method also authorizes the validation of certain attributes which the traditional methods are not able to do, such as to check if the input image being analyzed is from a living iris or not by determining if the subject to be validated responds to the illumination stimuli applied.

Liu and Li [81] study iris recognition based on tensor decomposition of Scale Invariant Feature Transform (SIFT) descriptors. A normalized iris image is divided into patches, each of which is represented by a SIFT descriptor. The low-dimensional features are encoded to binary codes by comparing with the mean value of every dimension. Iris matching is performed by counting the number of binary codes in agreement. The proposed method is validated on the UBIRIS v2 and CASIA-Iris v4 datasets.

Kumar and Chan [82] develop an approach for iris recognition using hypercomplex and sparse representations of unwrapped iris images. The orientation of local iris texture elements is extracted using a binarized dictionary of oriented atoms. The iris representation as quaternionic sparse coding is solved using a convex optimization strategy. The performance of this descriptor is evaluated on the UBIRIS v2 database. The quality of images in the UBIRIS v2 database is quite low, with an average estimated diameter of approximately 122 pixels. However, results indicate an improvement of 30% in rank-1 recognition over previously studied sparse representation approaches.

Zhang et al. [83] explore a color feature for iris classification in several different color spaces. The proposed feature, the iris color Texton, combines a pixel value in RGB, HSI, and LAB color spaces as a color feature. The image is represented by a histogram of the learnt iris color Texton vocabulary. The proposed method is robust to illumination variation. Extensive experiments performed on the UBIRIS v1, the UBIRIS v2, and the NICE II competition datasets indicate that the proposed iris color Texton indicates advantages for iris image classification based on only color information.

Wang et al. [84] propose a Robust Regularized Linear Programming feature selection model. The algorithm learns a compact ordinal feature set for iris recognition. A large margin loss function is adopted to learn a robust model. The discriminative information of each feature is considered to remove noise. The model is solved using the Simplex algorithm. Experiments conducted on the CASIA-Iris-v4 database show that the proposed method outperforms other state-of-the-art feature selection methods.

Nguyen et al. [85] show that feature-domain super-resolution is superior to pixel-domain super-resolution towards improving recognition performance of biometric systems. A framework is presented to perform super-resolution in the non-linear Gabor feature domain to improve the recognition performance of biometric systems. The authors employ non-linear 2D Gabor based features, which boost the recognition performance by capitalizing on the feature-domain super-resolution approach and the highly discriminant nature of Gabor features. Experiments conducted on the MBGC dataset confirm the validity of the proposed approach, demonstrating superior performance compared to existing linear approaches.

Zhang et al. [86] decompose iris images into lowpass components and bandpass components using Non-Subsampled Contourlet Transform (NSCT). Geometric features are extracted in bandpass components based on keypoint detection to align deformed iris patterns. Ordinal features are extracted from the lowpass component to characterize the ordinal measures of local iris regions. The proposed algorithm utilizes the shift-invariant, multi-scale, and multi-directional properties of the NSCT function efficiently. Match score level fusion is applied to the local features and keypoint features. Extensive experiments on the CASIA-Iris v4 and ICE 2005 databases demonstrate the effective performance of the proposed method.

Sun et al. [87] investigate texture analysis and propose a general framework for iris image classification. A nascent texture pattern representation method called Hierarchical Visual Codebook (HVC) is proposed to encode the texture primitives of iris images. The proposed method is an integration of the Vocabulary Tree method and the Locality-constrained Linear Coding method. The HVC adopts a coarse-to-fine visual coding strategy and provides a sparse representation of iris texture. An iris image database with four types of fake iris patterns, the CASIA-Iris-Fake database [88], is developed for the purpose of this experiment. Extensive experiments show that the proposed classification method achieves state-of-the-art performance for iris liveness detection, race classification, and coarse-to-fine iris identification.

Sun et al. [89] describe a formulation for ordinal feature selection with successful applications to iris and palm-print recognition. The objective function of the proposed feature selection considers the misclassification error of intra-class and inter-class matching samples and the weighted sparsity of ordinal feature descriptors. The Multi-lobe Ordinal Filter (MOF) is proposed to analyze the ordinal measures of the images. MOF has a number of positive and negative lobes which are specially designed in terms of distance, scale, orientation, number, and location so that the filtering result of MOF measures the ordinal relationship between image regions covered by the positive and negative lobes. Ordinal feature selection is formulated as a linear programming problem so that a solution can be efficiently obtained even on a large-scale feature pool and training database. Extensive experimental results for iris recognition are performed on the CASIA v4 dataset. The experiments demonstrate that the proposed formulation is advantageous over existing feature selection methods.

Tan and Kumar [90] propose a non-linear approach to simultaneously account for local consistency of iris bits and the overall quality of the weight map for iris recognition. The algorithm penalizes the fragile bits while simultaneously rewarding more consistent bits. A Zernike moment based phase encoding of iris features is deployed to achieve a stable characterization of local iris features. Experiments performed on subsets of UBIRIS v2, FRGC, and CASIA v4 databases ascertain the performance of the proposed iris matching strategy.

Tan and Kumar [91] propose a strategy for accurate iris recognition from distantly acquired face or eye images under less constrained environments. The algorithm randomly generates and exclusively assigns a set of coordinate-pairs to each subject in the system. This *geometric key* uniquely defines the manner in which iris features are encoded from the localized iris region pixels. The iris encoding scheme involves computationally efficient operations on the locally assembled image patches using the locations defined by the geometric key. The geometric key also accommodates scale and rotation changes in the localized iris region. The binary encoding of the local iris features allows efficient computation of their similarity using Hamming distance.

Nigam et al. [92] propose a novel iris recognition approach which takes into account the structure of the iris, variations in illumination and rotation, occlusion, and noise. The acquired iris image is segmented and normalized and the primary occlusion mask is computed to identify non-occluded pixels. The authors propose the Relational Measure feature that considers both radial and circumferential information. LBP descriptor is applied in a block-wise manner to the iris and dissimilarity scores are fused at the score level. Experimental results from the CASIA v4 and the IITK Iris databases demonstrate the efficacy of the proposed system.

The successful development of the above-mentioned feature extraction methods (Table 4) has allowed non-ideal iris recognition systems to become practically feasible. These algorithms permit the optimal functioning of matching algorithms, which we discuss in the next sub-section.

#### 2.1.5. Matching and indexing methods

Advancements in the field of iris recognition have led to the adoption of a number of feature representations for iris information. Consequently, matching techniques have also evolved with this diversification in iris representation. The large-scale deployment of iris recognition systems has also led to increasing interest in efficient indexing and retrieval of biometric templates. Generally, Gabor based features have been used for iris representation, and Hamming Distance is proposed to match these features.

Rathgeb et al. [97] present a generic approach to optimize the time complexity of iris recognition algorithms. The analysis of bit-error occurrences in the gallery of iris-codes is used to estimate a global ranking of bit positions, based on which the probes are rearranged, i.e. iris-codes are reordered. The most reliable bits are arranged in the first part of the iris-code, which allows a more efficient partial and incremental matching. Based on the outcome of partial matching, candidates with high Hamming Distance scores are rejected dynamically. Experiments on the CASIA-Iris v3 dataset suggest that the proposed algorithm can be applied to any iris-code recognition system and is capable of reducing bit comparisons significantly to about 5% of iris-code bits.

Gadde et al. [98] propose a novel method for indexing iris images based on the assignment of a code to every entry in the database, a small subset of which is retrieved based on the query code. The normalized gray-scale iris image is converted to a binary image and the Burrows Wheeler Transform is utilized due to its property of sorted context. A horizontal n-bit pattern is chosen and the locations of these patterns are found in the iris image. The normalized iris image is divided into vertical segments and, based on the maximum occurrence of the n-bit pattern among these segments, the iris image is assigned an index value based on the segment number. Experiments on the CASIA v3 Iris Database indicate a 99.83% Hit Rate at a Penetration Rate of 17.23% for the proposed method.

Vandal and Savvides [99] discuss the architecture of a parallelized iris template matching implementation using inexpensive Graphics Processing Units to achieve matching rates of approximately 44 million iris image template comparisons per second. The utilization of a CUDA architecture facilitates the parallel implementation of iris template matching with embedded rotational

**Table 4**
Summary of iris feature extraction approaches.

| Authors | Database | Summary |
|---|---|---|
| Sunder and Ross [65] | Miles Research Database [66] | Investigate macro-features (moles, freckles, nevi, melanoma) as soft biometric traits. SIFT descriptor is used to represent the macro-features |
| Zhou and Kumar [67] | IITD v1 [93], CASIA v3 | LRT exploits the orientation information from the local features. Dominant orientation is used to generate feature representation. Similarity is computed using matching distances |
| Scotti and Piuri [68] | In-house collection | RST features are extracted. Inductive classifier segments iris |
| Hosseini et al. [69] | UBIRIS v1, UBIRIS v2, CASIA v1 [94] | Shape features are extracted from pigment melanin in visible light |
| Roy et al. [70] | UBIRIS v1, ICE 2005, WVU Non-ideal | Active contour model is deployed to segment non-ideal iris. A Modified Contribution-Selection Algorithm selects informative features without affecting recognition performance |
| Hollingsworth et al. [71] | In-house collection | Improve recognition by masking fragile bits. Fragile Bit Distance is established to measure coincidence of fragile bit patterns |
| Zhang et al. [73] | CASIA v4 | DAISY descriptors are extracted from iris. Iris key points are localized on feature map. Extracted key points are matched |
| Bastys et al. [74] | CASIA v2 [95], ICE v1, MBGC [96] | A fusion of multi-scale Taylor expansion phase information and its local extrema is proposed as a hybrid descriptor |
| Proença and Santos [75] | NICE v2 | Segment iris into coherent regions. Color and shape information is extracted. Perform fusion with prior state-of-the-art approaches |
| Kumar et al. [76] | UBIRIS v2, FRGC, CASIA v4 | Recognition of distantly acquired irises using LRT based orientation features. Iris is modeled as sparse coding solution based on computationally efficient LRT dictionary |
| Li and Wu [77] | UBIRIS v2, CASIA v3 | Iris boundaries and eyelids are localized. Log-Euclidean Co-variance Matrices are used to model correlation of spatial coordinates, intensities, 1st and 2nd-order image derivatives |
| Rahulkar and Holambe [78] | UBIRIS, CASIA v3, IITD Iris | Features are extracted based on Triplet Half-Band Filter Bank. Post-classifier system achieves robustness against intra-class iris variations |
| Zhang et al. [79] | CASIA v4, ICE 2005 | Propose Perturbation-enhanced Feature Correlation Filter for robust iris matching. Correlation filters are utilized for Gabor images matching |
| da Costa and Gonzaga [80] | In-house collection | Capture information about manner in which eye reacts to light. Allows the validation of attributes such as to check if input image being analyzed is from a living iris |
| Liu and Li [81] | UBIRIS v2, CASIA v4 | Normalized iris image is divided into patches, represented by SIFT descriptors. The low-dimensional features are encoded to binary codes. Matching is performed by counting binary codes in agreement |
| Kumar and Chan [82] | UBIRIS v2 | Hyper-complex sparse representation is used. Orientation of iris texture is extracted using dictionary of oriented atoms. Iris representation as quaternionic sparse coding problem is solved using convex optimization strategy |
| Zhang et al. [83] | UBIRIS v1, UBIRIS v2, NICE v2 | Color Texton is combined with pixel value in multiple color spaces. The image is represented by histogram of the learnt Texton vocabulary |
| Wang et al. [84] | CASIA v4 | Large margin loss function is adopted to learn robust model. Information from each feature is considered to remove noise. The model is solved using Simplex algorithm. |
| Nguyen et al. [85] | MBGC | Feature-level super-resolution in non-linear Gabor feature domain is performed. Compared to classic pixel-level super-resolution approaches |
| Zhang et al. [86] | CASIA v4, ICE 2005 | Extract key-point features from bandpass component of iris images. Extract ordinal features from lowpass component and perform match-score fusion |
| Sun et al. [87] | CASIA Iris Fake [88] | Hierarchical Visual Codebook integrates Vocabulary Tree and Locality-constrained Linear Coding. Adopts coarse-to-fine visual coding strategy |
| Nigam et al. [92] | CASIA v4 database & IITK Iris database. | Propose Relational Measure feature and local binary pattern descriptor applied in block-wise manner. Dissimilarity scores are fused at the score level |
| Sun et al. [89] | CASIA v4 | Perform ordinal feature selection; objective function considers misclassification error of intra-class and inter-class matches. Multi-lobe Ordinal Filter is proposed to analyze ordinal measures of images |
| Tan and Kumar [90] | UBIRIS v2, FRGC, CASIA v4 | Propose non-linear approach to capture local consistency of iris bits and overall quality of weight map for recognition. Zernike moment based phase encoding of iris features is deployed |
| Tan and Kumar [91] | UBIRIS v2, FRGC, CASIA v4 | Propose strategy for accurate iris recognition from distantly acquired images. Algorithm generates geometric key - set of coordinate-pairs assigned to each subject |

invariance. The authors observe that the computation performance gain achieved by the GPU implementation of the shift-invariant Hamming distance is less for larger template sizes, which is suggested to occur due to shared memory constraints reducing the number of gallery templates that can be processed by each system thread block. Experiments demonstrate that the proposed implementation is capable of achieving accelerations outperforming state-of-the-art uni-core CPUs by a factor of 14.

Proença [100] propose a method that follows the syntactical pattern recognition paradigm. Each pattern (iris template) is regarded as a set of simpler sub-patterns. A pattern is expressed by its primitives and by the relationships between them. Symbolic data structures are used for the pattern representation. A probe pattern is labeled as a match if its representation is isomorphic with a pattern stored in the gallery. Experiments are performed on the CASIA and UBIRIS datasets. The proposed approach performs almost as well as Daugman's approach on the high-quality images in the CASIA database; it outperforms Daugman's approach on the challenging UBIRIS dataset which consists of images taken in non-ideal conditions.

Irises have unique visual patterns and features that vary across regions. This leads to significant differences in the robustness and the distinctiveness among feature codes derived from different iris regions. To effectively utilize this distinct information, Dong et al. [101] propose a personalized iris matching strategy using a class-specific weight map learned from training images of the same iris class. The weight map reflects the robustness of an encoding algorithm on different iris regions by assigning an appropriate weight to each feature code for iris matching. Such a weight map, which is trained by sufficient iris templates, is convergent and robust against noise. Comprehensive experimental results performed on the CASIA-Iris v3 dataset, the UBath Iris dataset, and the ICE2005 database demonstrate that the proposed strategy is effective for iris matching and greatly improves the performance of iris recognition systems. The advantages of the personalized iris matching strategy are observed to be more significant for poor quality images.

Farouk [102] presents a new method for iris recognition based on Elastic Graph Matching (EGM) and Gabor wavelets. The circular Hough transform is used to determine iris boundaries. The segmented irises are represented as labeled graphs; nodes are labeled with jets and edges are labeled with distance vectors. An EGM based similarity function is defined to account for the similarities of individual jets and the relative distortion of the graphs. Experiments performed on the CASIA Iris v3-Interval and UBIRIS datasets show that the EGM based method is an effective technique for iris matching.

Gyaourova and Ross [103] present a novel approach for generating fixed-length codes to index biometric databases. The index code is constructed by computing match scores between a probe image and a fixed set of reference images. Candidate identities are retrieved based on the similarity between the index code of the probe image and those of the identities in the database. In order to present indexing results on a substantially large dataset, the authors assemble a chimeric multimodal dataset using the FERET face database and the WVU Fingerprint database [62]. Experiments suggest that the proposed method results in an average reduction of 84% in the search space at a hit rate of 100%. The authors suggest that index codes for multiple modalities may be fused to improve the accuracy of indexing.

Dey and Samanta [104] propose an efficient indexing mechanism to retrieve iris biometric templates using Gabor energy features. The Gabor energy features are calculated from the iris texture at different scales and orientations to generate an index key. An index space is created based on the values of index keys of all the subjects present in the gallery. A candidate set is retrieved from the index space based on the values of the query index key. The authors conduct experiments on the Bath dataset, the CASIA-Iris v3 database, the CASIA-Iris v4 dataset, the MMU2 database, and the WVU Iris database. Experiments substantiate that the proposed approach is capable of retrieving biometric data with a higher hit rate and lower penetration rate compared to contemporary approaches present in the literature.

Tsai et al. [105] propose a novel possibilistic fuzzy matching strategy, which provides a robust matching scheme for two sets of iris feature points. The proposed methodology provides an alternative feature extraction method to avoid unwrapping the iris texture pattern by extracting features from the iris image directly. A nonlinear normalization model is adopted to provide accurate positioning before matching. The authors also present an effective iris segmentation method to refine the detected inner and outer boundaries to smooth curves. The proposed matching algorithm, which is based on the possibilistic fuzzy matching method, compares a pair of feature points by considering not only their local features but also the relative positions to all the other points. Experiments performed on the CASIA-Iris v3 database yield a correct identification rate of 99.97%. For similar experiments performed on the UBIRIS v1 database, a correct identification rate of 97.19% is achieved.

Several algorithms have been established to effectively tackle the UBIRIS v2 dataset as part of the NICE II contest. Tan et al. [106] propose a method for visible light iris matching by using multiple characteristics of the iris and eye images. The method consists of preprocessing, iris data matching, eye data matching, and multimodal fusion of the information from the two regions. Ordinal measures and color analysis are used for matching iris data, and texton representation and semantic information are used for matching eye data. The four matching scores obtained from these descriptors are used in a robust score level fusion strategy to generate a dissimilarity measure of the images. Extensive experiments on the UBIRIS v2 database and the NICE v2 dataset demonstrate the efficacy of the proposed method. Wang et al. [107] present an iris recognition framework which is learned by applying AdaBoost on a 2D Gabor based feature set. Irises are segmented and normalized and divided into different patches according to the normalization applied. A feature set is constructed based on 2D-Gabor for the entire iris as well as its constituent patches. Finally, two mutually exclusive AdaBoost frameworks are learned for accurately and inaccurately segmented irises separately. Santos and Hoyle [108] explore a novel fusion of multiple recognition approaches. There are primarily two forms of recognition techniques proposed by the authors. In the first approach, wavelet based feature extraction methods are applied to the iris and complemented with a zero-crossing representation. In the second approach, LBP and SIFT features are extracted from the ocular region outside the iris. It is shown that the fusion of these features increases the robustness of the algorithm on degraded data.

Shin et al. [109] propose several steps for classifying noisy iris images. First, the proposed technique discriminates the eye as either left or right on the basis of eye-lash distribution and specular reflection. Second, the separability between the classes is increased by using color information. Third, a 1D Gabor filter is applied to individual color channels. The obtained Hamming distance scores are combined on the basis of the weighted sum rule to produce a final matching score. Li et al. [110] present a weighted co-occurrence phase histogram for representing the local characteristics of texture patterns in irises. A weighting function is introduced to enable the phase angle of the image gradient at a pixel to contribute smoothly to several adjacent histogram bins. The authors assert that this accounts for the uncertainty of the phase angle estimation caused due to noise and illumination changes. De Marisco et al. [111] propose a Noisy Iris Recognition Integrated Scheme. The algorithm combines two local feature extraction techniques, linear binary patterns and discriminable textons, which independently characterize relevant regions of the iris. The authors investigate possible adaptations of the individual approaches and combine the two methods using a weighted mean scheme at the score level. Li and Ma [112] present a robust algorithm based on Random Sample Consensus for localization of non-circular iris boundaries. The authors describe an image registration method based on the Lucas–Kanade algorithm. A sequential forward selection method is used to select a subset of Gabor filters. Experiments suggest that recognition performance is greatly improved even with a very small number of filters. Szewczyk et al. [113] propose a reverse biorthogonal wavelet transform based recognition system. The blue color channel is removed and the image is mono-chromaticized. Eyelid occlusions and reflections are removed. Eye-lashes are eliminated and the resulting iris is histogram equalized. A 324-bit template is obtained using reverse biorthogonal wavelets. It is compared using a similarity score to the samples in the gallery.

In case of unconstrained data acquisition, iris images are degraded and the match-score distributions are poorly separated. Proença [72] propose an indexing method for degraded iris images which operates at the iris code level, i.e., after the feature encoding process, making it compatible with different feature encoding strategies. Gallery iris codes are decomposed at multiple scales and based on the most reliable components at each scale, the position in an N-ary tree is determined. At the time of retrieval, the probe iris code is decomposed similarly, and the distances between multi-scale centroids are used to penalize paths in the tree. As a result, only a subset of the branches is traversed up to the last level. The main contributions of the proposed method are that it is compatible with multiple signature encoding methods, it outperforms the state-of-the-art approaches when poor quality data is used to test the system, and it has a reduced computational cost compared to traditional exhaustive searches. The CASIA-Iris v4 database is used to predict performance in scenarios that correspond to prevalent iris recognition systems. Experiments on the UBIRIS v2

database report that the proposed algorithm outperforms all other systems, which indicates promising results for unconstrained iris acquisition and indexing.

Liu et al. [114] propose a code-level scheme for matching low resolution and high resolution iris images. The statistical relationship between the binary code of a low resolution iris image and a binary code corresponding to the latent high resolution iris image is established based on an adapted Markov network. The Markov network also produces a weight mask which measures the reliability of each bit in the enhanced iris code. Experimental results on the Quality-Face/Iris Research Ensemble database [115] demonstrate that code-level information fusion performs significantly better than prior pixel-level, feature-level, and score-level approaches for recognition of low resolution iris images.

Tomeo-Reyes and Chandran [116] investigate the impact of fused decisions on an iris recognition system. The authors explore multi-part fusion schemes, multi-sample fusion schemes, and an integration of these two schemes. The effectiveness of the proposed architecture is evaluated under the effects of miosis and mydriasis. Experiments conducted on a dataset collected by the authors show that statistically significant robustness towards such obfuscation attacks is achievable using their proposed architecture.

Liu et al. [117] attempt to learn a distance metric to transform heterogenous iris matching results (low-resolution and high-resolution) towards homogeneous (high-resolution and high-resolution) results. The proposed learning procedure utilizes label and local information to create the mapping. Ideal pairwise similarities are defined on the training set. A Mahalanobis distance is learnt by minimizing the divergence between the matching results measured by the target Mahalanobis distance and the matching results defined ideally. Extensive experiments performed on the Multi-PIE dataset [118] show that the proposed method outperforms prior state-of-the-art metric learning methods.

The large-scale deployment of iris recognition systems around the world has prompted researchers to work towards efficient and cost effective template matching techniques. Table 5 presents a summary of these techniques. The advent of specialized memory systems also motivates the community to utilize these systems to optimize template retrieval rates with the growing need for such features in large-scale systems.

### 2.1.6. Covariates

Iris biometrics has witnessed a significant diversification in the attempts to solve the problem of recognition in unconstrained environments (Fig. 6). Apart from studying iris recognition in the ideal scenario, biometrics community is actively pursuing problems such as the recognition of iris images which may not be orthogonal to the plane of signal acquisition. The problem of template spoofing has been explored for several different scenarios, with emphasis on the effect of contact lenses. The possibility of iris template aging has been studied. A few attempts have also been made to study cross-spectral iris recognition and cross-sensor iris recognition. This sub-section exhaustively summarizes the above-mentioned *iris covariates*. Table 6 also provides a concise summary of these covariates.

*2.1.6.1. Off-angle iris recognition.* Off-angle iris recognition refers to matching rotated iris images that are captured when iris and camera are not orthogonal. For example, such images are encountered when the face and iris acquisition sensor are significantly out of plane with respect to each other.

Chou et al. [121] propose a solution to the non-orthogonal view assumption (NOVA) iris recognition problem. The authors develop a custom camera to acquire four-spectral iris images to increase the robustness of the segmentation results. A circle rectification process is introduced to convert a non-orthogonal iris image into an approximately orthogonal iris image. The paper proposes an edge-type iris descriptor which characterizes an iris pattern with multi-scale edge-type maps, which are matched using an ensemble of weak classifiers. The equal error rate for the proposed system for iris images acquired at off-axis angles ranging from $-30^\circ$ to $+30^\circ$ is 0.04%. However, the high computation time required for processing 4-channel images, custom set-up required for acquisition, and the non-consideration of eye shadows presents several challenges to NOVA recognition.

Abhyankar and Schuckers [122] present a Biorthogonal Wavelet Network (BWN) based method to perform non-ideal iris recognition. A BWN is developed and trained for each class, where the non-ideal factors are adjusted by repositioning the BWN. The wavelet representation comprises of 10,080 bits, which is comparable to Daugman's algorithm which uses 9600 bits. Comprehensive experiments are performed on the CASIA, Bath, Clarkson, MAE, WVU, and VIIT datasets. Along with real data, synthetic iris images are generated by using affine and geometric transforms. Tests are carried out on experimentally collected off-angle data and synthetically generated data. Iris images that are off-angle by up to $42^\circ$ for synthetic data and by up to $45^\circ$ for experimental data are successfully recognized. The authors assert that the proposed method does not require knowledge of the angular orientation and may be used to account for other non-ideal conditions such as noise and rotation.

Santos-Villalobos et al. [123] propose a novel eye model and a method to reconstruct the off-angle eye to its frontal view. The focus of the paper is to allow existing biometric techniques to employ the proposed algorithm as a pre-processor to improve performance of existing recognition techniques. An anatomically accurate eye model and ray-tracing techniques are used to compute a transformation function, which reconstructs the off-angle iris to its frontal state. The authors study the *limbus effect*, which is used to aid the development of the Oak Ridge National Laboratory (ORNL) eye model and synthetic data is used to validate the efficacy of the proposed biological model.

Li et al. [124] propose a feature-level solution to off-angle iris recognition. Geometric features of corneal reflections are used to classify iris images into five classes according to the off-angle orientation of the iris. A linear programming based feature learning method is used to select the most effective ordinal features for each iris category. The off-angle iris image is recognized using the ordinal feature template belonging to the corresponding iris category. Experimental results indicate that the proposed solution significantly outperforms other methods based on off-angle iris recognition. An equal error rate of 2.41% is achieved on a subset of the Q-FIRE database.

*2.1.6.2. Iris recognition in spoofing scenarios.* Baker et al. [125] study iris recognition performance in the presence of contact lenses. Several systems are used to evaluate the recognition performance on the dataset collected by the authors for this study. The VeriEye system is reported to perform better than other recognition systems. Matches involving images of soft contact lenses with letter indicators or ill-fitting artifacts achieve a false reject rate about eighteen times that of matches between images with no contact lenses. Gas-permeable contact lenses cause a 50-fold increase in the false reject rate on the VeriEye system. The authors suggest that this degradation is primarily due to the distortion from the displacement of the lens for the acquired images. It is observed that intra-session images of a subject wearing cosmetic lenses results in true accepts, whereas inter-session images do not match well. These results indicate the importance of developing techniques to detect and mitigate the contact lens effect.

Venugopalan and Savvides [126] explore methods to generate alternate iris texture patterns for a subject to bypass a recognition

**Table 5**
Summary of iris matching and retrieval algorithms.

| Authors | Database | Summary |
|---|---|---|
| Rathgeb et al. [97] | CASIA v3 | Reorder bits, and dynamically reject high Hamming Distance score candidates |
| Gadde et al. [98] | CASIA v3 | Normalized image is divided into vertical segments. Based on occurrence of N-bit pattern among segments, iris is assigned index value based on segment number using Burrows-Wheeler Transform |
| Vandal and Savvides [99] | Not mentioned. | Parallel implementation of template matching with embedded rotational invariance on CUDA architecture is proposed |
| Proença [100] | CASIA, ICE, UBIRIS | Iris is regarded as a pattern, which is a set of simpler sub-patterns. Match occurs if pattern representation is isomorphic with a pattern stored in gallery |
| Dong et al. [101] | CASIA v3, UBath Iris [119], ICE2005 | Personalized iris matching strategy using class-specific weight map is learned from training images of an iris class. Appropriate weight is assigned to each feature code for matching |
| Farouk [102] | CASIA v3, UBIRIS | Circular Hough transform is used for segmentation. Elastic Graph Matching based similarity function is used to perform recognition |
| Gyaourova and Ross [103] | FERET [120], WVU Fingerprint [62] | Generate fixed-length codes. Index code is constructed by computing match scores between probe and a set of reference images. Candidate identities are retrieved based on the similarity between index codes |
| Dey and Samanta [104] | UBath, CASIA v3, CASIA v4, MMU2, WVU Iris | Gabor energy features are calculated from iris texture at different scales and orientations to generate index key. Index space is created based on values of index keys of all gallery subjects |
| Tsai et al. [105] | CASIA v3, UBIRIS v1 | Non-linear normalization model provides accurate iris positioning. Segmentation method refines detected inner and outer boundaries to smooth curves |
| Tan et al. [106] | UBIRIS v2 | Ordinal measures, color analysis are adopted for iris matching. Textons, semantic information are used for eye matching. Matching scores obtained are used for score-level fusion |
| Wang et al. [107] | UBIRIS v2 | Iris is segmented and normalized. Features are constructed based on 2D-Gabor transform. Two independent AdaBoost frameworks are learned for accurately and non-accurately segmented irises |
| Santos and Hoyle [108] | UBIRIS v2 | Wavelet based features are extracted from iris. Local descriptors are extracted from periocular region. Logistic regression is applied to outputs of the two approaches |
| Shin et al. [109] | UBIRIS v2 | Identify eye as "left or right". Separability between classes is increased.1D Gabor filter is applied to individual color channels. Hamming distance scores are combined using weighted sum rule |
| Li et al. [110] | UBIRIS v2 | Weighted Co-occurrence Phase Histogram represents local characteristics of texture patterns. Weighting function allows every pixel's phase angle to affect several histogram bins |
| De Marisco et al. [111] | UBIRIS v2 | Combines two local feature descriptors, Linear Binary Patterns, and discriminable textons. Individual methods are combined using weighted mean scheme at score level |
| Li and Ma [112] | UBIRIS v2 | Random Sample Consensus is used for localization of iris boundaries. Image registration method is applied. A subset of Gabor filters is used to enhance output |
| Szewczyk et al. [113] | UBIRIS v2 | Image is preprocessed and occluding artifacts are eliminated. 324-bit template is obtained using reverse biorthogonal wavelet. Similarity score is used for matching |
| Proença [72] | UBIRIS v2, CASIA v4 | Gallery iris codes are decomposed at multiple scales. Position in N-ary tree is determined. Distances between multi-scale centroids is used to penalize paths in tree for matching |
| Liu et al. [114] | Q-FIRE [115] | Statistical relationship between binary code of LR iris image and binary code of latent HR iris image is established based on a Markov network |
| Tomeo-Reyes and Chandran [116] | In-house collection | Explore multi-part fusion schemes, multi-sample fusion schemes, and integration of these two schemes. Effectiveness is evaluated under miosis and mydriasis |
| Liu et al. [117] | Multi-PIE [118] | Ideal pairwise similarities are defined on training set. Mahalanobis distance is learnt by minimizing divergence between matching results and ideal results |

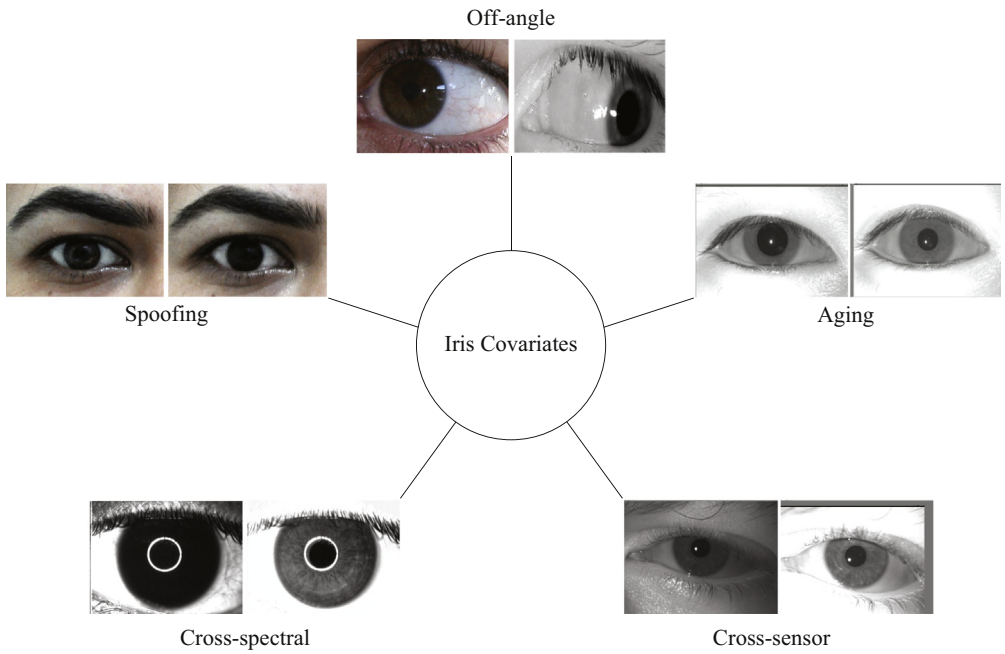


**Fig. 6.** Some covariates in iris biometrics.

**Table 6**
Summary of iris covariates' research.

| Category | Authors | Database | Summary |
|---|---|---|---|
| Off-Angle | Chou et al. [121] | UBIRIS v5, CASIA v3 | Circle rectification converts non-orthogonal iris to approximately orthogonal. Edge-type multi-scale maps characterize iris pattern. Matching is performed using an ensemble of weak classifiers |
| | Abhyankar and Schuckers [122] | CASIA, Bath, Clarkson [146], MAE and VIIT, WVU | Biorthogonal Wavelet Networks (BWN) are trained. Non-ideal factors are adjusted by repositioning BWN. Synthetic irises are generated. Tests are performed on real and synthetic data |
| | Santos-Villalobos et al. [123] | In-house collection | Human eye model and ray-tracing techniques are used to compute transformation function that reconstructs the off-angle iris to its frontal, non-refracted state |
| | Li et al. [124] | Q-FIRE | Predict orientation of the iris and apply orientation-specific template for preprocessing to perform classification |
| Spoofing | Baker et al. [125] | In-house collection | Study effect of soft lenses and gas-permeable lenses towards degradation of recognition performance. Use commercial off-the-shelf recognition systems |
| | Venugopalan and Savvides [126] | ICE 2005 | Attempt to bypass recognition system by generating alternate iris texture patterns. Discriminatory features are identified in the spoofed iris and embedded into the spoofing iris' texture |
| | Arora et al. [127] | IIITD Iris Alcohol [127] | Investigate effect of alcohol consumption. The pre-consumption and post-consumption overlap between genuine and impostor match scores increases by approximately 20% |
| | Yadav et al. [129] | IIITD CLI [128], ND-Contact Lens [147] | Investigate the role of contact lenses in obfuscation of iris texture and analyze the effect of contact lenses on the performance of iris recognition |
| | Gupta et al. [130] | IIITD Iris Spoofing [130] | Investigate iris recognition with respect to print spoofing attacks. Plausibility of identity obfuscation and identity impersonation is established |
| | Komulainen et al. [131] | Notre Dame Contact Lens Detection dataset | Address unseen lens patterns present in iris recognition. Introduce Binarized Statistical Image Features to capture difference in textural information between images |
| Unconstrained | Pillai et al. [133] | ICE2005, ND-IRIS-0405, MBGC | Propose quality measure that handles segmentation errors and alignment variations. Treats different regions separately and combines results depending on the quality of the region |
| | Huang et al. [134] | In-house collection | Algorithm is proposed for segmentation that can handle variable resolutions, illumination, and occlusion |
| Template Aging | Rankin et al. [136] | In-house collection | Investigate change in irides with time. Feature extraction is performed using 1D log-Gabor filter. Obtain information by decomposition of iris into complex-valued phase coefficients |
| | Fenker and Bowyer [135] | In-house collection | Iris template aging study over a time-lapse of 2 years. Investigates degree to which template aging effect is related to pupil dilation and contact lenses |
| | Fenker et al. [137] | In-house collection | Investigate factors which contribute towards template aging. Report change in pupil dilation, changes to enrollment and matching as significant factors |
| | Mehrotra et al. [139] | ND-Iris-Template-Aging-2008–2010 [148], ND TimeLapse-Iris 2012 [149] | Study whether fall in iris recognition performance occurs due to age or covariates such as poor acquisition, presence of occlusion, noise, and blur |
| | Bergmüller et al. [138] | In-house collection | Study aging effects developed in digital image sensors over time. Propose method to investigate sensor aging by simulative ageing of iris images |
| Cross-Spectral | Zuo et al. [140] | WVU Multispectral [150] | Non-linear adaptive model is proposed to use visible range iris to predict value of corresponding NIR iris. Predicted value is compared with real NIR iris using log-Gabor filter |
| | Gong et al. [141] | In-house collection | Most suitable wavelength for iris recognition is found based on amount of available texture information and matching performance |
| Cross-Sensor | Connaughton et al. [23] | In-house collection | Use three commercial iris sensors and three iris matching systems to investigate impact of cross-sensor matching on system performance in comparison to single-sensor performance |
| | Arora et al. [142] | IIITD Multi-Sensor [142], Notre Dame Cross Sensor [151] | Features are extracted and classification model for iris sensor is applied. Used to classify probe into a camera class. Selective enhancement algorithm is applied for respective sensor models |
| | Xiao et al. [143] | Notre Dame Cross Sensor [151] | Objective function minimizes misclassification error and achieves sparsity in coupled feature spaces. Employs regularization model based on half-quadratic optimization |
| | Pillai et al. [144] | ND Iris Dataset [145] | Propose framework to learn transformations on iris biometrics. Framework is applied to reduce distance between intra-class samples and increase distance between inter-class samples |

system based on the iris bit code. A framework is developed which, given a subjects iris code, can modify another subjects iris texture to resemble the former. Features are identified in the former subject's iris texture that discriminate it from the other iris. This discriminating information is embedded into the other person's iris texture. This ensures that the iris feature extraction module authenticates the hybrid pattern. The authors assert that spoof texture patterns generated by the proposed scheme generate the

same score response as that of the original iris. However, this approach assumes that the feature extraction mechanism of the iris matching scheme is known. Experiments performed on the ICE 2005 database confirm the efficacy of the proposed algorithm.

Arora et al. [127] investigate *alcohol consumption* as a covariate of iris recognition. The extent of change in iris images due to deformation caused by dilation or constriction of the pupil is dynamic and varies from person to person. The experiments performed on the IIITD Iris Under Alcohol Influence (IUAI) database indicate that if pre-consumption and post-consumption images are matched, the overlap between genuine and impostor match score distributions increases by approximately 20%. These results suggest that about one in five subjects under alcohol influence may be able to evade iris matching. Hence, iris recognition of a person under influence of alcohol can be viewed as a form of attack on the integrity of a biometric system.

Kohli et al. [128] investigate the role of contact lenses in obfuscation of iris texture and analyze the effect of contact lenses on the performance of iris recognition using the IIITD CLI database, which consists of images captured without lens, with transparent (prescription) lens, and with color cosmetic lens. The work presents an in-depth analysis of the effect of contact lenses on iris recognition performance. The results computed using VeriEye suggest that color cosmetic lenses significantly increase the false rejection at a fixed false acceptance rate. The authors also compare the performance of existing lens detection algorithms across different lens types and iris sensors. Yadav et al. [129] expand upon the preliminary investigation into the role of the presence of contact lenses, particularly textured cosmetic lenses, as they pose a challenge towards iris recognition due to obfuscation of the natural iris patterns. At a false match rate of 1 in 1 million, textured contact lenses can cause the false non-match rate to exceed 90%. Two databases, the IIITD Iris Contact Lens database and the ND-Contact Lens database, are employed to analyze the variations caused due to contact lenses. The authors also present a novel lens detection algorithm that can be used to reduce the effect of contact lenses. The proposed approach outperforms other lens detection algorithms on the two databases and shows improved iris recognition performance.

Gupta et al. [130] investigate iris recognition with respect to print spoofing attacks. A print attack in iris recognition is as an attack where the iris image is printed on a paper and scanned, or a photo is captured using an iris scanner. This image is used by an impostor to attack the iris recognition system. The authors study print attacks with contact lens variations as the spoofing mechanism. Experimental results on the IIITD Iris Spoofing database show that print attacks and contact lenses, individually and in conjunction, can significantly affect inter-personal and intra-personal distributions. It is observed that identity obfuscation is very easy with contact lenses and print attacks. The plausibility of identity impersonation is also established. The authors suggest that image descriptors such as LBP and HOG, if used together for the classification approach, are a cost effective solution to iris spoofing.

Komulainen et al. [131] study the issue of addressing unseen lens patterns while detecting contact lenses in iris recognition. The authors study the effect of preprocessing techniques and introduce a novel approach for contact lens detection using Binarized Statistical Image Features (BSIF) to capture the difference in textural information between iris image samples. Extensive experimental analysis on the Notre Dame Contact Lens Detection dataset [132] shows that the BSIF description extracted from preprocessed Cartesian iris texture images provides promising generalization capabilities across unseen texture patterns and multiple iris sensors.

*2.1.6.3. Unconstrained iris recognition.* Pillai et al. [133] propose a unified framework based on random projections and sparse representations for selection and recognition of iris images, which simultaneously addresses the problems associated with unconstrained acquisition, robust matching, and privacy enhancement. The proposed Sparsity Concentration Index quality measure handles segmentation errors and alignment variations for recognition using iris image videos. The proposed recognition algorithm treats different regions separately and combines the results depending on the quality of the region. The computational complexity of recognition is greatly reduced as matching of the different regions can be performed in parallel. Experiments performed on the ICE 2005 dataset, the Notre Dame ND-IRIS-0405 dataset, and videos from the MBGC database indicate that the selection algorithm can handle common distortions in iris image acquisition like blur, occlusions, and segmentation errors. The paper introduces a quality based matching score, which outperforms existing fusion schemes as demonstrated on the MBGC iris video dataset.

Huang et al. [134] propose a novel algorithm towards robust iris recognition in less intrusive environments. The proposed algorithm introduces a novel iris segmentation method that can handle variable resolutions, variable illumination, and partial occlusion, and a new feature encoding method that robustly treats non-ideal iris images. The study suggests that image noise reduces accuracy in low resolution images. The authors observe that the proposed algorithm applied on low noise high-quality images, acquired using a Digital Single-Lens Reflex camera, achieves state-of-the-art performance on very low resolution images.

*2.1.6.4. Iris recognition in presence of template-aging.* Fenker and Bowyer [135] report a template aging study on a dataset of 43 subjects collected over 2 years. The authors also explore the degree to which template aging may be related to pupil dilation and contact lenses. The VeriEye and IrisBEE commercial systems are used to evaluate recognition performance. Experiments are performed on a dataset collected by the authors. The authors report that the template aging effect does exist. Factors such as difference in pupil dilation between images and presence of contact lenses are considered while evaluating the results of the study.

Rankin et al. [136] perform a study of high resolution irides to investigate the degree of change that occurs in irides with time. The authors capture iris data in intervals of 3 months and 6 months using a specialized bio-microscope. Iris feature extraction is performed using a 1D log Gabor filter applied to each row of the normalized iris pattern to obtain information by decomposition of the iris image into complex-valued phase coefficients. The experiments measure failure rates resulting from the application of local and non-local feature extraction techniques. The minimum reported failure rate for local descriptor comparison is 20.3%, and 13.8% for non-local descriptor comparisons.

Fenker et al. [137] study the effects associated with template aging in iris recognition. Iris images acquired from 2008 through 2011 using an LG 4000 sensor are used for the experiment. Experimental results from the three-year time-lapse dataset suggest that the False Non-Match Rate increases by 150% at a decision threshold representing one in two million false matches. The authors report that there are several factors which contribute towards template aging such as age-related changes in pupil dilation and changes in enrollment and matching schemes.

Mehrotra et al. [139] try to determine whether the shift in genuine scores as reported in the above results can truly be attributed to aging. Experiments are performed on the ND-Iris-Template-Aging and ND-TimeLapse Iris datasets using VeriEye, a commercial iris matcher. Experiments suggest that the increase in false rejection is due to covariates such as poor acquisition, presence of occlusion, noise, and blur. The quality values of the falsely rejected gallery-probe pairs indicate that the quality of iris images taken from two independent sessions are different in comparison to the genuinely accepted pairs. Thus, even though results from the prior studies

are correct in reporting an increase in false rejection over time, the authors assert that this drop in matching performance is primarily due to the presence of covariates, and not due to the aging of the iris texture of the subjects. Bergmüller [138] study the aging effects developed in digital image sensors over time. The authors introduce a pixel model to study the effect, and an aging algorithm to create the test database. The simulation parameters are estimated from the aging effects observed of an iris scanner over a timespan of 4 years. Experimental results show that defects related to the sensor affect the recognition rate of an iris recognition system.

*2.1.6.5. Cross-spectral iris recognition.* Zuo et al. [140] introduce an adaptive method to create NIR channel images from color iris images. A non-linear adaptive model is proposed which uses visible range iris images to predict the value of the corresponding NIR channel iris image. The predicted value of the NIR channel is compared with real NIR iris images using the classical log-Gabor filter algorithm. Due to the predictive nature of the neighborhood based model, the predicted NIR image is observed to become over-smoothed compared to the original NIR image. Experiments demonstrate that a well designed predictive mapping, which is used to map a color image into a predicted NIR image is a promising approach to improve cross spectral iris recognition.

Gong et al. [141] investigate the existence of the most suitable wavelength band for heavily pigmented iris recognition. A multispectral acquisition system is designed for imaging the iris at narrow spectral bands in the range of 420–940 nm. The most suitable wavelength for the recognition of heavily pigmented iris is found based on the amount of available texture information as well as the matching performance. Such analysis is required to understand the texture from the structure and melanin of the iris that is revealed across all wavelengths from 400 nm to 940 nm. This work explores the possibility of finding a band of the electromagnetic spectrum, in which more texture can be extracted from heavily pigmented irises, beyond the wavelengths higher than 850 nm. Experimental results suggest that 700 nm is the most suitable wavelength for heavily pigmented iris recognition.

*2.1.6.6. Cross-sensor iris recognition.* Connaughton et al. [23] showcase the issue of interoperability between iris sensors in large-scale and long-term applications of iris biometric systems. The authors use three commercial sensors and three matching systems to explore the impact of cross-sensor matching on system performance in comparison to single-sensor performance. The study investigates the impact of several external factors on sensor performance, including environmental conditions, order of the sensors, and pupil dilation.

Arora et al. [142] address the increasing importance of sensor interoperability for iris recognition. The authors propose a pre-processing framework for iris sensor classification to address iris sensor interoperability. The framework involves extraction of features and learning of a classification model for iris sensor classification. The training model is used to classify the probe image into one of the iris camera classes. Selective enhancement algorithms are applied for respective sensor models, and the pre-processed image is provided to the recognition algorithm. Two commercial off-the-shelf recognition algorithms are used to study the effect of the image enhancement techniques applied. Experimental results on the IIITD Multi-Sensor Iris database and the Notre Dame Cross Sensor database present a significant improvement in cross-sensor iris recognition accuracy using the proposed approach.

Xiao et al. [143] propose a novel optimization model of coupled feature selection for cross-sensor iris recognition. The objective function of the proposed model minimizes misclassification error and achieves sparsity in coupled feature spaces. This is achieved by employing a novel $l_{2,1}$ regularization model and an efficient algorithm based on half-quadratic optimization. Experimental results on the Notre Dame Cross Sensor Iris Database and an in-house Cross Sensor database show that features selected by the proposed method perform better than those selected by conventional single-space feature selection methods such as Boosting and regularization methods.

Pillai et al. [144] propose a machine learning technique to mitigate the problem of cross-sensor performance degradation by adapting the iris samples from one sensor to another. A novel optimization framework for learning transformations on iris biometrics is developed. The framework is applied to iris samples to reduce the distance between samples of the same class, and increase the distance between samples of different classes. This is achieved by constraining samples from different sensors to behave in a similar manner in the transformed domain. The learned transformations are represented using kernel functions. Extensive experiments performed on iris data acquired from multiple sensors [145] demonstrate that the proposed method improves the cross-sensor recognition accuracy. The authors assert that the proposed solution leads to considerable improvement in cross-sensor matching. The algorithm is robust to alignment errors and is capable of handling real-valued feature representations.

*2.1.7. Other iris recognition techniques*

Boddeti and Kumar [152] challenge the limits of the operational range of iris acquisition systems using phase modulation masks. The authors investigate the feasibility of using unrestored wavefront coded images for recognition as it reduces the computational cost associated with image restoration. A custom phase mask is designed by formulating an optimization problem for iris segmentation and matching. Experiments are performed on images taken from the ICE database using a simulated wavefront coded imagery to study the results of Daugman's IrisCode algorithm as well as correlation-filter based iris recognition. The authors claim to achieve a practical trade-off between accuracy and depth-of-field: a slight degradation of accuracy results in an increase of the depth of the field by a factor of approximately four.

In human performance evaluation on iris images, Stark et al. [153] report results where subjects browse a set of 100 iris images and group them based on similarity of overall texture appearance. Five major iris texture categories and a natural categorization of iris images into a small number of high-level categories are identified, which reflect the ethnicity of the subject. The iris texture categorization has potential application in creating indexing algorithms to boost search for query templates in iris databases as well as towards determining soft biometric traits of subjects.

Nguyen et al. [154] propose a signal-level fusion approach which incorporates the quality score into a super-resolution based iris recognition system. A novel approach for assessing the focus level of the iris image is introduced. The score from focus of the iris is combined with several other quality factors using the Dempster–Shafer theory to produce one unified quality score. Experiments conducted on the MBGC dataset show that the proposed approach outperforms state-of-the-art signal-level and score-level fusion approaches for recognition of less constrained irises. The fusion technique takes advantage of multiple frames instead of simply selecting the best quality frame.

Hollingsworth et al. [155] report on the similarity in the left and right irises of individuals and in the irises of identical twins. It is established that comparisons between left and right irises are statistically indistinguishable from comparisons of unrelated peoples irises. The authors investigate how human observers view the overall iris texture pattern. It is reported that even though iris recognition systems observe no similarities in genetically identical irises based on the texture details, human observers are able to

detect similarities in genetically identical irises. The study suggests that the examination of pairs of iris images by humans for forensic purposes may be feasible.

Si et al. [156] propose several approaches to improve the overall performance of iris recognition systems. The authors propose a novel eyelash detection algorithm based on directional filters, which achieves a low rate of eyelash misclassification. A multi-scale multi-direction data fusion method is introduced to reduce the edge effect of wavelet transformation produced during iris segmentation. An iris indexing method based on corner detection is also proposed to accelerate matching. Two dimensional filtering is applied to iris features as it captures directional information which is proposed to contain discriminatory information. Experiments performed on the IITD v1 Iris database and CASIA-Iris v1 database suggest that the proposed methods are more robust, accurate and rapid compared with the present iris recognition algorithms.

Kong [157] present an algorithm to perform decompression of IrisCode by exploiting the graph composed of the bit pairs present in IrisCode and prior knowledge from iris image databases. In order to remove artifacts, two post-processing techniques in the Fourier domain are developed to remove interference and compression artifacts. Decompressed iris images obtained from the WVU Iris database and the UBIRIS v1 database are used to examine the proposed algorithms. Experimental results show that the decompressed iris images retain texture and the quality of the images is observed to be roughly equivalent to a JPEG quality factor of 10. Further, iris recognition methods match the original and decompressed images. The author asserts that if an attacker obtains the original IrisCodes and the Gabor filter parameters, the corresponding iris images can be compromised.

Rathgeb et al. [158] present a new strategy for comparing binary biometric templates. An improved iris-biometric comparator is proposed, which utilizes the comparison scores estimated at the time of template alignment in the training set. The proposed iris-biometric comparator fits comparison scores to an algorithm-dependent Gaussian function. For authentication, the scores are fitted onto the Gaussian and the normalized fitting score is fused with the minimal Hamming distance. Experiments are carried out for different iris biometric feature extraction methods achieving significant improvements in recognition accuracy on the CASIA-Iris v3 database.

Galbally et al. [159] propose a novel probabilistic approach to reconstruct iris images from binary templates. The reconstruction is performed by employing a genetic algorithm to optimize the similarity between a given iris template and the iris template which is being reconstructed. The authors also analyze the similarity between the reconstructed synthetic iris image and the original iris. The BioSecure Multimodal Database is used to verify the efficacy of the proposed method. Experimental results indicate that the reconstructed images are accurate enough to successfully deceive a commercial matching system. The authors claim that the possibility of reconstructing reasonably accurate irises using their proposed method poses a challenge to the security of iris biometric systems.

Sgroi et al. [160] present the results of an initial study to predict the relative age of a person from their iris images. The authors conclude that such classification is possible at levels of accuracy significantly greater than random chance. The texture features and classifier ensembles used are similar to those used by previous researchers for the prediction of gender and ethnicity from iris texture images. Experiments performed on a dataset collected for the purpose of the study show that iris texture can be used to classify subjects by age range at an accuracy of 64%.

McGinn et al. [161] investigate the ability of human examiners to determine if two iris images belong to the same person. The authors collect a dataset from 93 subjects using a LG 4000 infrared sensor. Human examiners perform matching with an average accuracy of approximately 91%. The level of accuracy increases to 96% when examiners are confident regarding their decision. It is reported that a majority of the incorrectly categorized image pairs belong to twins. The most frequently misclassified authentic pairs exhibit significant differences in pupil dilation between the two images. The results also suggest that a fusion of human interpreters and automated iris recognition may be able to boost the overall recognition performance.

#### 2.1.8. Current research directions in iris recognition

Section 2.1 exhaustively discusses the direction taken by biometrics researchers in iris recognition. The results reported in literature suggest that iris recognition in Near Infrared spectrum in controlled environments has been solved to a large extent. To advance the state-of-the-art, the research trends suggest that iris recognition is likely to be moving along the following directions in the future:

1. *Iris recognition at a distance*: Iris recognition has been extensively explored for constrained acquisition distances. Iris recognition in conjunction with the periocular modality holds potential for unconstrained recognition at a distance. The development of iris recognition at a distance would allow application of the modality in surveillance scenarios as well.
2. *Robust cross-spectral recognition*: While NIR iris recognition continues to form the basis of a majority of commercial iris recognition systems, there have been significant advancements in the research on iris recognition in visible spectrum. The development of robust cross-spectral systems is a research direction that holds significant practical value for real-world iris recognition systems.
3. *Iris recognition on mobile platforms*: The technological shift towards mobile platforms has resulted in an increasing number of identity-sensitive applications becoming prevalent on mobile devices. This trend has resulted in the need for enhanced security measures on such devices. Iris recognition on mobile platforms is an area of research that requires attention from academic as well as industrial researchers.
4. *Anti-spoofing measures*: As the reliability and acceptability of real-world iris recognition increases, a parallel need for strong anti-spoofing measures arises. The acquisition of iris biometric deviates from expected behavior in the presence of temporary agents such as eye-medicine and contact lenses, or due to permanent deviations introduced by eye diseases or cataract surgery. The performance of iris recognition systems in such cases is an important area of study, especially in the deployment of large scale public systems such as the Aadhar system in India.

### 2.2. Periocular

Unconstrained environments involving noise, non-cooperative subjects, occlusion, and other non-ideal scenarios call for exploring other ocular modalities which show reliable performance in real-world scenarios. In 2009, Park et al. [5] proposed *periocular* as a novel biometric trait. The periocular region is defined as the part of the face surrounding the eyes. This principal investigation, performed in the visible spectrum, studied the efficacy of the trait using global as well as local descriptors. The results of the study have motivated the research community to actively explore the periocular biometrics in diverse scenarios.

While periocular recognition has been established as an independent biometric modality, it has also been used in conjunction with face and iris biometrics. Several applications have been proposed for exploiting the information present in the periocular

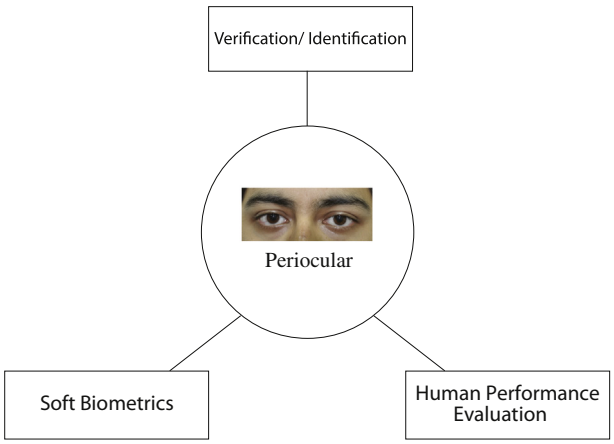


**Fig. 7.** Areas of study in Periocular biometrics.

region. Periocular features have also been used to determine gender, age, and ethnicity of subjects. Periocular recognition has also been deployed to supplement iris recognition, and in some cases, as a standalone modality when iris recognition fails. The remainder of this section is organized as illustrated in Fig. 7. Section 2.2.1 covers periocular verification and identification techniques. Section 2.2.2 summarizes research in the area of estimating gender, age, and ethnicity using periocular features. Section 2.2.3 surveys human performance studies for periocular information interpretation. Table 7 presents a summary of these periocular recognition studies.

### 2.2.1. Verification and identification using periocular region

The preliminary study by Park et al. [5] was followed by an exhaustive study of the periocular modality in [162]. The effects of various factors, including segmentation schemes, facial expression, and the discriminative information present in eyebrows were studied on the FRGC dataset. Comparison of periocular recognition

**Table 7**
Summary of periocular recognition.

| Category | Authors | Database | Summary |
|---|---|---|---|
| Recognition | Park et al. [5] | In-house collection | Proposed periocular biometric trait. HOG, LBP, SIFT features are extracted. LBP and SIFT are fused to achieve optimal recognition |
| | Park et al. [162] | FRGC v2 | Effect of pose variation, occlusion, template aging is studied. Score-level fusion of left and right periocular region using SIFT, HOG, LBP is applied |
| | Bharadwaj et al. [163] | UBIRIS v2 | GIST, circular LBP features for periocular recognition in visible spectrum are proposed. Normalized score-level fusion applied. Weighted sum-rule score fusion applied to left and right periocular regions |
| | Xu et al. [164] | FRGC | For verification, LW-T Binary Pattern is fused with Kernel Correlation Feature Analysis. Recognition using fusion of Discrete Wavelet Transform and LBP |
| | Woodard et al. [165] | FRGC v2, MBGC | LBP captures texture and color histograms are extracted followed by score-level fusion. Information from left and right periocular regions is fused at score-level |
| | Miller et al. [166] | FRGC | Study effect of illumination & resolution change, blurring. Highest performance degradation observed for blurring. Study conducted across sessions |
| | Miller et al. [167] | FRGC, FERET | Demonstrate performance of LBP. Suggest that skin texture, eye folds, periocular contours adequate for verification |
| | Adams et al. [168] | FRGC, FERET | Present genetic based Type II feature extraction for LBP. Feature optimization achieved and significant improvement in recognition accuracy reported |
| | Woodard et al. [169] | FRGC, MBGC | Score-level fusion of periocular skin texture (LBP) and color (histograms) information. Establishes that periocular appearance is unique for each eye |
| | Padole and Proença [170] | UBIPr | Studies performance variation for scale, pose, occlusion, pigmentation variation. Non-linear score-level fusion applied to LBP, SIFT, HOG descriptors |
| | Juefei-Xu and Savvides [171] | Compass [171] | Present periocular acquisition system using PTZ camera. Walsh-Hadamard transform encoded local binary pattern applied to extract information |
| | Padole and Proença [172] | UBIPosePr [172] | Non-ideal recognition: illumination variation using homomorphic filters and Self-Quotient images; pose change through geometric transformations |
| | Proença and Briceño [173] | FaceExpressUBI [173] | Study effectiveness of Globally Coherent Elastic Graph Matching to compensate distortions due to expressions |
| | Juefei-Xu and Savvides [174] | FRGC v2 | Apply subspace representations on Discrete Transform encoded LBP. Periocular performance is at par with face recognition. Gains tolerance to occlusion |
| | Sharma et al. [175] | IMP [175] | Neural networks train classifiers on cross-spectral images using Pyramid of HOG. Score-level sum rule fusion applied to NIR left and right eye images |
| | Mahalingam et al. [176] | HRT Transgender Dataset [177] | Study impact of hormone manipulation and its ability to disguise the face. Periocular using texture based matchers outperforms matching against the full face |
| | Proença et al. [178] | UBIRIS v2 | Posterior probability for each pixel of periocular region found. Appearance based information fused to geometrical constraints and shape priors to feed a two-layered MRF |
| Soft Biometrics | Juefei-Xu et al. [179] | FG-NET | Images are pre-processed. Walsh-Hadamard local binary pattern features with Unsupervised Discriminant Projection subspace modeling are extracted |
| | Lyle et al. [180] | FRGC | Grayscale intensities, LBP are extracted to predict gender, ethnicity. Scores fused with LBP features of periocular, face region for person recognition |
| | Lyle et al. [181] | FRGC, FERET | LBP, HOG, DCT, LCH information fused for periocular and eye regions for left and right regions |

with (partially occluded) face recognition indicated the reliability of using periocular recognition in non-ideal scenarios where face recognition may fail. The effects of pose variation, occlusion, cosmetic changes, and template aging were demonstrated on a dataset constructed for the purpose of the study. The extensive experiments conducted advocate the inclusion of eyebrows in the periocular region and the capture of neutral facial expressions for accurate recognition. Score-level fusion of left and right periocular region, using local matchers, such as SIFT, as well as global matchers, such as HOG and LBP, exhibits promising results with a rank-1 recognition rate of 87.32%.

Bharadwaj et al. [163] propose a texture based recognition system for the periocular region. The GIST descriptor is used as a global matcher, while circular LBP is used for capturing local texture information. Normalized score-level fusion is performed for the descriptors. Weighted sum-rule score fusion is performed for the left periocular and right periocular regions. For the experiments performed on the UBIRIS v2 database, it is observed that global features provide better discriminative information than local features. A rank-1 identification accuracy of 73.65% is achieved. Identification is performed at varying distances and a distance of 6 m from the subject is shown to be more useful for recognition.

Xu et al. [164] explore several filter based techniques and local feature extraction methods on the FRGC dataset. A Verification Rate of 17.0% at 0.1% false accept rate is reported using Local Walsh-Transform Binary Pattern approach. The verification rate, while quite low, outperforms the NIST reported baseline on the dataset. The best feature extraction method combined with Kernel Correlation Feature Analysis obtains a verification rate of 61.2%. The rank-1 accuracy achieved is 53.2%, using the fusion of discrete wavelet transform and local binary patterns. The accuracy rates reported are lower than prior work in periocular biometrics, but the database used for reporting results in the paper is approximately 24 times larger than databases used in prior works.

Woodard et al. [165] investigate the utility of various appearance cues including skin texture, color, and the spectrum used for capturing images. Several experiments are conducted using the FRGC v2 dataset, wherein local binary patterns are used to capture texture information and color histograms are used for representing the information encoded in the red and green channels. The experiments compare neutral expressions across sessions, alternate expressions from the same recording session, and also, alternate expressions across sessions. Color and texture information is combined using score-level fusion. Finally, information from the left and right periocular regions is combined using score-level fusion with min–max normalization. Experiments performed on the MBGC face-video dataset do not present good results; the authors suggest that this is due to blurring, scale-change, and illumination-change in the periocular images in the dataset. Miller et al. [166] build on this work to study the effect of illumination, resolution change, blurring, and information present in various color channels. In experiments conducted under the variations mentioned before, the highest performance drop due to blurring is observed to be from 94.10% to 54.49% for neutral expressions compared across sessions. The most significant variation in performance due to resolution change is from 94.90% to 84.70% for alternate expressions recorded across sessions. It is also observed that the red color channel does not constitute significant discriminatory information.

Miller et al. [167] demonstrate the performance of local binary pattern descriptor for recognition of individuals using periocular information on the FRGC dataset and the FERET dataset. The recognition accuracy for the FRGC dataset is reported at 89.76%, while the performance on the FERET dataset is 74.07%. Based on the performance of the proposed algorithm, the authors suggest that the skin texture, eye folds, and contours of the periocular region can adequately verify a person's identity.

Adams et al. [168] present a genetic based Type II feature extraction system for optimizing the feature sets returned by local binary pattern descriptors for periocular recognition. A significant recognition accuracy improvement (10.99%) is reported on the FERET dataset. Comparable feature optimizations are observed on the FRGC and FERET datasets.

Woodard et al. [169] investigate the utility of appearance cues such as periocular skin texture using local binary patterns, and color using Color Histograms, for periocular identification. 98.30% rank-1 recognition accuracy is achieved on the FRGC dataset, which demonstrates that the score-level fusion of periocular texture and color can be used as a biometric modality. The experiments performed on the MBGC dataset indicate that in non-ideal scenarios, periocular based matching significantly outperforms iris recognition. An interesting result emerging from the study comparing features between the right and the left periocular regions is that the periocular appearance is unique for each eye of an individual.

Padole and Proença [170] assess the effect in recognition performance with respect to change in scale, pose, occlusion, and pigmentation. UBIPr, a challenging dataset, is introduced for periocular recognition. A new strategy to initialize the periocular Region of Interest is explored and is observed to outperform the iris-centered recognition algorithms. Non-linear score-level fusion of LBP, SIFT, and Histogram of Oriented Gradient descriptors using neural networks is proposed. The paper effectively establishes the challenges associated with unconstrained periocular recognition.

Juefei-Xu and Savvides [171] propose a periocular acquisition and recognition system using a commercial off-the-shelf pan-tilt-zoom camera to tackle the difficulty of unconstrained periocular biometrics. The Compass dataset comprising of faces with 4 different expressions is introduced in the paper and the descriptor used for representing the images is the Walsh-Hadamard transform encoded local binary pattern. The proposed approach achieves a Verification Rate of 60.7% at 0.1% FAR, which supersedes the performance of face recognition on the same dataset.

Padole and Proença [172] assess the decrease in recognition performance due to change in illumination and the subject's pose. Homomorphic filters and Self-Quotient Images are used to compensate for varying lighting conditions. The authors describe a method to compensate for change in pose using landmark based geometric transformations. The proposed technique consistently improves performance when the subject's pose is moderately deviated, and scales well for angular deviations as large as 30°.

Proença and Briceno [173] address the effectiveness of the Globally Coherent Elastic Graph Matching algorithm to compensate for distortions due to expressions in periocular recognition. Experiments are performed on synthetic as well as real data (FaceExpressUBI dataset) to validate the algorithm. Consistent increments in the recognition performance are observed using the proposed algorithm. The improvements in handling distortions are achieved without a significant increase in the computational burden of the recognition process.

Juefei-Xu and Savvides [174] exhaustively demonstrate that subspace representations such as PCA, UDP, KCFA, and KDA on Discrete Transform encoded LBP features significantly outperform traditional subspace representations on raw pixel intensities as well as the standard LBP descriptor. Experiments are performed on the YaleB/YaleB+ datasets to test illumination pre-processing techniques prevalent in the literature. Multi-scale retinex is chosen for pre-processing the images for the experiments performed on the FRGC v2 dataset. With less than 40% of the face being utilized, periocular region has only a 2.5% drop in verification rate at 0.1% FAR compared to the complete face. However, the recognition

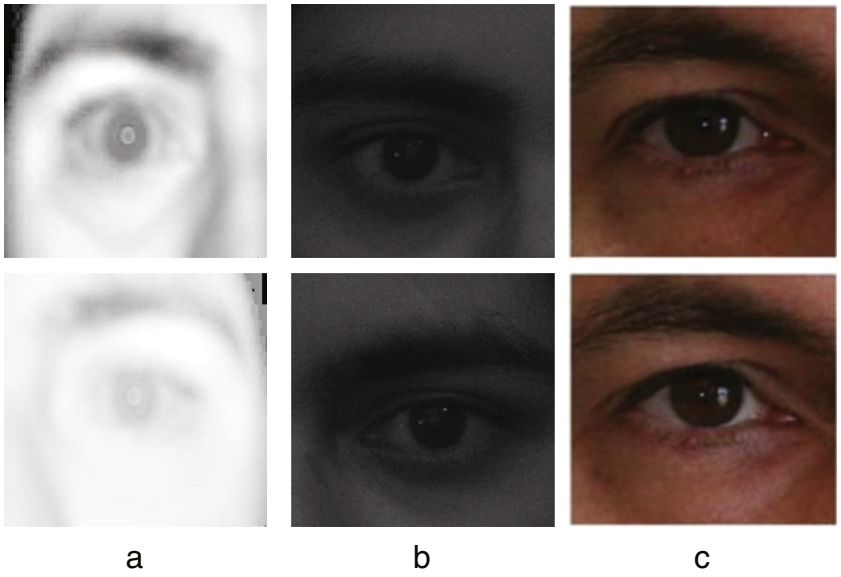


**Fig. 8.** Cross-spectral periocular recognition: (a) visible light, (b) Near Infrared, and (c) night vision.

system gains tolerance towards expression and occlusion, and the capability to match partial faces in crowds. The performance of the discrete transform encoded LBP feature in the Kernel Discriminant Analysis subspace representation is 75.1% verification rate at 0.1% FAR.

Sharma et al. [175] propose a cross-spectral periocular verification algorithm using neural networks. The proposed algorithm first trains the classifiers on individual spectrum images and then optimally combines them to mitigate the variations due to the difference in the spectra. The Pyramid of Histogram of Oriented Gradients feature is observed to outperform features used in prior works. Experiments are performed on the IIITD Multispectral Periocular database (Fig. 8), which includes images captured in three spectra: Near Infrared, Visible Light, and Night Vision. Among the three individual spectra, the best performance is achieved in the NIR spectrum with a Verification Rate of 92.50% at 1% FAR, using the score-level sum rule fusion of periocular information from the left and the right eye regions.

Mahalingam et al. [176] study the impact of changes in the face due to hormone manipulation and its ability to disguise the face and affect matching performance. A challenging dataset [177] that includes more than 1.2 million face images of 38 subjects is collected. Experiments on this dataset suggest that periocular region using simple texture based face matchers, namely, local binary patterns, histogram of gradients, and patch based local binary patterns outperforms matching against the full face. It is also observed that a fusion of the periocular using a texture based approach outperforms two Commercial Off The Shelf full face systems: PittPatt SDK and Cognetic FaceVACs.

Proença et al. [178] propose an approach for defining the periocular region-of-interest by segmenting all components in the periocular region: iris, sclera, eyelashes, eyebrows, hair, skin and glasses. A group of classification models predicts the posterior probabilities for each pixel in the periocular region for it to belong to one of the above component classes. The appearance based information is fused to geometrical constraints and shape priors to feed a two-layered Markov Random Field. Experiments performed on the UBIRIS v2 dataset show an equal error rate of 0.095.

### 2.2.2. Soft biometrics

Juefei-Xu et al. [179] have shown a feature extraction approach on periocular region to address the age-invariant face recognition problem. Images from the FG-NET dataset are pre-processed for illumination and pose correction, and periocular region normalization. Walsh-Hadamard Local Binary Pattern (WLBP) features are extracted from the preprocessed images. The WLBP featured periocular images with Unsupervised Discriminant Projection subspace modeling obtain a 100.00% rank-1 identification rate and 98.00% verification rate at 0.1% FAR. This algorithm significantly outperforms the baseline recognition rates, and proves that periocular recognition is a robust method for age-invariant biometric recognition.

Lyle et al. [180] describe a soft biometric classification approach using appearance based periocular feature. Information from the periocular region images is extracted using grayscale pixel intensities and periocular texture computed using local binary patterns in the FRGC dataset. Baseline gender and ethnicity classification accuracies of 93% and 91% are reported. The experiments indicate that the periocular modality can be effectively used in gender and ethnicity identification. The soft biometric information obtained also can be combined with existing periocular based recognition for improving recognition performance. This study is extended by the authors in Lyle et al. [181]. Experiments are performed in the visible spectrum on the FRGC dataset, and in the near infrared spectrum on the MBGC dataset. Local binary pattern, Histogram of Oriented Gradient (HOG), Discrete Cosine Transform (DCT), and Local Color Histogram (LCH) descriptors are used for performance evaluation. In all experiments, information is fused for the periocular and the eye region for both left and right regions. For the FRGC dataset, gender and ethnicity classifications of 97.3% and 94% respectively are observed. For the MBGC images, gender and ethnicity results of 90% and 89% are observed, respectively.

### 2.2.3. Human performance evaluation

In the past, gaining an understanding of how humans recognize faces enabled researchers to develop pragmatic feature extraction techniques for face recognition. Sinha et al. [182] describe a study of human face recognition and posit results that propose robust schemes towards the design of automated face recognition systems. Since periocular region is essentially a subset of the face region, it seems a worthy goal to explore how humans interpret periocular images.

The foremost study of features which humans found useful for making decisions in identifying individuals based on periocular information is attributed to Hollingsworth et al. [183]. It is found that humans can correctly classify the pairs as belonging to the

same person or different people, with an accuracy of about 92%. The authors report that the accuracy is observed to be about 97% when subjects are confident about their decision. It is established that the features that humans found most helpful for recognition of individuals were not the features used by contemporary researchers for automated periocular recognition. Features that subjects found helpful for recognition were eyelashes, the tear duct, and the shape of the eye, while eyebrows, the outer corner of the eye, and the skin texture were found to be of no assistance in recognition. Even though the feasibility study performed by Park et al. [5] suggests that eyebrows have significant discriminatory information, the reason that eyebrows received such a low ranking in the experiments is proposed to be that none of the images showed a complete eyebrow. The authors suggest that iris sensors with a larger field of view, which can capture eyebrows, are utilized to attempt to combine iris and periocular biometric information.

Hollingsworth et al. extend the study [183] to understand the effect of different factors on human performance in periocular recognition [184]. Firstly, the non-match queries are created by pairing subjects with the same gender, same ethnicity, and similar eye color, make-up, eye occlusion, and eyelash length. Secondly, the experiment limits the viewing time to 3 s for each query. Finally, it is ensured that all non-match periocular regions are paired so that the two subjects in a pair have the same gender and race. As compared to evaluations involving randomly selected non-match pairs with uncontrolled viewing time, the accuracy is observed to be 78.75%. This is a significant drop compared to the experiment involving randomly selected non-match pairs, which has an accuracy of 92.10%. The authors propose that explicit modeling and description of eyelids, eyelashes, and tear ducts can provide higher recognition power.

Hollingsworth et al. [185] perform an exhaustive human study on evaluating the region surrounding eyes for both periocular biometrics and iris biometrics. The study includes the irises and the periocular region of the subjects captured in the NIR spectrum using a LG2200 camera and in the visible spectrum using a Nikon D80 camera. The average score on the NIR periocular test is observed to be 78.8%, and the average score on the visible spectrum periocular test is observed to be 88.4% The machine performance for the periocular tests, averaged across three algorithms, which use SIFT, LBP, and HOG descriptors is 83.6%. In the human experiments, it is learnt that there was little evidence of correlation for pairs of subjects across different modalities. This result suggests that a difficult subject to match in one modality may be easier to match in other modalities. This suggests that fusing information from the two modalities is likely to lead to better recognition rates. The results of the study suggest that using visible spectrum periocular images instead of NIR images is a suitable direction for development of periocular recognition algorithms.

#### 2.2.4. Current research directions in periocular biometrics

Since it's inception in 2009, periocular biometrics has enjoyed significant attention from the biometrics community. The field has rapidly evolved from preliminary studies to competing with face recognition in the presence of occlusion. The trends discussed in Section 2.2 suggest that periocular recognition is likely to be moving along the following directions in the future:

1. *Cross-spectral periocular recognition*: Periocular recognition is used in conjunction with face recognition in the presence of occlusion. The periocular region is also critical in ocular recognition when the iris fails in unconstrained scenarios. Since iris recognition and face recognition are traditionally performed in the NIR and visible spectra, respectively, one of the important directions of research is to perform periocular recognition across spectra to potentially allow these modalities to work together.
2. *Anti-spoofing measures*: One of the factors on which acceptability of a biometric trait depends for real-world applications is its resilience to spoofing attacks. It is required that the biometric community focus on establishing measures to minimize spoofing of the trait.
3. *Unconstrained recognition at-a-distance*: Among all ocular biometric modalities, the periocular trait requires the least constrained acquisition process. It has the potential to allow ocular recognition at large stand-off distances, with applications in surveillance. It is likely that the research community will move towards exploring ocular recognition at a distance in more detail as compared to present studies.

### 2.3. Retina biometrics

The vasculature of the retina is rich in discriminatory information (Fig. 9). Retina based biometric recognition is believed to be the most secure biometric modality as it is extremely difficult to spoof the retinal vasculature. However, the modalities associated with the acquisition of retinal images require high user cooperation. Arakala et al. [186] explore the representation of retina vessel patterns as spatial relational graphs. The features are compared using error-correcting graph matching. The authors observe that apart from nodes, three other graph sub-structures are suitable for separating genuine comparisons from impostor comparisons. Two retina graph statistics are identified, the edge-to-node ratio and the variance of the degree distribution, which have low correlation with the node match score. Intra-class variation is accounted for by treating the two graphs (corresponding to two samples from the same subject) as noisy versions of the same graph. Two retina graphs are compared by error-correcting graph editing techniques using deletion, addition, and substitution of nodes and edges. The maximum common subgraph is generated from the set of nodes. Experiments on the VARIA [187] database show that using nodes as feature points, edges, and paths of length two units result in match scores which completely separate genuine from impostor comparisons.

Jeffers et al. [188] present theoretical genuine and impostor score distributions for retina templates by estimating normal kernel density. The estimates are based on 147 images, which are a part of the VARIA database. A common extraction and matching algorithm based on graph representation of retina images is used. The authors test seven normalized scoring functions on feature point based retina templates. Equal error rates in the range 0.3–1.3% are obtained using the scoring functions. False non-match rates of less than 10% and entropy estimates between 65 bits and 200 bits are also reported.

Lajevardi et al. [189] present a retina verification framework based on the Biometric Graph Matching (BGM) algorithm. The information from the retinal vasculature is extracted using filters in the frequency domain and other morphological operators. The retinal images are represented as formal spatial graphs derived from the vasculature. The BGM algorithm uses graph topology to define three distance measures between a pair of graphs. A SVM classifier is used to distinguish between genuine and impostor comparisons. The classifier is found to be able to perform separation on a training set of images from the VARIA database, which is the state-of-the-art for retina verification. Kernel density estimation is used to model the distribution of distances resulting from comparisons in the training set. This model is used to select an appropriate operating threshold for testing the system.

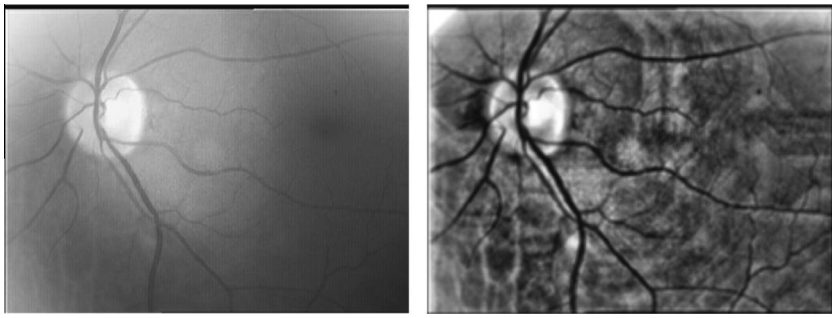

**Fig. 9.** VARIA database: retina sample (left); histogram equalized retina sample (right).

**Table 8**
Summary of retina recognition.

| Authors | Database | Summary |
|---|---|---|
| Arakala et al. [186] | VARIA [187] | Represent retina vessels as spatial relational graphs. Features are compared using error-correcting graph matching. Maximum common subgraph is generated from the set of nodes |
| Jeffers et al. [188] | | Theoretical genuine and impostor score distributions for retina templates are estimated. Test seven normalized scoring functions on feature point based retina templates |
| Lajevardi et al. [189] | | Retinal vasculature information is extracted using frequency domain filters. Images are represented as spatial graphs. Biometric Graph Matching algorithm defines distance measures |

Table 8 summarizes the research in the area of retina biometric recognition. The modality requires further research, especially in the acquisition stage, to improve user convenience and accuracy.

### 2.4. Emerging ocular biometrics

Komogortsev et al. [190] present an approach which estimates the unique Oculomotor Plant (OP) or eye globe muscle parameters from an eye movement trace. The muscle parameters model the human eye, including neuronal control signal, series elasticity, length tension, force velocity, and active tension. The authors propose a method to identify persons based on the Oculomotor Plant Mathematical Model (OPMM), which models a human eye as a system that consists of an eye globe driven by a set of extra-ocular muscles. Experimental results from an experiment consisting of 41 human subjects demonstrate the efficacy of the system. The authors assert that the Oculomotor Plant Mathematical Model (OPMM) includes both behavioral and physiological human attributes, is difficult to counterfeit, and is non-intrusive.

Eye movements are resistant to spoofing due to complex neurological interactions and the extra-ocular muscle properties involved in their generation. Holland and Komogortsev [191] present an objective evaluation of various eye movement based biometric features. The biometric candidates cover a number of basic eye movements and their scan-path characteristics. An information fusion method for combining these metrics is presented. Experiments performed on a dataset consisting of 32 subjects identifies individuals with an equal error rate of 27%. The results indicate that scan-path based biometric identification is a potential behavioral biometric technique.

Holland and Komogortsev [192] present an objective evaluation of the effects of eye tracking specification and stimulus presentation on the biometric viability of complex eye movement patterns. Six spatial accuracy and temporal resolution tiers, and five stimulus types are evaluated to identify acceptable conditions under which to collect eye movement data. The authors conduct three experiments to investigate the effects of environment and stimulus on the biometric viability of complex eye movement patterns. The first experiment examines the effects of varied stimulus type, the second experiment examines the effects of varied spatial accuracy and temporal resolution, and the third experiment provides data recorded on low-cost eye tracking equipment for cross-validation. The results suggest that eye tracking equipment is capable of achieving a spatial resolution of 0.5° and a temporal resolution of 250 Hz for biometric purposes, whereas stimulus has little effect on the biometric viability of eye movements.

Dong and Woodard [193] investigate the use of shape based eyebrow features for biometric recognition and gender classification. The eyebrows are manually segmented and shape based features are extracted. The features are compared using several different classifiers. The proposed algorithms are tested on the MBGC and FRGC databases. Identification rates of 90% and 75% are achieved on the MBGC database and FRGC database, respectively. Gender classification rates of 96% and 97% for each of the databases confirm the potential of the proposed biometric modality.

Crihalmeanu and Ross [194] design segmentation, enhancement, and matching routines for processing the conjunctival vasculature of multispectral eye images. A Redlake (DuncanTech) MS3100 multispectral camera is used to collect data from 49 participants. A double-density complex discrete wavelet transform is used to denoise the images. Specular reflections are in-painted using a partial differential equation to calculate the intensity of the pixel and the sclera is segmented. The segmented sclera is registered and matched using cross-correlation between the overlap of the two sclera regions being matched.

Zhou et al. [195] propose using the sclera present in the human eye as a biometric modality. The authors develop a novel technique for sclera segmentation, which works on color as well as grayscale images. Since the veins on the sclera surface are not rigid structures, the authors perform registration prior to feature extraction. A Gabor wavelet based sclera pattern enhancement method is designed as a pre-processor to feature extraction. A line-descriptor based feature extraction and matching method is proposed which is invariant to deformations in the pattern and thickness of the vasculatures. Experiments performed on the UBIRIS v1 dataset report an equal error rate of 3.83% for recognition. The authors also collect the IUPUI Multi-wavelength Database, which consists of images acquired from 44 subjects in 8 wavelength bands. The genuine accept rate for the proposed methodology is 81.51% at a false accept rate of 0.1%.

Oh and Toh [196] propose a cancelable sclera template matching scheme. The iris and the sclera are localized and an angular grid frame, whose origin is the iris centroid, is used to generate a region indicator matrix. Local binary pattern features are used to represent the texture information present in the grid. The authors assert that the templates are illumination and shift invariant. Recognition is performed by comparing normalized Hamming distances. Experiments performed on the UBIRIS v1 database demonstrate the efficacy of the proposed algorithm.

Rigas et al. [197] explore the dynamics of human eye movements as a biometric modality. Each sample is segmented into a number of parts, corresponding to fixations that occurred while the subject observed the stimuli. The sample is represented as a set of ten signals, corresponding to each fixation that took place. Each signal is passed through a low-pass filter to eliminate high-frequency effects. The signal is treated as a vector of velocity and acceleration parameters in 8D space: $[vel_{left_x}, vel_{left_y}, accel_{left_x}, accel_{left_y}, vel_{right_x}, vel_{right_y}, accel_{right_x}, accel_{right_y}]$. The multivariate Wald-Wolfowitz test is used to compare the distributions of saccadic velocity and acceleration features. Experiments performed on the Eye Movement Dataset [198] datasets show an accuracy of 91.5% for the proposed algorithm.

Crihalmeanu and Ross [199] present a novel algorithm for sclera segmentation based on a normalized sclera index measure. The authors collect a multispectral database of iris and sclera images. The sclera-eyelid and sclera-iris boundaries are individually segmented. Experiments performed on the collected dataset report that the SURF descriptor achieves an equal error rate of less than 0.8%. The authors assert that the descriptor is robust towards small variations in the viewing angle, affine deformations, and color shades. Score-level fusion of minutiae detected in the vasculature with direct correlation matching shows that sum-rule performs well for a number of correlation techniques. The authors suggest that multispectral images be used towards combining iris biometrics with sclera recognition for enhanced performance.

Rigas et al. [200] describe a study of human eye movements as a biometric modality. The authors observe the eye-movements of subjects while they observe face images. The subject's eye trajectories are modeled as 2D distributions of points on the image plane. The specific use of human faces as visual targets for subjects while they are being monitored allows for idiosyncratic eye-movements to be captured. A graph theoretic framework is implemented to process the captured eye movement patterns. The reported recognition performance, an equal error rate of approximately 30%, outperforms prior state-of-the-art techniques. The recognition performance indicates the feasibility of the proposed approach along with other methods to build a hybrid *physiological behavioral* recognition system.

Darwish and Pasquier [201] investigate the feasibility of using the dynamic features of the eyes for biometric identification. Eye movements are recorded and classified into segments that consist of saccades and fixations. The change in the size of the pupil is also considered during these movements. The authors propose to combine the proposed dynamic features, which consist of the eye movement features and iris constriction and dilation parameters, with iris biometrics. Experiments demonstrate a Half Total Error Rate (HTER) of 7.7% for iris and 30% for eye movements. The fusion of iris and eye movement data leads to an overall improvement of 5.3% in the HTER.

Lin et al. [202] propose a parallel sclera vein recognition method to improve the matching efficiency of the modality. A rotation-invariant and scale-invariant feature extraction method is designed to efficiently eliminate unlikely matches. A weighted polar line sclera descriptor structure is developed to optimize GPU memory requirements. Finally, a coarse-to-fine two-stage matching method is proposed. The Weighted Polar Line descriptor is developed as it is more suitable for parallel computing, which dramatically reduces data transfer and computation times. Experiments demonstrate that the proposed method dramatically improves the matching efficiency without compromising the recognition accuracy.

Rigas and Komogortsev [203] propose the extraction of biometric features from spatial patterns formed by eye movements during inspection of dynamic visual stimuli. The proposed framework transforms each eye movement signal into a time-constrained decomposition using a probabilistic representation of spatial and temporal features related to eye fixations. The experiments performed indicate that the Fixation Density Map performs well when eye movement data is captured at lower than optimum sampling frequencies. The authors posit that this is an important property of the proposed algorithm for future ocular biometric systems where existing iris recognition devices could be employed to combine eye movement traits with iris information for increased security and accuracy. The results on a dataset of 200 individuals collected by the authors indicate an equal error rate of 10.8% and a rank-1 accuracy of 51%.

Cantani et al. [204] present a novel Gaze ANalysis Technique (GANT) that uses a graph based representation of fixation points obtained through an eye tracker during human computer interaction. The authors examine dynamic aspects of eye behaviors to assess the relevance of eye movement patterns as a soft biometric trait. The proposed technique is applied to a dataset composed of 112 volunteer observers acquired through a Tobii 1750 remote eye tracker. For verification experiments on the data collected by the authors, an equal error rate of 0.224 is obtained.

Sun et al. [205] present a unified statistical framework for modeling saccadic eye movements and visual saliency based on super-Gaussian Component (SGC) analysis. The proposed algorithm sequentially obtains SGC using projection pursuit, and generates eye movements by selecting the location with maximum SGC response. Several key issues in saliency modeling research such as the effects of scale and blur are explored by the authors. The effectiveness of proposed algorithm is established based on extensive qualitative and quantitative experimental results performed on the York University Eye Tracking Dataset [206].

The ocular biometric recognition techniques discussed above are promising areas of research for extracting discriminatory biometric information. It is observed that eye-movement classification, in particular, has seen significant progression over the past 5 years. Table 9 summarizes the emerging ocular recognition techniques.

## 3. Fusing ocular information

The advent of periocular recognition and other emerging ocular modalities calls for the development of techniques which improve the overall recognition performance of biometric systems. The deployment of public large-scale recognition systems which enroll millions of individuals need reliable recognition in non-ideal scenarios. Under such scenarios, fusion of multiple modalities appears to be the most relevant and promising path forward in addressing the need for faster and more reliable recognition systems. Fusion in ocular biometrics can be performed in two ways: (1) Intra-ocular fusion - when information pertaining to two ocular modalities is fused, and (2) Fusion of ocular traits with other modalities (Fig. 10). This section summarizes multimodal biometric fusion literature with respect to ocular modalities.

### 3.1. Intra-ocular fusion

Fusion of ocular modalities may be performed in several different ways (Fig. 11). In the past, iris information has been combined

**Table 9**
Summary of emerging ocular biometrics research.

| Authors | Database | Summary |
|---|---|---|
| Komogortsev et al. [190] | In-house collection | Present the Oculomotor Plan Mathematical Model for biometric identification |
| Holland and Komogortsev [191] | In-house collection | Evaluation of eye movement based biometric features. Cover numerous basic eye movements and their scan-path characteristics. Information fusion is applied to combine metrics |
| Holland and Komogortsev [192] | EMBD v2 [207] | Evaluate effects of eye tracking specification and stimulus presentation on biometric viability of complex eye movements |
| Dong and Woodard [193] | FRGC, MBGC | Shape based eyebrow features are extracted. SVM, LDA, MD classifiers are used for recognition |
| Crihalmeanu and Ross [194] | In-house collection | Double-density complex discrete wavelet transform de-noises images. Segmented sclera is registered and matched using the cross-correlation of overlap of the sclera being matched |
| Zhou et al. [195] | UBIRIS v1, In-house collection | Sclera is segmented and vasculature is registered. Line descriptor based feature extraction and matching is applied |
| Oh and Toh [196] | UBIRIS v1 | Sclera is localized and region indicator matrix is generated centered on iris. LBP is applied on grid. Recognition by comparing Hamming Distances |
| Rigas et al. [197] | Eye Movement Dataset [198] | Eye-movement saccadic velocity and acceleration features are captured. Wald-Wolfowitx test is applied to measure correlation between samples |
| Crihalmeanu and Ross [199] | In-house collection | Segment sclera-eyelid boundary and sclera-iris boundary. SURF descriptor is applied. Score-level fusion of minutiae and direct correlation is explored |
| Rigas et al. [200] | In-house collection | Observe eye-movements of subjects. Subjects' eye trajectories are modeled as 2D distributions on image plane. Graph theoretic framework is implemented to process patterns captured |
| Darwish and Pasquier [201] | In-house collection | Eye movements are recorded. Classified into segments of saccades and fixations. Fusion of iris biometrics and proposed technique is performed |
| Lin et al. [202] | UBIRIS v1 | Weighted polar line descriptor is developed to optimize GPU requirements. Coarse-to-fine two-stage matching is applied |
| Rigas and Komogortsev [203] | In-house collection | Extract spatial features from eye movements. Transform eye movements into time-constrained decomposition using probabilistic representation of spatial and temporal features |
| Cantani et al. [204] | In-house collection. | [Emerging] Use graph based representation of fixation points using eye tracker. Examine dynamic aspects of eye behaviors to assess eye movement patterns as soft biometric trait |
| Sun et al. [205] | York University Eye Tracking Dataset [206] | [Emerging] Model saccadic eye movements and visual saliency based on SGC. Obtain SGC using projection pursuit and generate eye movements by selecting location with maximum SGC response |

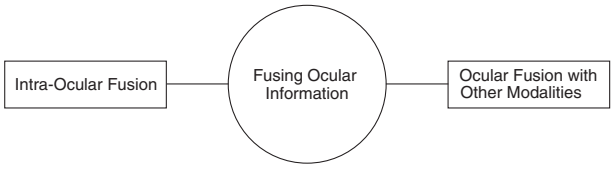


**Fig. 10.** Fusion in ocular biometrics.

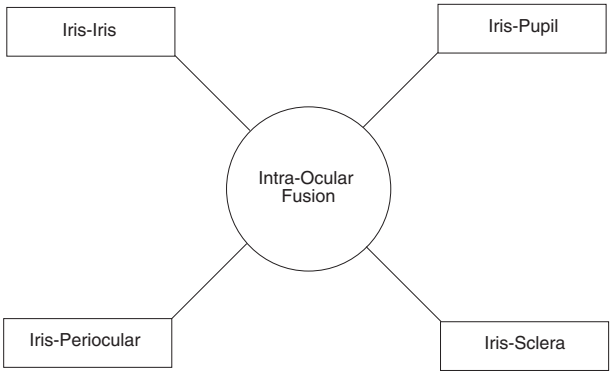


**Fig. 11.** Generally, intra-ocular fusion is performed in four combinations of ocular modalities.

with information from the pupil, the periocular region, and the sclera. This is a more intuitive approach because multiple ocular features can be combined in one image capture attempt. Table 10 summarizes the intra-ocular approaches to biometric fusion in the literature.

Vatsa et al. [208] propose a quality based fusion scheme for improving recognition accuracy using color iris images. The pairwise match score correlation for the red, green, and blue channels is used to combine information at the image level using a Redundant Discrete Wavelet Transform. The resultant image is used in a score-level fusion scheme with the remaining channel to improve recognition accuracy. Experimental results on the WVU Multispectral Iris database [150] demonstrate the efficacy of the technique when compared with other score-level and image-level fusion methods. The authors suggest that the proposed method can potentially benefit the use of color iris images in conjunction with their near infrared counterparts.

Kumar and Passi [209] perform a comparative study of iris recognition performance using log-Gabor filter, Haar wavelet, Discrete Cosine Transform, and Fast Fourier Transform based descriptors. Extensive experiments are performed on the CASIA v1, CASIA v3, and IITD Iris databases. The score level combination of log-Gabor filter and Haar wavelet using weighted-sum rule outperforms other descriptors and their combinations. The Haar wavelet based approach requires minimum computation time and its combination with log-Gabor filters is found to be computationally efficient as well. The authors also evaluate the comparative performance of various descriptors with singular training images. The performance from the proposed system is extensively evaluated using one training image on the CASIA and IITD databases.

Woodard et al. [210] investigate the utility of the periocular biometric in combination with the iris as a means to improve the overall recognition performance. The discriminatory information present in the iris is captured using Daugman's IrisCode algorithm. Local binary patterns are used to extract features from the periocular modality. Two match scores pertaining to the iris and the periocular region, respectively, are generated. Min–max normalization is applied to the scores, and weighted sum rule is used

**Table 10**
Summary of intra-ocular fusion approaches.

| Authors | Database | Summary |
|---|---|---|
| Vatsa et al. [208] | WVU Multispectral database[150] | Correlation of color channels is used to fuse information at image level. Fused image is used in score-level fusion framework with remaining channel |
| Kumar and Passi [209] | CASIA v1, CASIA v3, IITD Iris | Score level weighted sum rule fusion of Log-Gabor filter and Haar wavelet is performed. Recognition performance for singular training image systems is explored |
| Woodard et al. [210] | MBGC | Daugman's IrisCode is applied to iris. LBPs are extracted from periocular region. Min–max normalization is applied to match scores. Weighted sum rule is used for fusion |
| Rathgeb et al. [211] | CASIA v3 | Fuse two binary feature descriptors into a single template of the same size. Scheme is intended to effectively exploit error correction capacities of templates |
| Tan and Kumar [212] | CASIA v4 | Periocular information is extracted using Leung-Malik filters (LMF). Min–max normalization is applied, followed by weighted sum method score fusion |
| Gottemukkula et al. [213] | In-house collection | Information is extracted from iris and conjunctival vasculature in visible spectrum. Weighted sum rule fusion scheme is applied to match scores |
| Yano et al. [214] | In-house collection | Pre-process videos to reduce noise and adjust contrast. Pupil Light Reflex and iris pattern features are used to generate independent match scores. Information is fused at score level |
| Ross et al. [215] | FOCS [216], FRGC | GOH scheme extracts global information and SIFT extracts local edge anomalies. PDM handles non-linear deformations. Sum rule is used to combine generated match scores |
| Komogortsev et al. [217] | In-house collection | Extract Oculomotor Plant Characteristics (OPC), Complex Eye Movement (CEM) patterns, and physical structure of iris. OPC, CEM, and iris are combined for fusion |
| Mehrotra et al. [218] | CASIA v4 | Relevance Vector Machines (RVM) perform score-level fusion for multiple irises. RVM is observed to be computationally more efficient compared to SVM |
| Komogortsev and Holland [219] | In-house collection | Multiple features are extracted from oculomotor behavior. Score-level fusion is performed using likelihood ratios |
| Jillela and Ross [220] | Proprietary database | Iris matching is performed using VeriEye. Ocular regions are matched using LBP, NGC, and JDSR. Score-level fusion is performed |
| Proença [221] | UBIRIS v2, FRGC | Propose an ensemble of a strong expert which analyzes iris texture, and a weak expert which parameterizes the shape and geometrical features of the surrounding areas of the eye |

for score-level fusion. Experiments are performed on images extracted from Near Infrared face videos of the Multi Biometric Grand Challenge dataset. The experiments indicate that periocular based matching outperforms iris based matching by a large margin thereby indicating immense potential for its use in non-ideal imagery.

Rathgeb et al. [211] present a feature level fusion technique for fuzzy commitment schemes. The proposed fusion technique aims at fusing biometric templates of two binary feature descriptors into a single template of the same size. The fusion scheme is designed to balance average reliability across the entire biometric template on the basis of a small training set. The scheme is intended to effectively exploit error correction capabilities of the templates. Experiments performed on the CASIA v3 dataset demonstrate that the proposed fusion scheme significantly outperforms conventional multi-biometric fuzzy commitment schemes.

Tan and Kumar [212] propose a combination of iris and periocular fusion using Leung-Malik filters as the feature extractors for periocular recognition. Experiments performed on the CASIA v4 database achieve an improvement of 8.1% in recognition accuracy over prior state-of-the-art approaches. Min–max normalization is applied to the iris and periocular match scores. The match scores are combined using weighted sum method. The combination of simultaneously segmented iris and periocular images achieves average rank-1 recognition accuracy of 84.5%, i.e., an improvement of 52% over iris recognition.

Gottemukkula et al. [213] explore the feasibility of ocular biometric recognition in the visible spectrum by utilizing the iris along with the conjunctival vasculature. The authors design a weighted sum rule fusion scheme to combine the information from the two modalities. A dataset of 50 subjects is collected using a Nikon D3S FX camera. The proposed fusion scheme improves the equal error rate by 4.5% compared to an independent iris recognition system. The authors observe that unlike periocular biometrics, the proposed bimodal configuration explicitly uses the iris but only requires a small portion of the ocular region.

Yano et al. [214] propose a multimodal authentication method, which incorporates the use of the Pupil Light Reflex (PLR) and the iris pattern. The authors collect a database of videos from 59 subjects for the purpose of the study. The captured videos are pre-processed to reduce noise and adjust the contrast. The dynamic features of the PLR and the static features of the iris pattern are fused at the score level. Experimental results present an equal error rate of 2.44%.

Ross et al. [215] propose an information fusion framework to combine three distinct feature extraction and matching schemes to handle variability in the input data. The Gradient Orientation Histogram scheme is used to model global information. A variant of the Scale Invariant Feature Transform extracts local edge anomalies. A Probabilistic Deformation Model handles non-linear deformations. Sum rule is used to combine the match scores generated from the three feature extraction schemes. Experiments are performed on the Face and Ocular Challenge Series database [216] and a subset of the Face Recognition Grand Challenge database. It is observed that the equal error rate of iris recognition as compared to the proposed fusion approach is reduced from 34% to 19%.

Komogortsev et al. [217] explore a novel biometric approach that uses three disparate ocular traits acquired using a single camera sensor. The traits are the Oculomotor Plant Characteristics, the Complex Eye Movement (CEM) patterns, and the physical structure of the iris. A PlayStation Eye web camera is used to collect eye-movement and iris data for 87 subjects. The combination of OPC, CEM, and iris traits provides an error reduction of 19% when compared to the iris modality alone. The authors assert that the proposed combination of ocular traits has the potential to enhance the accuracy and counterfeit-resistance of biometric systems.

Mehrotra et al. [218] explore the application of Relevance Vector Machines (RVM) to perform score-level fusion from different classifiers. Experimental results on the CASIA v4 database show that the RVM achieves better accuracy compared to single iris recognition. The proposed fusion algorithm improves the recognition accuracy by 4% compared to single iris recognition. The time required for performing RVM fusion is observed to be significantly less than fusion using SVM, with comparable recognition performance.

Komogortsev and Holland [219] utilize patterns present in oculomotor behavior to recognize individuals. The features extracted

from the observed oculomotor behavior include saccadic dysmetria, compound saccades, dynamic overshoot, and express saccades. The authors perform score-level information fusion for these features, which is evaluated using likelihood ratios, support vector machines, and random decision forests. The EyeLink 1000 Eye Tracking System is used to acquire data from 32 subjects. Experimental results on the database achieve equal error rates of 25% and rank-1 identification rates of 47% using score-level fusion by applying likelihood ratio. The authors suggest that these results indicate that it is possible to identify subjects through the analysis of complex oculomotor behavior.

Jillela and Ross [220] propose matching ocular traits that are common between face and iris images for recognition. Iris matching is performed using a commercial software. Ocular regions are matched using local binary patterns, Normalized Gradient Correlation, and Joint Dictionary based Sparse Representation descriptors. Score-level fusion is performed for the match scores obtained from these ocular feature descriptors. Experimental results conducted on images obtained from 704 subjects suggest that the ocular region can provide better performance than iris under non-ideal conditions.

Proença [221] proposes a periocular recognition ensemble made of an expert which analyzes the iris texture and another expert which parameterizes the eyelid shapes and defines a surrounding region of interest. The strong expert (iris) analyzes the iris texture based on multi-lobe differential filters and uses the signal phase and magnitude to supplement the amount of information descriptor. The weak expert (ocular) analyses the shape of eyelids, the geometrical features of the eyelashes, and of the skin furrows near the cornea. The experts work on disjoint regions of the ocular area, thus producing practically independent responses. An empirical evaluation of the proposed methodology suggests an improvement of over 12% for the d-prime index on the UBIRIS v2 dataset and approximately 8% on the FRGC dataset.

### 3.2. Fusion of ocular traits with other biometric modalities

Different biometric modalities provide complementary information. The combination of such uncorrelated information descriptors is likely to help improve recognition performance. Here we summarize such algorithms (Fig. 12), which combine information from more than one source including iris and fingerprint, face and iris, face and periocular, and face and ocular traits. Table 11 presents a synopsis of these techniques.

Conti et al. [222] propose a template-level fusion algorithm integrating fingerprint and iris features. The proposed system is composed of two stages: preprocessing and matching. Iris and fingerprint images are preprocessed to extract the region of interest.

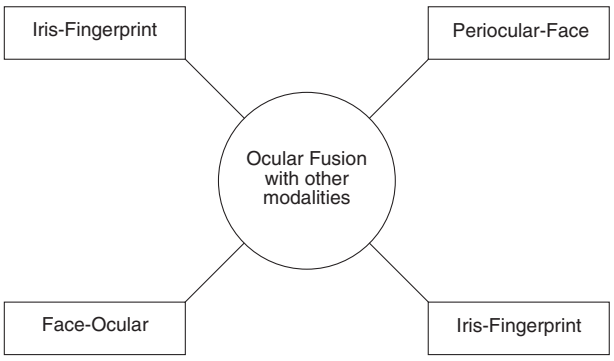


**Fig. 12.** Fusion of ocular traits with other modalities.

The fingerprint-singularity-regions based approach is employed as it requires low execution time. Iris image preprocessing is performed by segmenting the iris region and discarding the eyelids and eyelashes. The extracted regions of interest are used as input for the matching stage. The regions are normalized and processed through a frequency based approach to generate a homogeneous template. The Hamming distance between two templates is used to obtain the degree of similarity. The authors consider results at a false accept rate of 0% using the entire Fingerprint Verification Competition 2002 [223] database and a subset of the BATH Iris database [119]. False rejection rates of 5.71% and 7.28% are reported for two different subsets of the dataset.

Zhang et al. [224] propose a hierarchical fusion scheme for low quality images under uncontrolled situations. The authors employ Canonical Correlation Analysis to construct a statistical mapping from face to iris at the pixel level. The probe face image is used to obtain a subset of gallery candidates through this mapping. Score-level fusion of iris and face is performed on the gallery candidate subset for person identification. The dataset constructed by Dong et al. [225] is used to validate the proposed algorithm. The system achieves 100% accuracy for rank-58 recognition.

Johnson et al. [226] analyze several fusion strategies for combining face and iris biometrics. The FaceIT SDK is used to generate face match scores. Iris match scores are obtained using a modified version of Masek software. The authors utilize fixed sum rule, likelihood ratio, and quality based likelihood ratio for score-level fusion. Experiments performed on the Q-FIRE dataset demonstrate that the quality based likelihood ratio strategy performs optimally and achieves a genuine accept rate of 93.3% at a false accept rate of 0.1%.

Murakami and Takahashi [227] propose an identification technique which combines Bayes rule based score level fusion and distance based indexing. The algorithm selects the template of the

**Table 11**
Fusion of ocular traits with other biometric modalities.

| Authors | Database | Summary |
|---|---|---|
| Conti et al. [222] | FVC 2002 [223], Bath Iris [119] | Iris and fingerprint images are preprocessed to extract ROI. ROIs are processed through frequency based approach to generate homogeneous template. Hamming Distance is used for matching |
| Zhang et al. [224] | Dong et al. [225] | Canonical Correlation Analysis constructs statistical mapping from face to iris. Probe face image selects gallery candidates via constructed mapping. Score level fusion of iris and face is performed |
| Johnson et al. [226] | Q-FIRE | FaceIT SDK is used to generate face match scores. Iris match scores are obtained using modified version of Masek algorithm. Quality based likelihood ratio is used to perform optimal score-level fusion |
| Murakami and Takahashi [227] | Biosecure DS2 [228], CASIA v5 Fingerprint [229] | Bayes rule based score level fusion is used. Gallery template with highest posterior probability of being identical to probe template is identified |
| Nagar et al. [230] | FVC2002, CASIA v1, XM2VTS [231], WVU MultiModal | Fusion scheme combines homogeneous features to generate fused representation. Feasibility of framework is demonstrated using fuzzy vault and fuzzy commitment crypto-systems |
| Jillela and Ross [232] | IIITD Plastic Surgery [233] | VeriLook and PittPatt are used to obtain match scores for face. LBP and SIFT are applied to ocular region to obtain match scores. Weighted score-level fusion is applied |
| Bhatt et al. [234] | IIITD Plastic Surgery Database | Generates non-disjoint face granules, treating periocular as a specific component. Extended Uniform C-LBP and SIFT are used. Responses are combined using multi-objective genetic approach |

enrollee whose posterior probability of being identical to the probe template is the highest. Experimental evaluations using the Biosecure DS2 [228] dataset and the CASIA v5 Fingerprint [229] database demonstrate that the proposed algorithm significantly reduces identification error rates compared to unimodal biometrics.

Nagar et al. [230] propose a feature-level fusion framework to simultaneously protect multiple templates of a user as a single *secure sketch*. The feasibility of the framework is demonstrated using the fuzzy vault and fuzzy commitment crypto-systems. The proposed fusion scheme combines a set of homogeneous biometric features to generate a fused multi-biometric feature representation. For point-set based features, the authors suggest that a union of the representation may be utilized. A synthetic multimodal database is assembled using the FVC2002 database for fingerprints, the CASIA v1 database for irises, and the XM2VTS [231] database for faces. A genuine accept rate of 99% is achieved for this dataset. The algorithm does not perform as well on the WVU MultiModal dataset, a 75% genuine accept rate is reported. The experiments demonstrate that the proposed multibiometric crypto-system has higher security as well as recognition performance compared to uni-biometric systems.

Jillela and Ross [232] propose the fusion of information from the face and ocular regions to enhance recognition performance. Commercial face matching systems, VeriLook and PittPatt along with LBP and SIFT descriptors are applied to the ocular region for matching. Experiments are performed on a plastic surgery database consisting of 1800 images [233]. A rank-1 identification accuracy of 87.4% is obtained. Weighted score-level fusion is used to achieve these state-of-the-art recognition rates. Bhatt et al. [234] propose a multi-objective evolutionary granular algorithm to match individuals before and after plastic surgery. The algorithm generates non-disjoint face granules at multiple levels, which also treat periocular region as a specific component of the face image. The proposed algorithm yields higher identification accuracy as compared to prior algorithms and a commercial face recognition system. The Extended Uniform Circular local binary pattern and the Scale Invariant Feature Transform are used for extracting discriminating information from the face granules. The responses are combined in an evolutionary manner using a multi-objective genetic approach for improved performance.

## 4. Datasets and softwares

### 4.1. Datasets

Public datasets are an important component of active research in ocular biometrics. They provide an advantage in algorithm development, provide a platform for performance evaluation, and introduce new challenges to the research community. The availability of datasets associated with competitions such as the National Institute of Standards and Technology challenges and Noisy Iris Challenge Evaluation [36,235] motivates researchers to focus on exploring the algorithmic aspects of biometric recognition systems. Moreover, the performance of a new algorithm on an established dataset allows the algorithms to be benchmarked and be compared with prior state-of-the-art approaches. Table 12 lists commonly used ocular datasets and some of the major ocular datasets are described below.

- **CASIA Iris Datasets**: The CASIA v1 dataset [94], is the first in a series of datasets collected at the Chinese Academy of Sciences for the purpose of iris recognition. Iris images are captured using a homemade iris camera with eight 850 nm near infrared illuminators circularly arranged around the sensor to uniformly illuminate the iris. The dataset includes 756 iris images from 108 eyes, having a resolution of 320 × 280 pixels. The CASIA v2 dataset [95] was released in 2004. The dataset includes data acquired using a OKI Irispass-h sensor as well as a device developed by the authors, the CASIA-IrisCamV2. Each of the systems is used to collect 1200 images from 60 classes. The CASIA v3 dataset [61] was released to promote research in iris localization, nonlinear normalization, occlusion segmentation, liveness detection, and large-scale identification. It includes three subsets, each subset intended for research into specific modalities of iris recognition. All iris images in the CASIA v3 are 8 bit grayscale images, collected under near infrared illumination. A total of 22,034 iris images from more than 700 subjects and 1500 eyes are present in the CASIA v3. The CASIA v4 [34] dataset is an extension of the CASIA-IrisV3 and contains six subsets. The three subsets which comprise the CASIA v3 are extended in the CASIA v4. Additionally, three new subsets are introduced. The CASIA-Iris v4 contains a total of 54,601 iris images from more than 1800 genuine subjects as well as synthetic data. All iris images are 8 bit grayscale images, collected under near infrared illumination or are artificially synthesized.
- **Notre Dame and NIST Datasets**: Phillips et al. [28] describe the characteristics of the ND-IRIS-0405 dataset. The dataset contains 64,980 iris images obtained from 356 subjects using a

**Table 12**
List of ocular biometrics' datasets.

| Ocular modalities | Dataset | Authors/organization |
|---|---|---|
| Iris | BMDB | Ortega-Garcia et al. [237] |
| | CASIA Iris v1 | CAS-IA [94] |
| | CASIA Iris v2 | CAS-IA [95] |
| | CASIA Iris v3 | CAS-IA [61] |
| | CASIA Iris v4 | CAS-IA [34] |
| | IITD Iris | IIT Delhi [93] |
| | Herta Iris | Herta Security [51] |
| | ICE 2005 | NIST [39] |
| | IIITD CLI | IIIT Delhi [129] |
| | IIITD Iris Spoofing | IIIT Delhi [130] |
| | IIITD Multi Sensor | IIIT Delhi [142] |
| | Miles Research Database | Miles Research [66] |
| | Multi-PIE | Gross et al. [118] |
| | ND Time Lapse Iris | Baker et al. [149] |
| | ND-IRIS-0405 | Phillips et al. [28] |
| | ND Cross Sensor | University of Notre Dame [151] |
| | NICE v1 | NICE [36] |
| | NICE v2 | NICE [235] |
| | Q-FIRE | Johnson et al. [115] |
| | UBath Iris | University of Bath [119] |
| | UBIRIS v1 | Proença and Alexandre [18] |
| | WVU Non-Ideal | West Virginia University [62] |
| | WVU Off Angle | West Virginia University [238] |
| Periocular | Compass | Juefei-Xu and Savvides [171] |
| | IIITD Multispectral Periocular | IIIT Delhi [175] |
| | IIITD Plastic Surgery | IIIT Delhi [233] |
| | UBIPr | Padole and Proença [170] |
| Iris, Periocular | FERET | DARPA [120] |
| | FRGC v1 | NIST [64] |
| | FRGC v2 | NIST [236] |
| | MBGC | Phillips et al. [96] |
| | UBIRIS v2 | Proença et al. [19] |
| Eye movement | EMBD v2 | Komogortsev and Holland [207] |
| Ocular | FOCS | NIST [216] |
| Retina | VARIA | VARFA [187] |

LG 2200 infrared sensor. The images in the dataset simulate several real-world conditions including blur, occlusion, non-frontal irises, and artifacts induced due to contact lenses. Notre Dame CVRL group thereafter proposes several iris databases. For example, Fenker and Bowyer [148] prepared the ND-Iris-Template-Aging dataset. The dataset contains 22,156 images from 644 irises, acquired using an LG 4000 iris sensor over a period of 2 years.

- **UBIRIS and NICE Datasets**: Proença and Alexandre collected the UBIRIS v1 dataset [18] using a Nikon E5700 sensor. It is the first large-scale visible light iris database. The database contains 1877 images collected from 241 persons. The UBIRIS v2 dataset [19] contains visible-spectrum images from 261 subjects, having a resolution of $300 \times 400$ pixels. The primary purpose of the UBIRIS v2 database is to provide a tool to supplement visible wavelength iris recognition under non-ideal imaging conditions. Apart from iris recognition, the dataset has been used by a number of researchers to validate their proposed approaches to periocular recognition.
- **The VARIA Retina Database**: The VARIA database [187] is a set of retinal images used for authentication purposes. The database includes 233 images acquired from 139 different individuals. The images have been acquired with a TopCon non-mydriatic NW-100 camera and are centered on the optic disk. The resolution of the images is $768 \times 584$ pixels.
- **Face Datasets used for Ocular Recognition**: The data for the Face Recognition Grand Challenge v1 (FRGC) [64] consists of 50,000 recordings. It consists of high resolution facial images with an average inter-eye distance of 250 pixels. The FRGC is intended to facilitate the development of new algorithms that take advantage of the additional information inherent in high resolution images. It is suitable for benchmarking periocular recognition algorithms. The Face Recognition Grand Challenge 2.0 [236] contains visible spectrum frontal images of 568 subjects, having a resolution of $1704 \times 2272$ pixels. The high resolution images of the FRGC v2 dataset have been successfully used for validating several periocular recognition algorithms.

  Phillips et al. [96] describes the Multiple Biometrics Grand Challenge (MBGC). The dataset is acquired using several different sensors: the LG 2200 near infrared camera, the Sarnoff Iris on the Move system, and a high definition video camera having a resolution of $1440 \times 1080$. The face videos, having a resolution of $2048 \times 2048$ pixels, are suitable for validating periocular recognition algorithms. The goal of MBGC is to facilitate research in face and iris recognition for data acquired in non-ideal conditions.

  The Face Recognition Technology (FERET) database [120] is sponsored by the Department of Defense's Counterdrug Technology Development Program. However, it was originally collected to develop automatic face recognition capabilities. The database consists of 14051 face images in a number of orientations. The database is of significant interest for researchers working on constrained as well as unconstrained periocular recognition as well.
- **Multimodal databases that include ocular modalities**: Ortega-Garcia et al. [237] describe the multi-scenario Biosecure Multimodal DataBase (BMDB), collected within the framework of the European BioSecure Network of Excellence. Several biometric modalities are captured in multiple environments. Iris information is acquired from 667 subjects using an LG Iris Access EOU 3000. The novel and varied acquisition conditions of the BMDB allow for a variety of biometric techniques to be validated on the dataset. Johnson et al. [115] describe the Q-FIRE dataset, which is a set of face and iris videos consisting of subjects at a distance of 5–25 feet. Iris videos are captured in the near infrared spectrum with a Dalsa 4M30 camera. The iris data consists of variations in blur, orientation angle, and occlusion.

### 4.2. Open-source and commercial softwares

Fast-paced progress in the research on ocular biometrics has led to the development of software suites to facilitate experiments. Among ocular biometric traits, iris recognition has enjoyed majority of the attention of biometric researchers. As a result, a number of available open-source and commercial softwares focus on recognizing individuals from iris patterns. A few of the major ocular biometric softwares/open-source are described below.

1. Libor Masek's *MATLAB Source Code for a Biometric Identification System Based on Iris Patterns* [239] is an open-source implementation of Daugman's algorithm. The system performs segmentation, normalization, and feature encoding of eye images. The software suite also includes a program to measure the Hamming Distance between the biometric templates to perform matching.
2. The *Video-based Automatic System for Iris Recognition (VASIR)* [240] is an open-source iris recognition system designed at NIST for recognizing irises in videos. The system is capable of processing videos of human subjects walking through the system in unconstrained environments apart from robustly handling constrained stationary-image iris recognition. VASIR supports the following matching scenarios – non-ideal video sequences to non-ideal video sequences, non-ideal video sequences to ideal stationary images, and ideal stationary images to ideal stationary images. VASIR is capable of automatically detecting and extracting the eye region and assessing the quality of the iris image, apart from performing a comprehensive image comparison analysis. The performance and practical feasibility of VASIR has been empirically established on the Iris Challenge Evaluation (ICE) dataset and the Multiple Biometric Grand Challenge (MBGC) dataset [241].
3. *VeriEye* [242] is a commercial Software Development Kit for iris identification. The technology includes multiple proprietary solutions that allow robust iris enrolment under various conditions. The system is capable of verification as well as identification. The recognition time and recognition accuracy of the system has been tested at the NIST Iris Exchange (IREX). VeriEye performs robust recognition and can process non-frontal unconstrained images. The system can efficiently detect irises in the presence of visual noise, lighting reflections, or obstructed eye images. VeriEye matches up to 40,000 irises per second on a standard desktop computer, and enrolls an iris image in 0.6 s.
4. The *Eye Movement Classification Software* [243,244] developed at the Human Computer Interaction Laboratory at the Texas State University performs offline classification of eye movement trajectories. The software suite performs extraction of fixations and saccades from the observed positions of the eye trace. The software contains implementation of several eye movement classification algorithms: Velocity Threshold Identification, Hidden Markov Model Identification, Dispersion Threshold Identification, Minimum Spanning Tree Identification, and Kalman Filter Identification. The software also computes standardized behavior scores that allow selection of threshold and input parameters for any eye movement classification method.

## 5. Path forward

Ocular biometrics has been well explored and there are several systems that yield state-of-the-art results with cooperative users. However, for unconstrained environment and non-cooperative users, operations such as recognition at a distance, in the presence of contact lens, under the influence of drugs, and spoofing are

challenging scenarios where significant effort is required. Moreover, currently available ocular recognition systems, except periocular, require cooperation from users for acquisition. To achieve good recognition accuracies in unconstrained environments, research efforts can be extended in multiple areas. For future research, we believe that there are five major directions:

1. **Improved sensing technology**: Improving the accuracy of a biometric system is always conditioned by the acquisition technology and the algorithms utilized. With improvements in sensing technology, the captured data can be significantly improved thereby improving the recognition accuracies. Further, acquisition devices are also vital to increase the coverage area of any biometric modality. For instance, if the devices cannot capture samples at a distance, then the usage of that modality is always constrained in controlled environments. Therefore, one important research direction for ocular biometrics would be to design improved devices for non-intrusive and "at-a-distance" capture. Along with this, mobile and inexpensive devices for ocular biometrics can also increase the usage of these modalities. With new devices, improved preprocessing, feature extraction and matching algorithms will also be required.
2. **Exploration of advanced machine learning algorithms for better representation and classification algorithms**: Among different ocular modalities, iris is the most studied and deployed. One of the primary reasons for not deploying other biometrics is comparatively lower state-of-the-art of periocular and other ocular biometrics in unconstrained environments. Recently, several advancements have been proposed in the machine learning community to improve both representation and classification, for instance dictionary learning, deep learning, and distance metric learning. Researchers can explore these advanced machine learning algorithms to improve the performance of ocular modalities.
3. **Heterogeneous recognition**: With the availability of novel devices, interoperability is an ever increasing challenge. For instance, iris region can be captured in both NIR and visible spectra. Similarly, periocular recognition has also been explored in both the spectra. The scanners working in the same spectrum also have variations in resolutions, illumination source (such as different number and arrangement of NIR light emitting diodes), and field of view, thus bringing the challenge of interoperability in same spectrum devices as well. Another interesting example comes from Aadhaar project where iris biometrics is being used for verification. One device has been used for enrollment whereas for authentication, several inexpensive devices will be used by different registrars all over the country. To maintain high levels of authentication accuracy, the algorithms should be interoperable. Therefore, it is important that interoperability challenges such as cross spectrum and cross resolution are addressed in ocular biometrics.
4. **Ocular recognition at a distance**: Iris and periocular recognition have been studied extensively for scenarios involving constrained acquisition. The two modalities have achieved accurate recognition performance at short acquisition distances. Advances in acquisition sensors as well as the deployment of real-world biometric systems have led to the exploration and nascent development of unconstrained recognition systems. Iris and the periocular region, along with information fusion from the two modalities, holds significant potential for recognition of individuals at large stand-off distances.
5. **Multimodal ocular biometrics**: In literature, researchers have generally focused on single ocular modality only. However, it has been well established that multimodal biometrics approach yields better recognition results than unimodal approach. Therefore, efficiently fusing some ocular or non-ocular biometric modality with ocular ones can yield improved recognition results. Context switching or selection algorithms [9,245] can also be utilized to recognize individuals in certain conditions where it is difficult to process all the modalities together. For instance, face and iris biometrics can be combined to improve the accuracy. However, in unconstrained environments where it is difficult to capture iris, context switching can be performed to recognize the query image only using face images. This helps in increasing the number of probes that can be identified and also improves the overall accuracy.
6. **Benchmarking standards and open-source software**: The field of ocular biometrics enjoys the availability of a number of public datasets. However, apart from a few open competitions such as the Multiple Biometric Grand Challenge and the Noisy Iris Challenge Evaluations, there is a dearth of well-set protocols to benchmark the performance of ocular recognition algorithms. In the field of face recognition, the Point and Shoot Face Recognition Challenge and the Labeled Faces in the Wild Challenge provide common datasets as well as protocols to streamline the comparison between competing algorithms. Such standards allow a clear understanding of the relative merits of various recognition techniques. We assert that the ocular biometric recognition community requires such protocols to be established to allow the comparison of recognition techniques to benchmark the relative strengths and weaknesses of these algorithms. The need for benchmarking protocols is accompanied by the requirement for an initiative towards a culture of open-source software. Reproducibility of state-of-the-art results is necessary to constructively build upon the fast paced research conducted in the field of ocular biometrics.

## Acknowledgements

A part of this research is supported through a grand by the Department of Electronics and Information Technology, Government of India. The authors would like to thank the Editor-in-Chief, Associate Editor, and reviewers for their insightful feedback on the paper. The authors also acknowledge Dr. Maria De Marsico and Dr. Hugo Proença for their insightful comments.

## References

[1] M.J. Burge, K.W. Bowyer, Handbook of Iris Recognition, first ed., Springer-Verlag, London, 2013.
[2] L. Flom, A. Safir, Iris Recognition System, US Patent 4,641,349, 1987.
[3] L. Thomas, Y. Du, Z. Zhou, A new approach for sclera vein recognition, in: SPIE Conference on Mobile Multimedia/Image Processing, Security, and Applications, 2010, http://dx.doi.org/10.1117/12.849706.
[4] R.B. Hill, Apparatus and Method for Identifying Individuals through their Retinal Vasculature Patterns, US Patent 4,109,237, 1978.
[5] U. Park, A. Ross, A. Jain, Periocular biometrics in the visible spectrum: a feasibility study, in: Third IEEE International Conference on Biometrics: Theory, Applications, and Systems, 2009, pp. 1–6.
[6] The United Arab Emirates Immigration Program. <https://www.adpolice.gov.ae/> (accessed 15.03.15).
[7] Retinal Recognition: Biometric Technology in Practice. <http://www.biometricnews.net/Publications/BiometricsArticleRetinalRecognition.pdf>.
[8] A.A. Ross, K. Nandakumar, A.K. Jain, Handbook of Multibiometrics, vol. 6, Springer, 2006.
[9] M. Vatsa, R. Singh, A. Noore, A. Ross, On the dynamic selection of biometric fusion algorithms, IEEE Transactions on Information Forensics and Security 5 (3) (2010) 470–479.
[10] Unique Identification Authority of India. <http://uidai.gov.in/>.
[11] Office of Biometric Identity Management, National Protection and Programs Directorate. <http://www.dhs.gov/obim>.
[12] K.W. Bowyer, K. Hollingsworth, P.J. Flynn, Image understanding for Iris Biometrics: a survey, Comput. Vis. Image Underst. 110 (2) (2008) 281–307.
[13] K.W. Bowyer, K. Hollingsworth, P.J. Flynn, A survey of iris biometrics research: 200–2010, in: Handbook of Iris Recognition, Springer, 2013, pp. 15–54.

[14] J. Daugman, High confidence visual recognition of persons by a test of statistical independence, IEEE Trans. Pattern Anal. Mach. Intell. 15 (11) (1993) 1148–1161.

[15] J. Daugman, The importance of being random: statistical principles of iris recognition, Pattern Recogn. 36 (2) (2003) 279–291.

[16] J. Daugman, New methods in iris recognition, IEEE Trans. Syst. Man Cybern. Part B: Cybern. 37 (5) (2007) 1167–1175.

[17] A. Kong, D. Zhang, M. Kamel, An analysis of IrisCode, IEEE Trans. Image Process. 19 (2) (2010) 522–532.

[18] H. Proença, L.A. Alexandre, UBIRIS: a noisy iris image database, in: IARP Conference on Image Analysis and Processing, 2005, pp. 970–977.

[19] H. Proença, S. Filipe, R. Santos, J. Oliveira, L. Alexandre, The UBIRIS.v2: a database of visible wavelength iris images captured On-the-Move and At-a-Distance, IEEE Trans. Pattern Anal. Mach. Intell. 32 (8) (2010) 1529–1535.

[20] S. Venugopalan, M. Savvides, Unconstrained iris acquisition and recognition using COTS PTZ camera, EURASIP J. Adv. Signal Process 2010 (2010) 381–3820.

[21] S. McCloskey, W. Au, J. Jelinek, Iris capture from moving subjects using a fluttering shutter, in: Fourth IEEE International Conference on Biometrics: Theory Applications and Systems, 2010, pp. 1–6.

[22] S. Venugopalan, U. Prasad, K. Harun, K. Neblett, D. Toomey, J. Heyman, M. Savvides, Long range iris acquisition system for stationary and mobile subjects, in: International Joint Conference on Biometrics, 2011, pp. 1–8.

[23] R. Connaughton, A. Sgroi, K. Bowyer, P. Flynn, A multialgorithm analysis of three iris biometric sensors, IEEE Trans. Inf. Forensics Secur. 7 (3) (2012) 919–931.

[24] S. Tankasala, V. Gottemukkula, S. Saripalle, V. Nalamati, R. Derakhshani, R. Pasula, A. Ross, A video-based hyper-focal imaging method for iris recognition in the visible spectrum, in: IEEE Conference on Technologies for Homeland Security, 2012, pp. 214–219.

[25] C. Boehnen, D. Barstow, D. Patlolla, C. Mann, A multi-sample standoff multimodal biometric system, in: Fifth IEEE International Conference on Biometrics: Theory, Applications and Systems, 2012, pp. 127–134.

[26] E. Ortiz, K. Bowyer, P. Flynn, An optimal strategy for dilation based iris image enrollment, in: IEEE International Joint Conference on Biometrics, 2014, pp. 1–6.

[27] S. Bharadwaj, M. Vatsa, R. Singh, Biometric quality: a review of fingerprint, iris, and face, EURASIP Journal on Image and Video Processing 2014 (1).

[28] P. Phillips, W. Scruggs, A. O'Toole, P. Flynn, K. Bowyer, C. Schott, M. Sharpe, FRVT 2006 and ICE 2006 large-scale experimental results, IEEE Trans. Pattern Anal. Mach. Intell. 32 (5) (2010) 831–846.

[29] J. Liu, Z. Sun, T. Tan, A novel image deblurring method to improve iris recognition accuracy, in: IEEE International Joint Conference on Biometrics, 2011, pp. 1–8.

[30] E. Ortiz, K. Bowyer, Dilation aware multi-image enrollment for iris biometrics, in: International Joint Conference on Biometrics, 2011, pp. 1–7.

[31] Y.-H. Li, M. Savvides, An automatic iris occlusion estimation method based on high-dimensional density estimation, IEEE Trans. Pattern Anal. Mach. Intell. 35 (4) (2013) 784–796.

[32] A. Sgroi, K. Bowyer, P. Flynn, The impact of diffuse illumination on iris recognition, in: 6th IAPR International Conference on Biometrics, 2013, pp. 1–7.

[33] C.-W. Tan, A. Kumar, Adaptive and localized iris weight map for accurate iris recognition under less constrained environments, in: Sixth IEEE International Conference on Biometrics: Theory, Applications and Systems, 2013, pp. 1–7.

[34] CASIA Version 4 Database. <http://biometrics.idealtest.org/dbDetailForUser.do?id=4> (accessed 15.03.15).

[35] T. Tan, Z. He, Z. Sun, Efficient and robust segmentation of noisy iris images for non-cooperative iris recognition, Image Vis. Comput. 28 (2) (2010) 223–230.

[36] The Noisy Iris Challenge Evaluation: Part I. <http://nice1.di.ubi.pt/index.html>.

[37] X. Zhang, Z. Sun, T. Tan, Texture removal for adaptive level set based iris segmentation, in: 17th IEEE International Conference on Image Processing, 2010, pp. 1729–1732.

[38] K. Roy, C. Suen, P. Bhattacharya, Segmentation of Unideal Iris Images Using Game Theory, in: 20th International Conference on Pattern Recognition, 2010, pp. 2844–2847.

[39] NIST, Iris Challenge Evaluation Competition, 2005. <http://iris.nist.gov/ICE/> (accessed 15.03.15).

[40] S. Pundlik, D. Woodard, S. Birchfield, Iris segmentation in non-ideal images using graph cuts, Image Vis. Comput. 28 (12) (2010) 1671–1681.

[41] J. Zuo, N. Schmid, On a methodology for robust segmentation of nonideal iris images, IEEE Trans. Syst. Man Cybern. Part B: Cybern. 40 (3) (2010) 703–718.

[42] M. De Marsico, M. Nappi, R. Daniel, $IS_{IS}$: Iris Segmentation for Identification Systems, in: 20th International Conference on Pattern Recognition, 2010, pp. 2857–2860.

[43] H. Proença, Iris recognition: on the segmentation of degraded images acquired in the visible wavelength, IEEE Trans. Pattern Anal. Mach. Intell. 32 (8) (2010) 1502–1516.

[44] J. Koh, V. Govindaraju, V. Chaudhary, A robust iris localization method using an active contour model and hough transform, in: 20th International Conference on Pattern Recognition, 2010, pp. 2852–2856.

[45] Y. Du, E. Arslanturk, Z. Zhou, C. Belcher, Video-based noncooperative iris image segmentation, IEEE Trans. Syst. Man Cybern. Part B: Cybern. 41 (1) (2011) 64–74.

[46] C.-W. Tan, A. Kumar, Automated segmentation of iris images using visible wavelength face images, in: IEEE Computer Society Conference on Computer Vision and Pattern Recognition Workshops, 2011, pp. 9–14.

[47] C.-W. Tan, A. Kumar, Unified framework for automated iris segmentation using distantly acquired face images, IEEE Trans. Image Process. 21 (9) (2012) 4068–4079.

[48] G. Sutra, S. Garcia-Salicetti, B. Dorizzi, The viterbi algorithm at different resolutions for enhanced iris segmentation, in: 5th IAPR International Conference on Biometrics, 2012, pp. 310–316.

[49] H. Li, Z. Sun, T. Tan, Robust iris segmentation based on learned boundary detectors, in: 5th IAPR International Conference on Biometrics, 2012, pp. 317–322.

[50] C. Fernandez, D. Perez, C. Segura, J. Hernando, A novel method for low-constrained iris boundary localization, in: 5th IAPR International Conference on Biometrics, 2012, pp. 291–296.

[51] Herta Iris Database. <http://research.hertasecurity.com/datasets/HID> (accessed 15.03.15).

[52] C.-W. Tan, A. Kumar, Efficient iris segmentation using Grow-Cut algorithm for remotely acquired iris images, in: Fifth IEEE International Conference on Biometrics: Theory, Applications and Systems, 2012, pp. 99–104.

[53] A. Uhl, P. Wild, Weighted adaptive Hough and ellipsopolar transforms for real-time iris segmentation, in: 5th IAPR International Conference on Biometrics, 2012, pp. 283–290.

[54] H. Li, Z. Sun, T. Tan, Accurate iris localization using contour segments, in: 21st International Conference on Pattern Recognition, 2012, pp. 3398–3401.

[55] F. Alonso-Fernandez, J. Bigun, Iris boundaries segmentation using the generalized structure tensor. A study on the effects of image degradation, in: Fifth International Conference on Biometrics: Theory, Applications and Systems, 2012, pp. 426–431.

[56] F. Alonso-Fernandez, J. Bigun, Quality factors affecting iris segmentation and matching, in: 6th IAPR International Conference on Biometrics, 2013, pp. 1–6.

[57] J. Fierrez, J. Ortega-Garcia, D.T. Toledano, J. Gonzalez-Rodriguez, Biosec baseline corpus: a multimodal biometric database, Pattern Recogn. 40 (4) (2007) 1389–1392.

[58] C.-W. Tan, A. Kumar, Towards online iris and periocular recognition under relaxed imaging constraints, IEEE Trans. Image Process. 22 (10) (2013) 3751–3765.

[59] R.R. Jillela, A. Ross, Segmenting iris images in the visible spectrum with applications in mobile biometrics, Pattern Recognit. Lett. (2014), http://dx.doi.org/10.1016/j.patrec.2014.09.014.

[60] Y. Hu, K. Sirlantzis, G. Howells, A robust algorithm for colour iris segmentation based on $l_1$-norm regression, in: IEEE International Joint Conference on Biometrics, 2014, pp. 1–8.

[61] CASIA Version 3 Database. <http://biometrics.idealtest.org/dbDetailForUser.do?id=3> (accessed 15.03.15).

[62] S. Crihalmeanu, A. Ross, S. Schuckers, L. Hornak, A protocol for multibiometric data acquisition, storage and dissemination, WVU, Lane Department Computer Science, Technical Report.

[63] Center for Identification Technology Research (CITeR), West Virginia University Off-angle Iris Database, <http://www.citer.wvu.edu/> (accessed 15.03.15).

[64] NIST, Face Recognition Grand Challenge Version 1. <http://www.nist.gov/itl/iad/ig/frgc.cfm> (accessed 15.03.15).

[65] M. Sunder, A. Ross, Iris image retrieval based on macro-features, in: 20th International Conference on Pattern Recognition, 2010, pp. 1318–1321.

[66] Miles Research Database. <http://www.milesresearch.com/> (accessed 15.03.15).

[67] Y. Zhou, A. Kumar, Personal identification from iris images using localized radon transform, in: 20th International Conference on Pattern Recognition, 2010, pp. 2840–2843.

[68] F. Scotti, V. Piuri, Adaptive reflection detection and location in iris biometric images by using computational intelligence techniques, IEEE Trans. Instrum. Meas. 59 (7) (2010) 1825–1833.

[69] M. Hosseini, B. Araabi, H. Soltanian-Zadeh, Pigment melanin: pattern for iris recognition, IEEE Trans. Instrum. Meas. 59 (4) (2010) 792–804.

[70] K. Roy, P. Bhattacharya, C. Suen, J. You, Recognition of unideal iris images using region-based active contour model and game theory, in: 17th IEEE International Conference on Image Processing, 2010, pp. 1705–1708.

[71] K. Hollingsworth, K. Bowyer, P. Flynn, Improved Iris recognition through fusion of hamming distance and fragile bit distance, IEEE Trans. Pattern Anal. Mach. Intell. 33 (12) (2011) 2465–2476.

[72] H. Proença, Iris biometrics: indexing and retrieving heavily degraded data, IEEE Trans. Inf. Forensics Secur. 8 (12) (2013) 1975–1985.

[73] M. Zhang, Z. Sun, T. Tan, Deformable DAISY Matcher for robust iris recognition, in: 18th IEEE International Conference on Image Processing, 2011, pp. 3189–3192.

[74] A. Bastys, J. Kranauskas, V. Krger, Iris recognition by fusing different representations of multi-scale Taylor expansion, Comput. Vis. Image Underst. 115 (6) (2011) 804–816.

[75] H. Proença, G. Santos, Fusing color and shape descriptors in the recognition of degraded iris images acquired at visible wavelengths, Comput. Vis. Image Underst. 116 (2) (2012) 167–178.

[76] A. Kumar, T.-S. Chan, C.-W. Tan, Human identification from at-a-distance face images using sparse representation of local iris features, in: 5th IAPR International Conference on Biometrics, 2012, pp. 303–309.

[77] P. Li, G. Wu, Iris recognition using ordinal encoding of log-euclidean covariance matrices, in: 21st International Conference on Pattern Recognition, 2012, pp. 2420–2423.
[78] A. Rahulkar, R. Holambe, Half-iris feature extraction and recognition using a new class of biorthogonal triplet half-band filter bank and flexible k-out-of-n: a postclassifier, IEEE Trans. Inf. Forensics Secur. 7 (1) (2012) 230–240.
[79] M. Zhang, Z. Sun, T. Tan, Perturbation-enhanced feature correlation filter for robust iris recognition, IET Biometrics 1 (1) (2012) 37–45.
[80] R. da Costa, A. Gonzaga, Gonzaga, dynamic features for iris recognition, IEEE Trans. Syst. Man Cybern. Part B: Cybern. 42 (4) (2012) 1072–1082.
[81] X. Liu, P. Li, Tensor decomposition of SIFT descriptors for person identification, in: 5th IAPR International Conference on Biometrics, 2012, pp. 265–270.
[82] A. Kumar, T.-S. Chan, Iris recognition using quaternionic sparse orientation code (QSOC), in: IEEE Computer Society Conference on Computer Vision and Pattern Recognition Workshops, 2012, pp. 59–64.
[83] H. Zhang, Z. Sun, T. Tan, J. Wang, Iris image classification based on color information, in: 21st International Conference on Pattern Recognition, 2012, pp. 3427–3430.
[84] L. Wang, Z. Sun, T. Tan, Robust regularized feature selection for iris recognition via linear programming, in: 21st International Conference on Pattern Recognition, 2012, pp. 3358–3361.
[85] K. Nguyen, S. Sridharan, S. Denman, C. Fookes, Feature-domain super-resolution framework for Gabor-based face and iris recognition, in: IEEE Conference on Computer Vision and Pattern Recognition, 2012, pp. 2642–2649.
[86] M. Zhang, Z. Sun, T. Tan, Deformed iris recognition using bandpass geometric features and lowpass ordinal features, in: 6th IAPR International Conference on Biometrics, 2013, pp. 1–6.
[87] Z. Sun, H. Zhang, T. Tan, J. Wang, Iris image classification based on hierarchical visual codebook, IEEE Trans. Pattern Anal. Mach. Intell. 36 (6) (2014) 1120–1133.
[88] Institute of Automation, Chinese Academy of Sciences, CASIA-Iris-Fake Database. <http://www.cripac.ia.ac.cn/people/znsun/irisclassification/CASIA-Iris-Fake.rar> (accessed 15.03.15).
[89] Z. Sun, L. Wang, T. Tan, Ordinal feature selection for iris and palmprint recognition, IEEE Trans. Image Process. 23 (9) (2014) 3922–3934.
[90] C.W. Tan, A. Kumar, Accurate Iris Recognition at a Distance Using Stabilized Iris Encoding and Zernike Moments Phase Features, IEEE Transactions on Image Processing 23 (9) (2014) 3962–3974.
[91] C.-W. Tan, A. Kumar, Efficient and Accurate At-a-Distance Iris Recognition Using Geometric Key-Based Iris Encoding, IEEE Transactions on Information Forensics and Security 9 (9) (2014) 1518–1526.
[92] A. Nigam, V. Krishna, A. Bendale, P. Gupta, Iris recognition using block local binary patterns and relational measures, in: International Joint Conference on Biometrics, 2014, pp. 1–6.
[93] IIT Delhi Iris Database (Version 1.0). <http://www4.comp.polyu.edu.hk/csajaykr/IITD/DatabaseIris.htm> (accessed 15.03.15).
[94] CASIA Version 1 Database. <http://biometrics.idealtest.org/dbDetailForUser.do?id=1> (accessed 15.03.15).
[95] CASIA Version 2 Database. <http://biometrics.idealtest.org/dbDetailForUser.do?id=2> (accessed 15.03.15).
[96] P. Phillips, P. Flynn, J. Beveridge, W. Scruggs, A. OToole, D. Bolme, K. Bowyer, B. Draper, G. Givens, Y. Lui, H. Sahibzada, I. Scallan, JosephA, S. Weimer, Overview of the multiple biometrics grand challenge, in: Advances in Biometrics, Lecture Notes in Computer Science, vol. 5558, Springer, Berlin Heidelberg, 2009, pp. 705–714.
[97] C. Rathgeb, A. Uhl, P. Wild, Incremental iris recognition: a single-algorithm serial fusion strategy to optimize time complexity, in: Fourth IEEE International Conference on Biometrics: Theory Applications and Systems, 2010, pp. 1–6.
[98] R. Gadde, D. Adjeroh, A. Ross, Indexing iris images using the Burrows-Wheeler Transform, in: IEEE International Workshop on Information Forensics and Security, 2010, pp. 1–6.
[99] N. Vandal, M. Savvides, CUDA accelerated iris template matching on Graphics Processing Units (GPUs), in: Fourth IEEE International Conference on Biometrics: Theory Applications and Systems, 2010, pp. 1–7.
[100] H. Proença, An iris recognition approach through structural pattern analysis methods, Expert Syst. 27 (1) (2010) 6–16.
[101] W. Dong, Z. Sun, T. Tan, Iris matching based on personalized weight map, IEEE Trans. Pattern Anal. Mach. Intell. 33 (9) (2011) 1744–1757.
[102] R. Farouk, Iris recognition based on elastic graph matching and Gabor wavelets, Comput. Vis. Image Underst. 115 (8) (2011) 1239–1244.
[103] A. Gyaourova, A. Ross, Index codes for multibiometric pattern retrieval, IEEE Trans. Inf. Forensics Secur. 7 (2) (2012) 518–529.
[104] S. Dey, D. Samanta, Iris data indexing method using Gabor energy features, IEEE Trans. Inf. Forensics Secur. 7 (4) (2012) 1192–1203.
[105] C.-C. Tsai, H.-Y. Lin, J. Taur, C.-W. Tao, Iris recognition using possibilistic fuzzy matching on local features, IEEE Trans. Syst. Man Cybern. Part B: Cybern. 42 (1) (2012) 150–162.
[106] T. Tan, X. Zhang, Z. Sun, H. Zhang, Noisy iris image matching by using multiple cues, Pattern Recogn. Lett. 33 (8) (2012) 970–977.
[107] Q. Wang, X. Zhang, M. Li, X. Dong, Q. Zhou, Y. Yin, Adaboost and multi-orientation 2D Gabor-based noisy iris recognition, Pattern Recogn. Lett. 33 (8) (2012) 978–983.
[108] G. Santos, E. Hoyle, A fusion approach to unconstrained iris recognition, Pattern Recogn. Lett. 33 (8) (2012) 984–990.
[109] K.Y. Shin, G.P. Nam, D.S. Jeong, D.H. Cho, B.J. Kang, K.R. Park, J. Kim, New iris recognition method for noisy iris images, Pattern Recogn. Lett. 33 (8) (2012) 991–999.
[110] P. Li, X. Liu, N. Zhao, Weighted co-occurrence phase histogram for iris recognition, Pattern Recogn. Lett. 33 (8) (2012) 1000–1005.
[111] M. De Marsico, M. Nappi, D. Riccio, Noisy iris recognition integrated scheme, Pattern Recogn. Lett. 33 (8) (2012) 1006–1011.
[112] P. Li, H. Ma, Iris recognition in non-ideal imaging conditions, Pattern Recogn. Lett. 33 (8) (2012) 1012–1018.
[113] R. Szewczyk, K. Grabowski, M. Napieralska, W. Sankowski, M. Zubert, A. Napieralski, A reliable iris recognition algorithm based on reverse biorthogonal wavelet transform, Pattern Recogn. Lett. 33 (8) (2012) 1019–1026.
[114] J. Liu, Z. Sun, T. Tan, Code-level information fusion of low-resolution iris image sequences for personal identification at a distance, in: Sixth IEEE International Conference on Biometrics: Theory, Applications and Systems, 2013, pp. 1–6.
[115] P. Johnson, P. Lopez-Meyer, N. Sazonova, F. Hua, S. Schuckers, Quality in face and iris research ensemble (Q-FIRE), in: Fourth IEEE International Conference on Biometrics: Theory Applications and Systems, 2010, pp. 1–6.
[116] I. Tomeo-Reyes, V. Chandran, Decision fusion from parts and samples for robust iris recognition, in: Sixth IEEE International Conference on Biometrics: Theory, Applications and Systems, 2013, pp. 1–6.
[117] J. Liu, Z. Sun, T. Tan, Distance metric learning for recognizing low-resolution iris images, Neurocomputing 144 (2014) 484–492.
[118] R. Gross, I. Matthews, J. Cohn, T. Kanade, S. Baker, Multi-PIE, Image Vis. Comput. 28 (5) (2010) 807–813.
[119] BATH Iris Database, University of Bath Iris Image Database. <http://www.bath.ac.uk/eleceng/research/sipg/irisweb/> (accessed 15.03.15).
[120] DARPA, The Facial Recognition Technology Database. <http://www.itl.nist.gov/iad/humanid/feret/feretmaster.html> (accessed 15.03.15).
[121] C.-T. Chou, S.-W. Shih, W.-S. Chen, V. Cheng, D.-Y. Chen, Non-orthogonal view iris recognition system, IEEE Trans. Circuits Syst. Video Technol. 20 (3) (2010) 417–430.
[122] A. Abhyankar, S. Schuckers, A novel biorthogonal wavelet network system for off-angle iris recognition, Pattern Recogn. 43 (3) (2010) 987–1007.
[123] H. Santos-Villalobos, D. Barstow, M. Karakaya, C. Boehnen, E. Chaum, ORNL biometric eye model for iris recognition, in: Fifth International Conference on Biometrics: Theory, Applications and Systems, 2012, pp. 176–182.
[124] X. Li, L. Wang, Z. Sun, T. Tan, A feature-level solution to off-angle iris recognition, in: 6th IAPR International Conference on Biometrics, 2013, pp. 1–6.
[125] S.E. Baker, A. Hentz, K.W. Bowyer, P.J. Flynn, Degradation of iris recognition performance due to non-cosmetic prescription contact lenses, Comput. Vis. Image Underst. 114 (9) (2010) 1030–1044.
[126] S. Venugopalan, M. Savvides, How to generate spoofed irises from an iris code template?, IEEE Trans Inf. Forensics Secur. 6 (2) (2011) 385–395.
[127] S. Arora, M. Vatsa, R. Singh, A. Jain, Iris recognition under alcohol influence: a preliminary study, in: 5th IAPR International Conference on Biometrics, 2012, pp. 336–341.
[128] N. Kohli, D. Yadav, M. Vatsa, R. Singh, Revisiting iris recognition with color cosmetic contact lenses, in: 6th IAPR International Conference on Biometrics, 2013, pp. 1–7.
[129] D. Yadav, N. Kohli, J. Doyle, R. Singh, M. Vatsa, K. Bowyer, Unraveling the effect of textured contact lenses on iris recognition, IEEE Trans. Inf. Forensics Secur. 9 (5) (2014) 851–862.
[130] P. Gupta, S. Behera, M. Vatsa, R. Singh, On iris spoofing using print attack, in: IEEE International Conference on Pattern Recognition, 2014, pp. 205–208.
[131] J. Komulainen, A. Hadid, M. Pietikainen, Generalized textured contact lens detection by extracting BSIF description from Cartesian iris images, in: IEEE International Joint Conference on Biometrics, 2014, pp. 1–7.
[132] J. Doyle, K. Bowyer, P. Flynn, Variation in accuracy of textured contact lens detection based on sensor and lens pattern, in: Sixth IEEE International Conference on Biometrics: Theory, Applications and Systems, 2013, pp. 1–7.
[133] J. Pillai, V. Patel, R. Chellappa, N. Ratha, Secure and robust iris recognition using random projections and sparse representations, IEEE Trans. Pattern Anal. Mach. Intell. 33 (9) (2011) 1877–1893.
[134] X. Huang, B. Fu, C. Ti, A. Tokuta, R. Yang, Robust varying-resolution iris recognition, in: Fifth IEEE International Conference on Biometrics: Theory, Applications and Systems, 2012, pp. 47–54.
[135] S.P. Fenker, K.W. Bowyer, Experimental evidence of a template aging effect in iris biometrics, in: IEEE Workshop on Applications of Computer Vision, 2011, pp. 232–239.
[136] D. Rankin, B. Scotney, P. Morrow, B. Pierscionek, Iris recognition failure over time: the effects of texture, Pattern Recogn. 45 (1) (2012) 145–150.
[137] S. Fenker, E. Ortiz, K. Bowyer, Template aging phenomenon in iris recognition, IEEE Access 1 (2013) 266–274.
[138] T.Bergmüller, L.Debiasi, A.Uhl, Z.Sun, Impact of sensor ageing on iris recognition, in:IEEE International Joint Conference on Biometrics, 2014, pp. 1–8.
[139] H. Mehrotra, M. Vatsa, R. Singh, B. Majhi, Does iris change over time? PloS ONE 8(11), <http://dx.doi.org/10.1371/journal.pone.0078333>.

[140] J. Zuo, F. Nicolo, N. Schmid, Cross spectral iris matching based on predictive image mapping, in: Fourth IEEE International Conference on Biometrics: Theory Applications and Systems, 2010, pp. 1–5.
[141] Y. Gong, D. Zhang, P. Shi, J. Yan, An optimized wavelength band selection for heavily pigmented iris recognition, IEEE Trans. Inf. Forensics Secur. 8 (1) (2013) 64–75.
[142] S. Arora, M. Vatsa, R. Singh, A. Jain, On iris camera interoperability, in: Fifth International Conference on Biometrics: Theory, Applications and Systems, 2012, pp. 346–352.
[143] L. Xiao, Z. Sun, R. He, T. Tan, Coupled feature selection for cross-sensor iris recognition, in: Sixth IEEE International Conference on Biometrics: Theory, Applications and Systems, 2013, pp. 1–6.
[144] J.K. Pillai, M. Puertas, R. Chellappa, Cross-sensor iris recognition through kernel learning, IEEE Trans. Pattern Anal. Mach. Intell. 36 (1) (2014) 73–85.
[145] A. Sgroi, K. Bowyer, P. Flynn, Cross sensor iris recognition competition, in: IEEE International Conference on Biometrics: Theory, Applications, and Systems, 2012.
[146] A. Abhyankar, S. Schuckers, Iris quality assessment and bi-orthogonal wavelet based encoding for recognition, Pattern Recogn. 42 (9) (2009) 1878–1894.
[147] J.S. Doyle, K.W. Bowyer, P.J. Flynn, Variation in accuracy of textured contact lens detection based on sensor and lens pattern, in: Sixth IEEE International Conference on Biometrics: Theory, Applications and Systems, IEEE, 2013, pp. 1–7.
[148] S. Fenker, K. Bowyer, Analysis of template aging in iris biometrics, in: IEEE Computer Society Conference on Computer Vision and Pattern Recognition Workshops, 2012, pp. 45–51.
[149] S. Baker, K. Bowyer, P. Flynn, P. Phillips, Template aging in iris biometrics: evidence of increased false reject rate in ICE 2006, Handbook Iris Recogn. (2013) 205–218.
[150] C. Boyce, A. Ross, M. Monaco, L. Hornak, X. Li, Multispectral iris analysis: a preliminary study, in: IEEE International Conference on Computer Vision and Pattern Recognition Workshops, 2006, pp. 51–51.
[151] ND-Cross Sensor Database, University of Notre Dame. <http://www3.nd.edu/cvrl/CVRL/DataSets.html> (accessed 15.03.15).
[152] V. Boddeti, B. Kumar, Extended-depth-of-field iris recognition using unrestored wavefront-coded imagery, IEEE Trans. Syst. Man Cybern. Part A: Syst. Humans 40 (3) (2010) 495–508.
[153] L. Stark, K. Bowyer, S. Siena, Human perceptual categorization of iris texture patterns, in: Fourth IEEE International Conference on Biometrics: Theory Applications and Systems, 2010, pp. 1–7.
[154] K. Nguyen, C. Fookes, S. Sridharan, S. Denman, Quality-driven super-resolution for less constrained iris recognition at a distance and on the move, IEEE Trans. Inf. Forensics Secur. 6 (4) (2011) 1248–1258.
[155] K. Hollingsworth, K.W. Bowyer, S. Lagree, S.P. Fenker, P.J. Flynn, Genetically identical irises have texture similarity that is not detected by iris biometrics, Comput. Vis. Image Underst. 115 (11) (2011) 1493–1502.
[156] Y. Si, J. Mei, H. Gao, Novel approaches to improve robustness, accuracy and rapidity of iris recognition systems, IEEE Trans. Ind. Inf. 8 (1) (2012) 110–117.
[157] A.-K. Kong, IrisCode decompression based on the dependence between its bit pairs, IEEE Trans. Pattern Anal. Mach. Intell. 34 (3) (2012) 506–520.
[158] C. Rathgeb, A. Uhl, P. Wild, Iris-biometric comparators: exploiting comparison scores towards an optimal alignment under Gaussian assumption, in: 5th IAPR International Conference on Biometrics, 2012, pp. 297–302.
[159] J. Galbally, A. Ross, M. Gomez-Barrero, J. Fierrez, J. Ortega-Garcia, Iris image reconstruction from binary templates: an efficient probabilistic approach based on genetic algorithms, Comput. Vis. Image Underst. 117 (10) (2013) 1512–1525.
[160] A. Sgroi, K. Bowyer, P. Flynn, The prediction of old and young subjects from iris texture, in: 6th IAPR International Conference on Biometrics, 2013, pp. 1–5.
[161] K. McGinn, S. Tarin, K. Bowyer, Identity verification using iris images: performance of human examiners, in: Sixth IEEE International Conference on Biometrics: Theory, Applications and Systems, 2013, pp. 1–6.
[162] U. Park, R. Jillela, A. Ross, A. Jain, Periocular biometrics in the visible spectrum, IEEE Trans. Inf. Forensics Secur. 6 (1) (2011) 96–106.
[163] S. Bharadwaj, H. Bhatt, M. Vatsa, R. Singh, Periocular biometrics: when iris recognition fails, in: Fourth IEEE International Conference on Biometrics: Theory Applications and Systems, 2010, pp. 1–6.
[164] J. Xu, M. Cha, J. Heyman, S. Venugopalan, R. Abiantun, M. Savvides, Robust local binary pattern feature sets for periocular biometric identification, in: Fourth IEEE International Conference on Biometrics: Theory Applications and Systems, 2010, pp. 1–8.
[165] D. Woodard, S. Pundlik, J. Lyle, P. Miller, Periocular region appearance cues for biometric identification, in: IEEE Computer Society Conference on Computer Vision and Pattern Recognition Workshops, 2010, pp. 162–169.
[166] P. Miller, J. Lyle, S. Pundlik, D. Woodard, Performance evaluation of local appearance based periocular recognition, in: Fourth IEEE International Conference on Biometrics: Theory Applications and Systems, 2010, pp. 1–6.
[167] P.E. Miller, A.W. Rawls, S.J. Pundlik, D.L. Woodard, Personal identification using periocular skin texture, in: ACM Symposium on Applied Computing, ACM, 2010, pp. 1496–1500.
[168] J. Adams, D. Woodard, G. Dozier, P. Miller, K. Bryant, G. Glenn, Genetic-based type II feature extraction for periocular biometric recognition: less is more, in: Twentieth IEEE International Conference on Pattern Recognition, 2010, pp. 205–208.
[169] D. Woodard, S. Pundlik, P. Miller, J. Lyle, Appearance-based periocular features in the context of face and non-ideal iris recognition, SIViP 5 (4) (2011) 443–455.
[170] C. Padole, H. Proença, Periocular recognition: analysis of performance degradation factors, in: Fifth IAPR International Conference on Biometrics, 2012, pp. 439–445.
[171] F. Juefei-Xu, M. Savvides, Unconstrained periocular biometric acquisition and recognition using COTS PTZ camera for uncooperative and non-cooperative subjects, in: IEEE Workshop on Applications of Computer Vision, 2012, pp. 201–208.
[172] C.N. Padole, H. Proença, Compensating for pose and illumination in unconstrained periocular biometrics, Int. J. Biometrics 5 (3) (2013) 336–359.
[173] H. Proença, J.C. Briceño, Periocular biometrics: constraining the elastic graph matching algorithm to biologically plausible distortions, IET Biometrics 3 (2014) 167–175 (8).
[174] F. Juefei-Xu, M. Savvides, Subspace-based discrete transform encoded local binary patterns representations for robust periocular matching on face recognition grand challenge, IEEE Trans. Image Process. 23 (8) (2014) 3490–3505.
[175] A. Sharma, S. Verma, M. Vatsa, R. Singh, On cross spectral periocular recognition, in: IEEE International Conference on Image Processing, 2014, pp. 5007–5011.
[176] G. Mahalingam, K. Ricanek, A. Albert, Investigating the periocular-based face recognition across gender transformation, IEEE Trans. Inf. Forensics Secur. 9 (12) (2014) 2180–2192.
[177] G. Mahalingam, K. Ricanek, Is the eye region more reliable than the face? A preliminary study of face-based recognition on a transgender dataset, in: Sixth IEEE International Conference on Biometrics: Theory, Applications and Systems, 2013, pp. 1–7.
[178] H. Proença, J. Neves, G. Santos, Segmenting the periocular region using a hierarchical graphical model fed by texture/shape information and geometrical constraints, in: IEEE International Joint Conference on Biometrics, 2014, pp. 1–7.
[179] F. Juefei-Xu, K. Luu, M. Savvides, T. Bui, C. Suen, Investigating age invariant face recognition based on periocular biometrics, in: IEEE International Joint Conference on Biometrics, 2011, pp. 1–7.
[180] J. Lyle, P. Miller, S. Pundlik, D. Woodard, Soft biometric classification using periocular region features, in: Fourth IEEE International Conference on Biometrics: Theory Applications and Systems, 2010, pp. 1–7.
[181] J.R. Lyle, P.E. Miller, S.J. Pundlik, D.L. Woodard, Soft biometric classification using local appearance periocular region features, Pattern Recogn. 45 (11) (2012) 3877–3885.
[182] P. Sinha, B. Balas, Y. Ostrovsky, R. Russell, Face recognition by humans: nineteen results all computer vision researchers should know about, Proc. IEEE 94 (11) (2006) 1948–1962.
[183] K. Hollingsworth, K. Bowyer, P. Flynn, Identifying useful features for recognition in near-infrared periocular images, in: Fourth IEEE International Conference on Biometrics: Theory Applications and Systems, 2010, pp. 1–8.
[184] K. Hollingsworth, K.W. Bowyer, P.J. Flynn, Useful features for human verification in near-infrared periocular images, Image Vis. Comput. 29 (11) (2011) 707–715.
[185] K. Hollingsworth, S. Darnell, P. Miller, D. Woodard, K. Bowyer, P. Flynn, Human and machine performance on periocular biometrics under near-infrared light and visible light, IEEE Trans. Inf. Forensics Secur. 7 (2) (2012) 588–601.
[186] A. Arakala, S. Davis, K. Horadam, Retina features based on vessel graph substructures, in: International Joint Conference on Biometrics, 2011, pp. 1–6.
[187] VARIA, Varia Retinal Images for Authentication. <http://www.varpa.es/varia.html> (accessed 15.03.15).
[188] J. Jeffers, S. Davis, K. Horadam, Estimating individuality in feature point based retina templates, in: 5th IAPR International Conference on Biometrics, 2012, pp. 454–459.
[189] S. Lajevardi, A. Arakala, S. Davis, K. Horadam, Retina verification system based on biometric graph matching, IEEE Trans. Image Process. 22 (9) (2013) 3625–3635.
[190] O.V. Komogortsev, S. Jayarathna, C.R. Aragon, M. Mahmoud, Biometric identification via an oculomotor plant mathematical model, in: Proceedings of the 2010 Symposium on Eye-Tracking Research, 2010, pp. 57–60.
[191] C. Holland, O. Komogortsev, Biometric identification via eye movement scanpaths in reading, in: International Joint Conference on Biometrics, 2011, pp. 1–8.
[192] C. Holland, O. Komogortsev, Complex eye movement pattern biometrics: the effects of environment and stimulus, IEEE Trans. Inf. Forensics Secur. 8 (12) (2013) 2115–2126.
[193] Y. Dong, D. Woodard, Eyebrow shape-based features for biometric recognition and gender classification: a feasibility study, in: International Joint Conference on Biometrics, 2011, pp. 1–8.
[194] S. Crihalmeanu, A. Ross, On the use of multispectral conjunctival vasculature as a soft biometric, in: IEEE Workshop on Applications of Computer Vision, 2011, pp. 204–211.
[195] Z. Zhou, E. Du, N. Thomas, E. Delp, A new human identification method: sclera recognition, IEEE Trans. Syst. Man Cybern. Part A: Syst. Humans 42 (3) (2012) 571–583.

[196] K. Oh, K.-A. Toh, Extracting sclera features for cancelable identity verification, in: 5th IAPR International Conference on Biometrics, 2012, pp. 245–250.
[197] I. Rigas, G. Economou, S. Fotopoulos, Human eye movements as a trait for biometrical identification, in: Fifth IEEE International Conference on Biometrics: Theory, Applications and Systems, 2012, pp. 217–222.
[198] P. Kasprowski, J. Ober, Enhancing eye-movement-based biometric identification method by using voting classifiers, 2005.
[199] S. Crihalmeanu, A. Ross, Multispectral scleral patterns for ocular biometric recognition, Pattern Recogn. Lett. 33 (14) (2012) 1860–1869.
[200] I. Rigas, G. Economou, S. Fotopoulos, Biometric identification based on the eye movements and graph matching techniques, Pattern Recogn. Lett. 33 (6) (2012) 786–792.
[201] A. Darwish, M. Pasquier, Biometric identification using the dynamic features of the eyes, in: Sixth IEEE International Conference on Biometrics: Theory, Applications and Systems, 2013, pp. 1–6.
[202] Y. Lin, E. Du, Z. Zhou, N. Thomas, An efficient parallel approach for sclera vein recognition, IEEE Trans. Inf. Forensics Secur. 9 (2) (2014) 147–157.
[203] I. Rigas, O. Komogortsev, Biometric Recognition via Probabilistic Spatial Projection of Eye Movement Trajectories in Dynamic Visual Environments, IEEE Transactions on Information Forensics and Security 9 (10) (2014) 1743–1754.
[204] V. Cantoni, C. Galdi, M. Nappi, M. Porta, D. Riccio, GANT: gaze analysis technique for human identification, Pattern Recogn. 48 (4) (2015) 1027–1038.
[205] X. Sun, H. Yao, R. Ji, X.M. Liu, Toward statistical modeling of saccadic eye-movement and visual saliency, IEEE Trans. Image Process. 23 (11) (2014) 4649–4662.
[206] N. Bruce, J. Tsotsos, Saliency based on information maximization, Advances in Neural Information Processing Systems, vol. 18, MIT Press, 2006, pp. 155–162.
[207] Eye Movement Biometric Database v2. <http://cs.txstate.edu/ok11/embdv2.html> (accessed 15.03.15).
[208] M. Vatsa, R. Singh, A. Ross, A. Noore, Quality-based fusion for multichannel iris recognition, in: 20th International Conference on Pattern Recognition, 2010, pp. 1314–1317.
[209] A. Kumar, A. Passi, Comparison and combination of iris matchers for reliable personal identification, in: IEEE Computer Society Conference on Computer Vision and Pattern Recognition Workshops, 2008, pp. 1–7.
[210] D. Woodard, S. Pundlik, P. Miller, R. Jillela, A. Ross, On the fusion of periocular and iris biometrics in non-ideal imagery, in: 20th International Conference on Pattern Recognition, 2010, pp. 201–204.
[211] C. Rathgeb, A. Uhl, P. Wild, Reliability-balanced feature level fusion for fuzzy commitment scheme, in: International Joint Conference on Biometrics, 2011, pp. 1–7.
[212] C.-W. Tan, A. Kumar, Human identification from at-a-distance images by simultaneously exploiting iris and periocular features, in: 21st International Conference on Pattern Recognition, 2012, pp. 553–556.
[213] V. Gottemukkula, S. Saripalle, S. Tankasala, R. Derakhshani, R. Pasula, A. Ross, Fusing iris and conjunctival vasculature: Ocular biometrics in the visible spectrum, in: IEEE Conference on Technologies for Homeland Security, 2012, pp. 150–155.
[214] V. Yano, A. Zimmer, L.L. Ling, Multimodal biometric authentication based on iris pattern and pupil light reflex, in: 21st International Conference on Pattern Recognition, 2012, pp. 2857–2860.
[215] A. Ross, R. Jillela, J. Smereka, V. Boddeti, B. Kumar, R. Barnard, X. Hu, P. Pauca, R. Plemmons, Matching highly non-ideal ocular images: An information fusion approach, in: 5th IAPR International Conference on Biometrics, 2012, pp. 446–453.
[216] NIST Face and Ocular Challenge Series Database. <http://www.nist.gov/itl/iad/ig/focs.cfm> (accessed 15.03.15).
[217] O. Komogortsev, A. Karpov, C. Holland, H. Proença, Multimodal ocular biometrics approach: A feasibility study, in: Fifth IEEE International Conference on Biometrics: Theory, Applications and Systems, 2012, pp. 209–216.
[218] H. Mehrotra, M. Vatsa, R. Singh, B. Majhi, Biometric match score fusion using RVM: a case study in multi-unit iris recognition, in: IEEE Computer Society Conference on Computer Vision and Pattern Recognition Workshops, 2012, pp. 65–70.
[219] O. Komogortsev, C. Holland, Biometric authentication via complex oculomotor behavior, in: Sixth IEEE International Conference on Biometrics: Theory, Applications and Systems, 2013, pp. 1–8.
[220] R. Jillela, A. Ross, Matching face against iris images using periocular information, in: IEEE International Conference on Image Processing, 2014, pp. 4997–5001.
[221] H. Proença, Ocular Biometrics by Score-Level Fusion of Disparate Experts, IEEE Transactions on Image Processing 23 (12) (2014) 5082–5093.
[222] V. Conti, C. Militello, F. Sorbello, S. Vitabile, A frequency-based approach for features fusion in fingerprint and iris multimodal biometric identification systems, IEEE Trans. Syst. Man Cybern. Part C: Appl. Rev. 40 (4) (2010) 384–395.
[223] Fingerprint Verification Competition 2002 Database. <http://bias.csr.unibo.it/fvc2002/> (accessed 15.03.15).
[224] X. Zhang, Z. Sun, T. Tan, Hierarchical fusion of face and iris for personal identification, in: 20th International Conference on Pattern Recognition, 2010, pp. 217–220.
[225] W. Dong, Z. Sun, T. Tan, A design of iris recognition system at a distance, in: Chinese Conference on Pattern Recognition, 2009, pp. 1–5.
[226] P. Johnson, F. Hua, S. Schuckers, Comparison of quality-based fusion of face and iris biometrics, in: International Joint Conference on Biometrics, 2011, pp. 1–5.
[227] T. Murakami, K. Takahashi, Fast and accurate biometric identification using score level indexing and fusion, in: International Joint Conference on Biometrics, 2011, pp. 1–8.
[228] N. Poh, T. Bourlai, J. Kittler, A multimodal biometric test bed for quality-dependent, cost-sensitive and client-specific score-level fusion algorithms, Pattern Recogn. 43 (3) (2010) 1094–1105.
[229] CASIA v5 Fingerprint Database. <http://biometrics.idealtest.org/> (accessed 15.03.15).
[230] A. Nagar, K. Nandakumar, A. Jain, Multibiometric cryptosystems based on feature-level fusion, IEEE Trans. Inf. Forensics Secur. 7 (1) (2012) 255–268.
[231] The Multi Modal Verification for Teleservices and Security applications Database. <http://www.ee.surrey.ac.uk/CVSSP/xm2vtsdb/> (accessed 15.03.15).
[232] R. Jillela, A. Ross, Mitigating effects of plastic surgery: fusing face and ocular biometrics, in: Fifth IEEE International Conference on Biometrics: Theory, Applications and Systems, 2012, pp. 402–411.
[233] R. Singh, M. Vatsa, H. Bhatt, S. Bharadwaj, A. Noore, S. Nooreyezdan, Plastic surgery: a new dimension to face recognition, IEEE Trans. Inf. Forensics Secur. 5 (3) (2010) 441–448.
[234] H. Bhatt, S. Bharadwaj, R. Singh, M. Vatsa, Recognizing surgically altered face images using multiobjective evolutionary algorithm, IEEE Trans. Inf. Forensics Secur. 8 (1) (2013) 89–100.
[235] The Noisy Iris Challenge Evaluation: Part II. <http://nice2.di.ubi.pt/index.html>.
[236] NIST, Face Recognition Grand Challenge Version 2. <http://www.frvt.org/FRGC/> (accessed 15.03.15).
[237] J. Ortega-Garcia, J. Fierrez, F. Alonso-Fernandez, J. Galbally, M. Freire, J. Gonzalez-Rodriguez, C. Garcia-Mateo, J.-L. Alba-Castro, E. Gonzalez-Agulla, E. Otero-Muras, S. Garcia-Salicetti, L. Allano, B. Ly-Van, B. Dorizzi, J. Kittler, T. Bourlai, N. Poh, F. Deravi, M. Ng, M. Fairhurst, J. Hennebert, A. Humm, M. Tistarelli, L. Brodo, J. Richiardi, A. Drygajlo, H. Ganster, F. Sukno, S.-K. Pavani, A. Frangi, L. Akarun, A. Savran, The multiscenario multienvironment biosecure multimodal database (BMDB), IEEE Trans. Pattern Anal. Mach. Intell. 32 (6) (2010) 1097–1111.
[238] West Virginia University Off-Angle Dataset. <http://www.clarkson.edu/citer/research/collections/wvuoffaxisrelease1.html> (accessed 15.03.15).
[239] L. Masek, P. Kovesi, A Biometric Identification System Based on Iris Patterns. Available: http://www.csse.uwa.edu.au/~pk/studentprojects/libor/, Accessed: 2015-03-15 (2003).
[240] Video-based Automatic System for Iris Recognition (VASIR), <http://www.nist.gov/itl/iad/ig/vasir.cfm> (accessed 15.03.15).
[241] Y. Lee, R.J. Micheals, J.J. Filliben, P.J. Phillips, VASIR: an open-source research platform for advanced iris recognition technologies, J. Res. Nat. Inst. Stand. Technol. 118 (2013) 218.
[242] VeriEye SDK. <http://www.neurotechnology.com/verieye.html> (accessed 15.03.15).
[243] O.V. Komogortsev, D.V. Gobert, S. Jayarathna, D.H. Koh, S.M. Gowda, Standardization of automated analyses of oculomotor fixation and saccadic behaviors, IEEE Trans. Biomed. Eng. 57 (11) (2010) 2635–2645.
[244] O.V. Komogortsev, A. Karpov, Automated classification and scoring of smooth pursuit eye movements in the presence of fixations and saccades, Behav. Res. Methods 45 (1) (2013) 203–215.
[245] M. Vatsa, R. Singh, A. Noore, Unification of evidence-theoretic fusion algorithms: a case study in level-2 and level-3 fingerprint features, IEEE Trans. Syst. Man Cybern. Part A: Syst. Humans 39 (1) (2009) 47–56.